NASA

National Aeronautics and Space Administration

- Multipurpose Hydrogen Test Bed - System Definition and Insulated Tank Development

Final Report

Contract NAS8-39201 - CFM Technologies for Space Transportation: Multipurpose Hydrogen Test Bed System Definition and Tank Procurement

Martin Marietta Astronautics

July, 1993

Prepared for
George C. Marshall Space Flight Center

Final Report
July, 1993

Contract NAS8-39201 - CFM Technologies for Space Transportation: Multipurpose Hydrogen Test Bed System Definition and Tank Procurement

Abstract: This report covers the development of a Test Bed Tank and Thermal Control System designed to simulate an upper stage liquid hydrogen tank. The tank is 10 ft long and is 10 ft in diameter, and is an ASME certified tank constructed of 5083 aluminum. The tank is insulated with a combination of sprayed on foam insulation, covered by 45 layers of double aluminized mylar separated by dacron net. The mylar is applied by a continuous wrap system adapted from commercial applications, and incorporates variable spacing between the mylar to provide more space between those layers having colder temperatures near the walls, which minimizes heat leak. It also incorporates a unique venting system which uses fewer large holes in the mylar rather than the multitude of small holes used conventionally. This significantly reduces heat transfer, provided adequate venting occurs. The test bed consists of an existing vacuum chamber at MSFC, the test bed tank and its thermal control system, a thermal shroud (which may be heated) surrounding the tank, and a zero-g vent subsystem developed by another contractor. Provisions are made in the tank and chamber for inclusion of a variety of cryogenic fluid management concepts.

Martin Marietta Astronautics
PO Box 179
Denver Colorado 80201
Internal Mail Number S5060

Authors:
E. C. Fox
E. R. Kiefel
G. L. McIntosh
J. B. Sharpe
D. R. Sheahan
M. E. Wakefield

NASA Project Managers: Mark Fisher and Leon Hastings
Space Propulsion Branch, Propulsion Systems Division, Propulsion Laboratory
George C. Marshall Space Flight Center

Martin Marietta Program Managers: M. E. Wakefield and E. C. Fox
Flight Systems
Martin Marietta Astronautics

Table of Contents

Abbreviations

ASME	American Society of Mechanical Engineers
CDR	Critical Design Review
CFM	Cryogenic Fluid Management
CTS	Cryogenic Technical Services, Inc.
DAM	Double Aluminized Mylar
ET	External Tank
LH_2	Liquid Hydrogen
MHTB	Multipurpose Hydrogen Test Bed
MLI	Multilayer Insulation
MSFC	Marshall Space Flight Center
OFHC	Oxygen Free High Purity Copper
PCS	Pressure Control Subsystem
PDR	Preliminary Design Review
RPM	Rotations per Minute
STF	Slush Hydrogen Test Facility
TCS	Thermal Control Subsystem
TML	Total Mass Loss
TVL	Thermal Vacuum Stability
VCM	Volatile Condensable Materials
VCS	Vapor Cooled Shield
SOFI	Spray On Foam Insulation

1.0 Background

Space transportation is expected to evolve from Earth based operations to space based operations after the Space Station becomes operational in the early 2000 time frame. The efficient management of subcritical cryogenic propellants is one of the key drivers for future programs. The cryogenic fluid management (CFM) technologies must be able to reliably maintain the cryogens at proper thermodynamic conditions in the following broad range of space operations; low earth orbit, planetary injections, manned sorties, life support, power systems,and accommodation of on-orbit resupply.

The objective of the multipurpose hydrogen test bed (MHTB) program is to provide a safe and reliable Phase 1 test tank and Thermal Control Subsystem for multi-use ground based technology demonstrations. As additional CFM technologies are defined, they will be integrated into the Phase 1 configuration for continued system level demonstrations. Table 1-1 summarizes the applicability of the CFM technologies to the emerging missions. This report summarizes the Phase 1 program activities for the Thermal Control Subsystem and the test bed tank.

Table 1-1 Upper Stage Cryogenic Fluid Management Needs for the Next Ten Years

CFM Technology	Length of Space Mission			
	24 Hr Mission	45 Day Mission	6 Month Mission	9 Month + Mission
Thermal Control (TCS)	Foam/Coated Helium Purge	Foam/MLI 0.75/2.00"	Foam/MLI 0.75/2.00"	Foam/MLI 1.00/4.00"
Pressure Control (PCS)	Settle/vent	Settle/vent or TVS/mixer	TVS/mixer	TVS/mixer
Vapor Cooled Shield (VCS)	None	None	Integrated With PCS	Integrated With PCS
Active Refrigeration	None	None	None	Yes
Ascent Heat Protection	None	Yes, Shroud For TLI	Yes, Payload Fairing	Yes, Payload Fairing
Meteoroid Protection	None	Integrated With TCS	Integrated With TCS	Integrated With TCS
Propellant Transfer	None	None	Topoff	Topoff

2.0 Introduction

This contract includes the design and development of the test tank as well as the Thermal Control Subsystem (TCS). An integrated design is necessary to satisfy the cryogenic liquid hydrogen loading and storage requirements for ground and orbital operations. Transient thermal performance testing was sacrificed in fovor of unlimited cycle life. Therefore, the test tank is a 5083 aluminum alloy, ASME-coded pressure vessel designed for safe operation under multiple test conditions in both atmospheric and vacuum environments. The design includes a large manhole

cover at the top that can be removed for access into the tank to install various CFM components that are developed on other CFM technology programs. Two instrumentation ports on the top dome provide access to silicon diode temperature transducers on the removable instrumentation rakes. These instruments are used to determine the thermodynamic state (stratification) of the liquid hydrogen during various test conditions. A detailed description of the test tank is found in Section 8.0.

Table 2-1 summarizes the TCS requirements defined for the MHTB test program. The TCS baseline includes a Spray On Foam Insulation (SOFI) directly bonded to the tank to prevent condensation of the ground purge gas during loading and ground hold, and a Multilayer Insulation (MLI) which is applied over the SOFI to provide low heat transfer during orbital operations. The Thermal Control Subsystem includes the insulation systems, a thermal shroud, low heat leak tank supports, an MLI application fixture, and a SOFI/MLI rotation fixture. Figure 2-1 illustrates several of these features in the Marshall Space Flight Center (MSFC) Test Stand 300 vacuum

Table 2-1, Thermal Control Subsystem Application Requirements

MHTB Requirements

- **Ground Hold Conditions**
  - Hold Fully loaded Tank for 3 Hours
  - GN2 Purge with -65 °F Dew Point
  - Final Topoff to 98% Two Minutes Before Liftoff
    - Maintain SOFI Surface Temp at or Above -200 °F
- **Ascent Flight Conditions for Design**
  - Altitude = 5×10^{-5} Ft (3.5×10^{-6} Torr) 420 Seconds after Liftoff
  - Vibration Loads: Saturn V Acoustic Environment
  - Acceleration History for Loads

Time (Sec)	Acceleration (a/g_o)
0	1.26
100	2.20
195	4.50
196	1.00
400	2.00
460	2.80

- **Orbital Conditions**
  - Average MLI External Surface Temperature = 540 °R
  - Orbit Hold time = 45 Days

Prototype Reference*

- **Ground Hold**
  - External Tank
    - Fully Loaded Tank for 5 Hours 20 Minutes before Launch
    - Final Topoff at T-2.5 Minutes
    - GN2 Purge Dew Point = -65°F
  - Centaur
    - Fully Loaded Tank for 25 Minutes to 1 Hour 25 Minutes before Launch
    - Final Topoff at T-90 Sec, 99.8% Full
- **Ascent Flight Condtions**
  - Utilize NLS Conditions
- **Orbital Conditions**
  - Translunar Injection Stage:
  - Assume Dual Launch, 45 Day Mission
  - Max. Avg. Surface Temp = 540 °R
  - Min. Avg. Surface Temp = 200° R

* For Reference Only

chamber. Past programs have dealt with the problem of bonding SOFI to liquid hydrogen tanks in various ways, however this program selected the proven materials and processes developed for the Space Shuttle External Tank liquid hydrogen tank as its point of departure for the new space applications. For the MLI systems, the materials include conventional aluminized radiation shields and non-metallic spacers, but applies them in a unique method for improved performance.

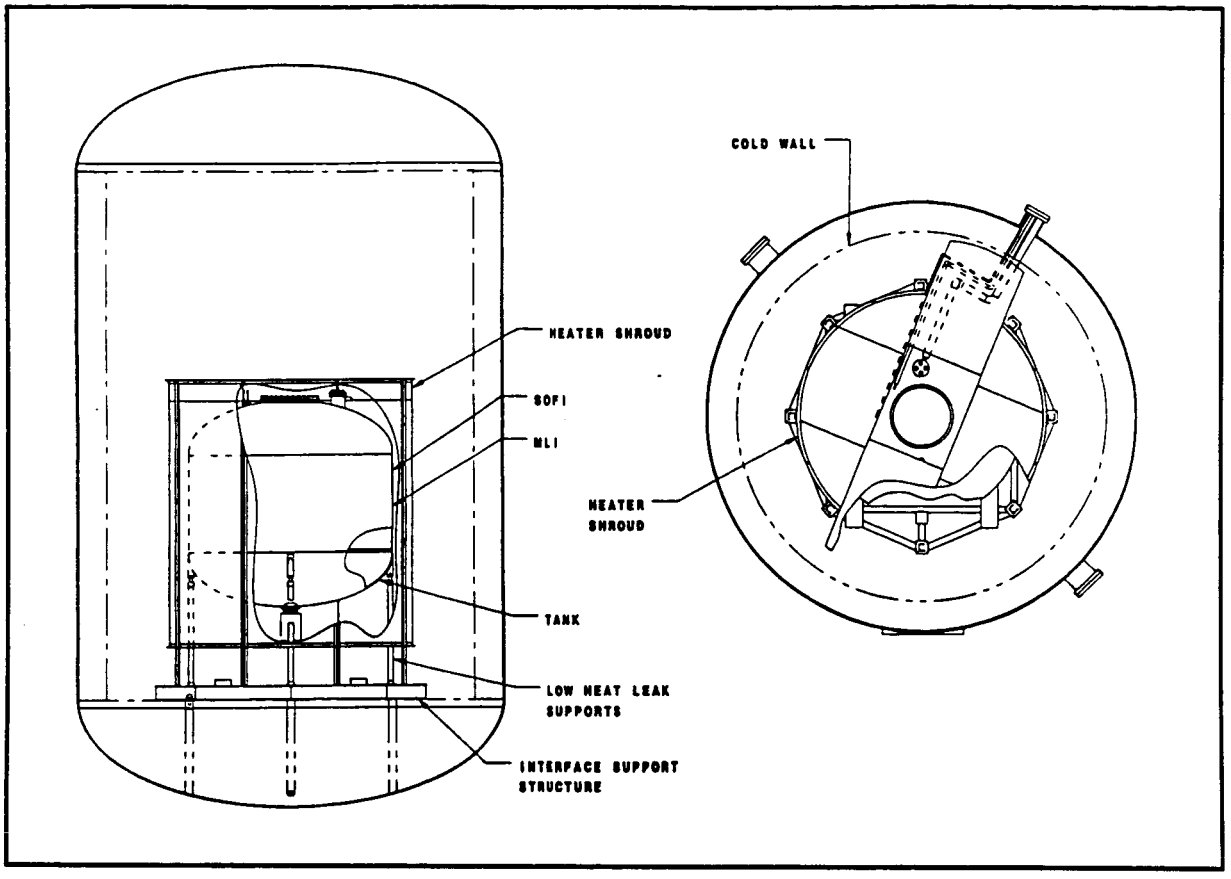

Figure 2-1, Thermal Control Subsystem Components

The purpose of the MHTB thermal control study is to develop a lightweight, robust insulation system that can maintain a cryogenic tank for an on-orbit hold period of up to 45 days. The thermal insulation system for the MHTB test tank was developed based on past program experience, extensive analysis, and commercial application techniques. Cryogenic insulation systems have been studied and tested for at least 30 years with improved performance as the years progress. Figure 2-2 summarizes the performance improvement over the years of various high performance insulation systems which have been built and tested. The density-thermal conductivity product (ρk) is an indicator of overall performance of an insulation system by accounting for both the mass and thermal performance of a system. The tested systems are all different materials, tested at different boundary temperatures and installed differently on different sized tanks. Yet, the ρk value provides a means of comparing performance in a normalized manner. Prior programs used an MLI installed density of 60 layers per inch based on demonstrated fabrication capabilities. We have added a data point (number 9) for a typical 45 layer constant density system using double aluminized Mylar (DAM) for radiation shields and two layers of Dacron net as the spacer material. For this program, we developed a variable density MLI

fabrication approach which reduces the density, reduces solid conduction within the insulation and yet is robust and can survive the ascent flight loads. We have included several data points (number 10) for 45 layer variable density systems which use DAM for radiation shields but eliminates one layer of spacer by adding discrete bumper strips of Dacron net at several locations within the insulation. The effect is to reduce the density and the solid conduction simultaneously. The graph illustrates the ability to improve the overall performance of an insulation system by employing a SOFI/variable-density MLI layup. The predicted performance of the MHTB tank with variable density MLI is shown to improve the previous performance by a factor of two.

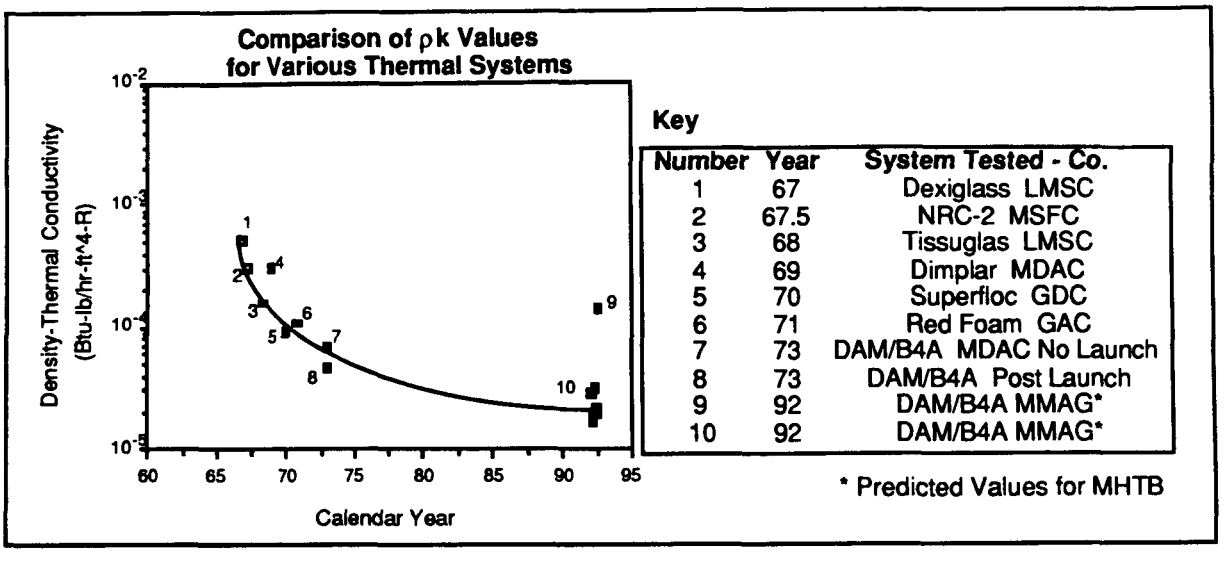

Figure 2-2 Comparison of Density - Thermal Conductivity Values

3.0 Insulation Concepts

The insulation concept selected for the MHTB technology effort is a SOFI and MLI system. The combination of the foam and MLI provide thermal protection for both the ground hold and space hold conditions. The SOFI provides thermal insulation during the ground hold period by reducing the conductive heat transfer into the tank and eliminating the condensation of nitrogen on the tank by increasing the surface temperature of the foam above the nitrogen liquefaction temperature. The insulation system will be purged with gaseous nitrogen during the ground hold period to remove trapped moisture within the blankets. The multilayer insulation provides thermal protection in space by reducing the radiation heat transfer into the tank. These two systems, when combined, reduce the overall heat transfer into the tank for the entire mission. A system optimization determined the desirable SOFI and MLI thickness. These will be discussed in more detail later in the report.

The selection of SOFI was based upon the desire to reduce the ground hold heat transfer using a robust design. Currently, the Space Shuttle External Tank (ET) utilizes SOFI for its insulation system. An alternative ground hold concept is to apply MLI directly to the tank and use a helium purge through the entire MLI blanket. The helium prevents condensation of air (formation of liquid air is a safety hazard), but it increases the ground boiloff rate. Te helium purge concept eliminates the SOFI application operation and reduces the insulation weight carried on-orbit, but there are other consequences which much be considered. The helium purge system must be designed into the MLI system and this component weight must be carried through the mission. A larger impact is the thermal conductivity of helium purge gas which is five times larger than nitrogen (the heat transfer into the tank is five times greater) which can ultimately lower the hydrogen bulk density at launch. During a top-off ground hold operation, this heat transfer rate is not a large problem. However, when the vehicle is launched, the helium remains in the blanket for a period of time and the heat transfer and subsequent boiloff can impact the vehicle design. This subsequent boiloff rate can exceed the mass of a SOFI system. Based upon these considerations, a SOFI insulation system was selected for the ground hold.

The next consideration was the multilayer insulation design. Past programs have investigated numerous materials, designs and systems. A multilayer insulation system consists of a highly reflective material which is separated by a spacer material. The reflective material reduces the radiative heating while the spacer material reduces the solid conduction between the layers of reflective material. Alternating layers of reflective and spacer material are placed together to make up a multilayer insulation system. Past programs have shown that a low density MLI system provides the best thermal performance. In order to achieve a low density insulation system, a new technique was considered for the MLI layup. This technique is employed in the commercial cryogenic dewar industry and has proven successful on many liquid hydrogen dewars and several liquid helium dewars. The low density is achieved by using narrow strips of the spacer material as bumper strips between layers of reflective material. The application technique involves a continuous roll-wrap process which applies DAM, Dacron net and bumper strips simultaneously to the barrel section of the tank. The tank is rotated in a fixture at a controlled rate as the insulation material is rolled on. This technique minimizes the seams on the barrel section which greatly reduces the heat flux into the tank. This technique is described in more detail in Section 3.2.3 MLI Sensitivity Analysis.

3.1 Spray On Foam Insulation Concept at CDR

3.1.1 Selection of SOFI Materials and Application Processes

The primary objective during ground hold is to eliminate the condensation of nitrogen on the tank surface. This nitrogen condensation is of concern during ground and flight operations because the additional mass of liquefied nitrogen reduces flight performance and the vaporization of condensed nitrogen affects the multilayer insulation performance on-orbit.

A typical ground hold scenario uses nitrogen as the purge gas around a tank to provide an inert, controlled environment. Nitrogen condenses at 150°R (85°K) and will readily condense on a non-insulated liquid hydrogen tank. One solution to eliminating the potential of nitrogen liquefaction is to apply a foam substrate directly to the tank. A polyurethane foam is currently in use on the Shuttle ET and is the basis for the insulation being used on the MHTB tank. The required thickness of SOFI is determined from the thickness of MLI applied over the foam and the desired SOFI surface temperature. A thick blanket of MLI will maintain a stagnant layer of nitrogen gas and subsequently lower the temperature of the foam surface. Therefore, the desirable foam thickness is driven by the MLI thickness and the nitrogen condensation temperature. Typically, a margin for error is included in the foam thickness to account for areas where the MLI thickness may be greater than the nominal thickness. This test program set a desirable foam surface temperature at 260°R (140°K) to provide a margin of safety in the design. In order to achieve this foam surface temperature, approximately one inch (2.54 cm) of foam is required with a two inch MLI blanket. Figure 3.1.1-1 illustrates the effect of foam thickness and MLI thickness on the tank surface temperature.

Closed cell polyurethane foam was used in earlier MLI test program and difficulty was encountered during evacuation of the MLI during ascent. Post test examinations disclosed the foam had cracked and debonded from the tank in several areas of the foam application. This allowed the nitrogen purge gas, which was used during loading and ground hold operations, to condense on the tank and foam surfaces. This condensed nitrogen would continue to vent in orbit, contributing to a higher than expected residual gas pressure in the MLI, until sublimation and venting was completed. To alleviate these materials and application problems, the newest materials and processes from the External Tank program were used. The materials, processes, data base, and application tooling were available for this program. This decision to use ET SOFI materials limited the scope to only BX-250 and Isofoam SS-1171. The properties of the two foams which were considered are shown in Table 3.1.1-1. The SS-1171 foam was selected because of its superior application capability and synergistic data which would be available from the ongoing ET materials improvement and robotic applications programs.

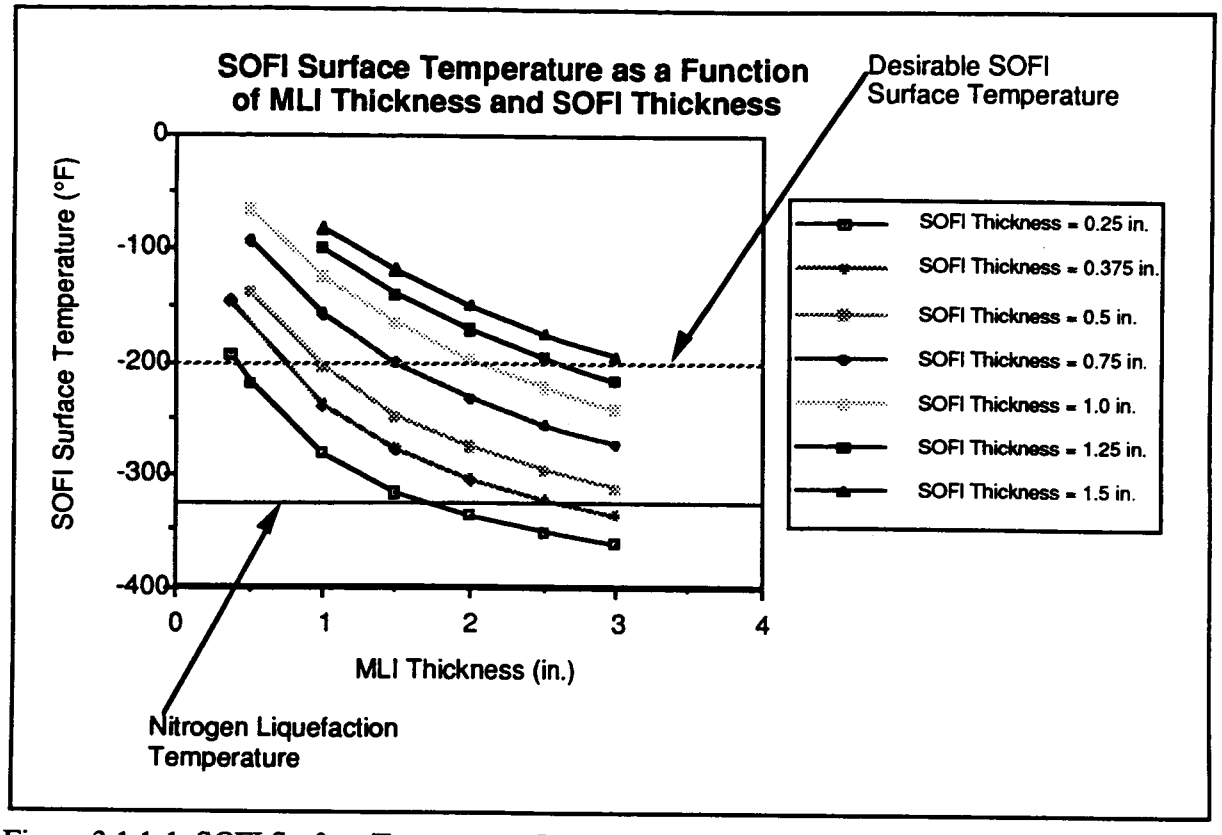

Figure 3.1.1-1 SOFI Surface Temperature Parametrics

Table 3.1.1-1 Foam Property Comparison

Property	BX-250	Isofoam SS-1171
Density (lb/ft^3)	2.2	2.3
Compressive Strength (psi)	39	32
Bond Tensile Strength (psi)		
Ambient	76	78
-320 °F	88	84
-423 °F	66	72
Cryoflex (-423 °F, 78 ksi)	pass	pass
Flammability (per NHB 8060.1A)	pass	pass
Outgassing		
Total Mass Loss (%)	11.01	9.45
Volatile Condensable Materials	0.17	TBD

For flight applications on Expendable Launch Vehicles, no problems are anticipated with usage of either foam. Shuttle vehicle usage for these foam systems would require compatibility with the selection criteria for materials usage in the payload bay. A review of NASA procedure MSFC-PROC-1301, "Guidelines for the Implementation of Required Materials Control Procedures" revealed six criteria for selection/approval of materials for use in the Shuttle payload bay. These are corrosion, stress corrosion, cracking, fluid compatibility, flammability, and thermal vacuum stability (TVS). The first three apply to metals and therefore, were not considered to be applicable. The fourth applies to any hazardous fluid used in the payload bay so it was not an issue with the foam. The last two criteria apply to the foam and all considered foam materials have been submitted to the MSFC Materials and Processing Laboratory for testing. The Isofoam SS-1171 met the flammability criteria during its qualification for ET usage. The Isofoam SS-1171 does not meet the TVS criteria with an "A" rating because it has a Total Mass Loss (TML) of 9.45%. An "A" rating requires a TML of less than 1.0% and a Volatile Condensable Materials (VCM) of less the 0.1%. Since the SS-1171 does not meet the "A" rating, sufficient rationale for its use in the payload bay will be required.

For this program, the SOFI application is performed in an environmentally controlled room in building 4707 at MSFC. The foam application uses robotic tooling and ET processing parameters. The robot moves the spray gun along the tank surface as the tank rotates. This results in a "barber pole" type of application, typical of the ET. With this technique, successive spray passes of foam overlap previous passes until the complete coverage of the tank is achieved. For the domes, the rotational velocity (surface speed) of the tank approaches zero at the apex. To compensate for this reduction in surface speed the output of the spray gun is reduced on the domes to minimize excessive thickness. This process results in a nominal foam thickness of 1.0 ± 0.25 inches, with the thickness of each pass being about 0.5 inches. Manual trimming operations are performed on the SOFI to terminate the sprayed foam at penetrations, then either a hand spray operation or PDL 4034 pour foam application must be performed to close out the penetrations. A rotational fixture was supplied as a part of this contract to rotate the tank during the application process. It includes an MSFC provided electrical drive system, which interfaces with the robotic programmed controller in the SOFI spray booth.

3.2 Multilayer Insulation Concept at CDR

The original MHTB tank design included a vapor cooled shield (VCS) to meet a thermal requirement of less than 2% boiloff/month. The 2% boiloff/month was a requirement derived for long term cryogenic storage applications. As the MHTB program developed, the VCS was eliminated from the design to focus the program on more near term space storage requirements. A VCS is advantageous for tanks that will be on-orbit for more than approximately 60 days. Figure

3.2-1 shows the impact of an operational and non-operational VCS on the boiloff rate. The mass penalty associated with a VCS can be a benefit for long term cryogenic storage because it outweighs the boiloff mass. For short term cryogenic storage, the mass of the VCS does not outweigh the mass loss of the hydrogen boiloff. Therefore, the VCS is not included in the final design of the tank.

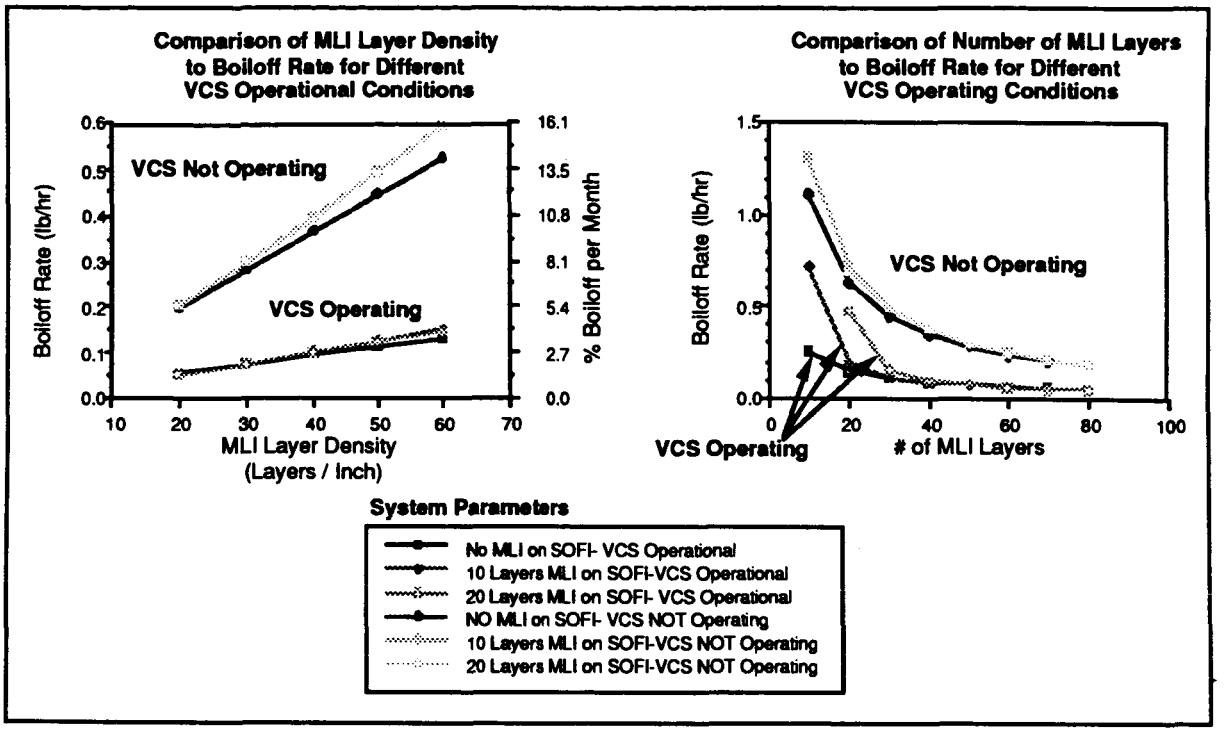

Figure 3.2-1 VCS Non-Operational Parametrics

Once the VCS was eliminated from the design, alternate design concepts were evaluated for the multilayer insulation. Past programs have used many layers of the reflective material-spacer material combination (up to 200 layers) to reduce the heat leak into the tank. The heat transfer into the tank is governed by three modes: radiation, solid conduction, and interstitial gas conduction. The radiation heat transfer is governed by the number of reflective layers, so increasing the reflective material layers reduces the radiation heat transfer. Yet, each reflective layer increases the potential of solid conduction throughout the blanket due to the possibility of contact between surrounding layers. Separation of reflective layers is achieved by placing spacer material between each reflective layer. The third heat transfer mode is gas conduction. For good vacuum conditions (less than 10^{-5} torr), the interstitial gas conduction is small in comparison to the radiation and solid conduction heat transfer. Therefore, gas conduction is not a driver in the MLI design except during launch ascent profile and the first few hours on-orbit. An objective of the reflective/spacer

material layup is to optimize the number of layers to produce the most efficient thermal barrier. An MLI system optimization was performed to determine the best MLI layup.

3.2.1 MLI Material Selection

The first consideration for the multilayer insulation was the material selection. The reflective material candidates were double aluminized Mylar (DAM) and double aluminized Kapton. Other reflective materials are available such as goldized Mylar and goldized Kapton, but the cost is prohibitive for these materials. The double aluminized Mylar was selected for the reflective material because of cost considerations. The Kapton material is ten times more expensive than Mylar and does not improve the performance of the reflector. The only purpose for using Kapton would be to meet the non-flammability requirement for Shuttle launch.

Another consideration was the use of organic coatings to increase the Mylar reusability. Sheldahl produces a corrosion resistant acrylic overcoat to prevent degradation of the reflective material when exposed to salt fog, humidity, abrasion and temperature cycling. The organic coating doubles the cost of Mylar and these data are not pertinent to this phase of the program, therefore the coating was not included in the design. The MHTB test program can provide data on the degradation of the material after thermal cycling and exposure to moisture.

Several candidate spacer materials were considered including Dacron net, silk net, spunbonded polyester fiber mat, and glass paper. Dacron net was selected for the spacer material based on its low mass, low cost, and low outgassing. Table 3.2.1-1 shows the physical properties of the candidate spacer materials. Two different types of Dacron net were considered for the spacer material - B2A and B4A Dacron net. The B2A Dacron net is a heavier, tighter mesh net than the B4A. The B2A net has a minimum mesh of 190 per square inch while the B4A net has a minimum of 43 per square inch. The B4A net weighs half as much as the B2A net, which decreases the solid conduction through the multilayer insulation to approximately one half of the B2A value.

Table 3.2.1-1 Spacer Material Properties

Spacer Material	Thickness (mil)	Mass g/m^2 (lb/ft^2)	Cost $/ft^2
Reemay Style 2250	4	17 (0.0035)	$0.014
Silk Net	5	6.0 (0.0012)	$2.67
Dacron Net B4A	6.5	7.1 (0.0015)	$0.155
Decron Net B2A	6	14.9 (0.0031)	$0.143

The silk net was originally recommended for the spacer material because of its physical and thermal properties. Silk net has the lowest heat transfer properties of all the materials, as well as being light weight. The biggest detriment of the silk net is the cost and its water moisture retention

characteristic. The silk net is sixteen times more expensive than the Dacron net and yet has only a 15% improvement in thermal properties. The high outgassing rate coupled with the cost increase eliminated silk net from further consideration. The spunbonded polyester fiber mat is produced by Reemay and these fiber mats are utilized in many industries. The reason for considering the Reemay was its good thermal properties and its low cost. After further analysis, the Reemay was dropped from consideration because its high fiber content increased the solid conduction component of the heat transfer. The glass paper was rejected because it has low tensile strength and it is heavier and thicker than the other separators.

3.2.2 MLI Optimization

The optimization of the MLI system requires certain assumptions and ground rules. The optimization considers the mass of the SOFI, MLI and resultant hydrogen boiloff which are summed to evaluate an overall system mass. This system mass is an indicator of the overall mass effectiveness of the insulation system. A constant density MLI layup was evaluated to ensure consistency between results. A constant density system refers to maintaining the same number of reflector and spacer layers throughout the MLI blanket. Three layer density systems (25, 45 and 60 layers/in.) were evaluated for the optimization. Two mission durations were considered - a 30 day mission and a 45 day mission. All the optimizations maintained the SOFI surface temperature for the ground hold above 260°R (145°K).

The MLI performance analysis tool was developed by CTS in Boulder Colorado which is a thirteen year old spinoff of Cryenco Sciences, Inc. which itself was founded in 1958 by the three CTS principles: Glen E. McIntosh, Gerald D. Mordhorst, and Kenneth P. Leonard. CTS has designed many kinds of cryogenic dewars, complex transfer and distribution systems, and cryogenic process equipment. Dr. McIntosh developed the MLI performance analysis tool, which considers radiation and solid conduction heat transfer through the MLI, based upon many years of experience with cryogenic dewars.

Dr. McIntosh developed a layer by layer thermal conductivity equation to evaluate the temperature gradient and overall heat flux of an MLI blanket design. This equation accounts for radiation, solid and gas conduction heat transfer.

$$k = \sigma[\epsilon/(2-\epsilon)(T_w^2 + T_c^2)(T_w + T_c) - 4T_m^3 \cdot L_f/N \cdot \alpha^2] \quad \text{Radiation Term}$$

$$+ 1.1666 \cdot P[1 - (0.2)(T_w - 80)/220] \quad \text{Gas Conduction}$$

$$+ (10^{-2} \cdot f/\Delta x)[0.017 + 7x10^{-5}(800 - T_w) + 0.0228 \cdot \ln(T_w)] \quad \text{Solid Conduction}$$

where:

k = thermal conductivity, W/m•K

σ = Stefan-Boltzmann constant, $5.675x10^{-8}$ W/m2•K4

L_f = Fiber pore size, m

= $(\pi/4)$(fiber diameter/f)

f = fractional fiber density = (rho)/spacer material solid density - (dimensionless)

N = reflector layer/m

α = radiation absorptivity of separator

P = gas pressure, Pa (1.1666 assumes N_2 residual gas)

rho = effective density of spacer material - Kg/M^3

T_W = warm reflector layer temperature

T_C = cold reflector layer temperature

ϵ = reflector layer emissivity

T_m = mean temperature between layer $(T_W + T_C)/2$

Δx = thickness of spacer material

Notes on equation:

1. This equation is intended for layer by layer MLI calculations.
2. The radiation term assumes parallel surfaces with equal emissivities as shown. Different emissivities can actually be used by re-arranging the first part of the first term.
3. The second part of the first term represents radiation that is absorbed by the separator material.
4. The bracketed item in the gas conduction term, the accommodation coefficient, is unity below 80K.
5. The 10^{-2} term in the solid conduction equation is an empirical multiplier to account for random orientation of separator fibers perpendicular to the heat flow.
6. The bracketed item in the solid conduction equation is an empirical fit to Dacron thermal conductivity data.
7. The gas conduction coefficient is calculated from kinetic theory. The 1.1666 value for nitrogen is satisfactory for air but a different (and higher) value must be used if hydrogen or helium is the residual gas in the vacuum space. The helium value is 2.05.
8. For some calculations, the Stefan-Boltzmann constant has been increased by 3% to account for an increase in radiation heat transfer due to 1% area being perforated to permit rapid evacuation without excess stress on the double aluminized Mylar reflector.
9. The equation validity decreases at high interstitial pressures.

A sample calculation is included in Appendix A. This analysis tool predicts the temperature distribution through the entire MLI blanket using the sum of squares approach. With knowledge of the external MLI temperature, the number of layers and the tank temperature, an appropriate temperature difference for each layer is predicted and the thermal conductivity calculated based upon this temperature difference. This is repeated for each layer until the appropriate temperature

range is determined. The development of the equations is a tedious and time consuming process, but once the equations are developed for a particular MLI design, analysis of that design is straightforward.

This MLI thermal conductivity equation developed by CTS appears to accurately characterize MLI performance. This equation combined with a constant difference of squares method of calculating reflector temperatures has been used to calculate MLI heat transfer for a number of applications with results that are reasonably consistent with existing data. This thermal conductivity equation was used to predict the performance of an 11,000 gallon liquid helium transport dewar for a Japanese company. The dewar demonstrated a boiloff rate 5% lower than the predicted value, and recorded a pressure rise of only 5 psi during its ocean transport. This is the lowest pressure rise ever observed by the Japan Helium Center.

The advantages of using the proposed equation are two-fold. First, the equation, which closely follows analytical expressions, takes into account, as directly as possible, all of the modes of MLI heat transfer. The only adjusting coefficient is the 10^{-2} factor on solid conduction which reflects the combination of contact resistance and parallel orientation of the separator material fibers. Secondly, the equation is intended for layer by layer calculation of the MLI apparent thermal conductivity. This permits adjustment of reflector layer density in any way desired with printout of overall results and individual "k" values. Thus, given sufficient time to adjust the constants, it is possible to optimize an MLI system layer by layer. In fact, the calculation flexibility is greater that the practical range of spacer options since a new equation is required for every new spacer configuration.

The proposed thermal conductivity equation was used to determine the number of MLI layers which produce the best insulation performance for the minimum mass. Figures 3.2.2-1 through 3.2.2-3 illustrate the results of the optimizations for the 45 day mission and different layer densities. The low density system (25 layers/in.) has a minimum system mass at 65 layers of MLI which is approximately 2.6 inches (6.6 cm). This minimum value is found on the flat portion of the system mass line. Virtually the same system mass value can be achieved by using just 40 layers (less than 2 inches) of a low density system. The same trends can be observed with the 45 and 60 layer/inch systems. A relatively flat optimization is observed with a minimum of approximately 2 inches of MLI. The higher density systems just increase the mass of the overall system. Therefore, by producing a low density MLI layup, the best performing system can be obtained for minimum mass impact.

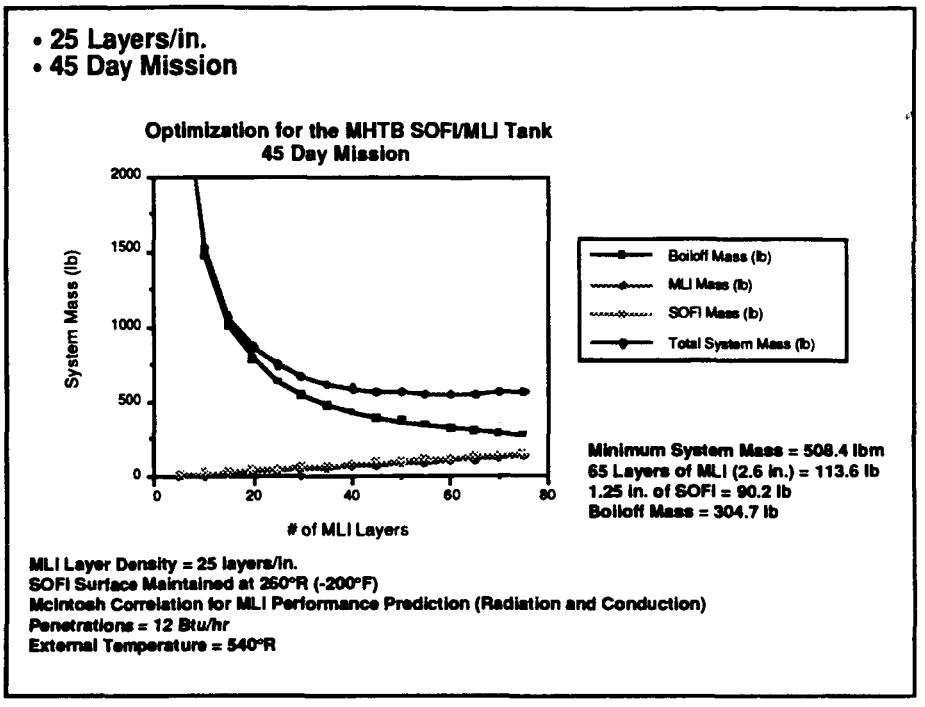

Figure 3.2.2-1 SOFI/MLI Optimization

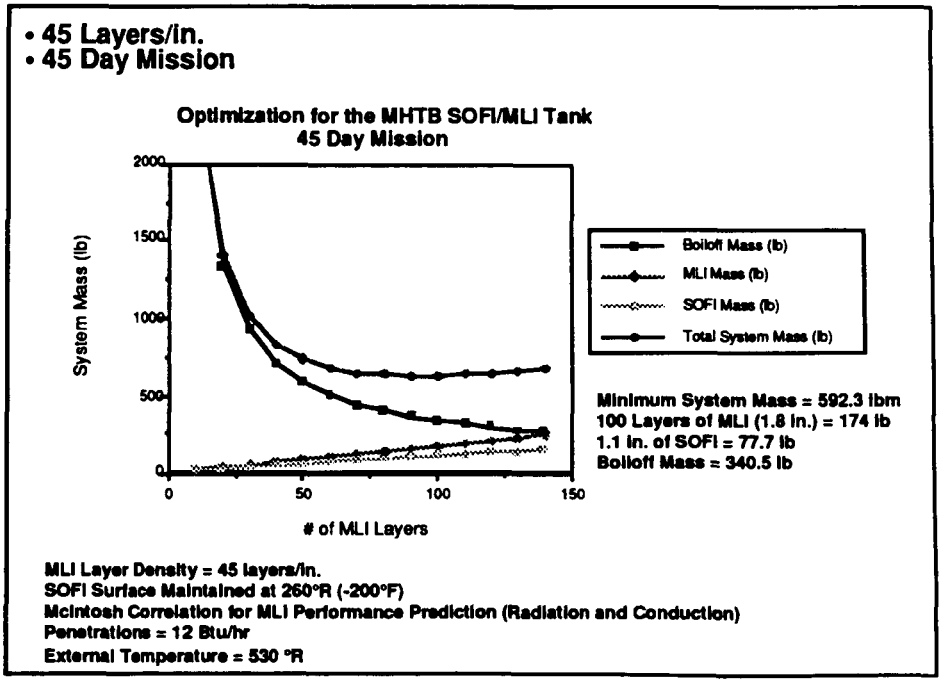

Figure 3.2.2-2 SOFI/MLI System Optimization

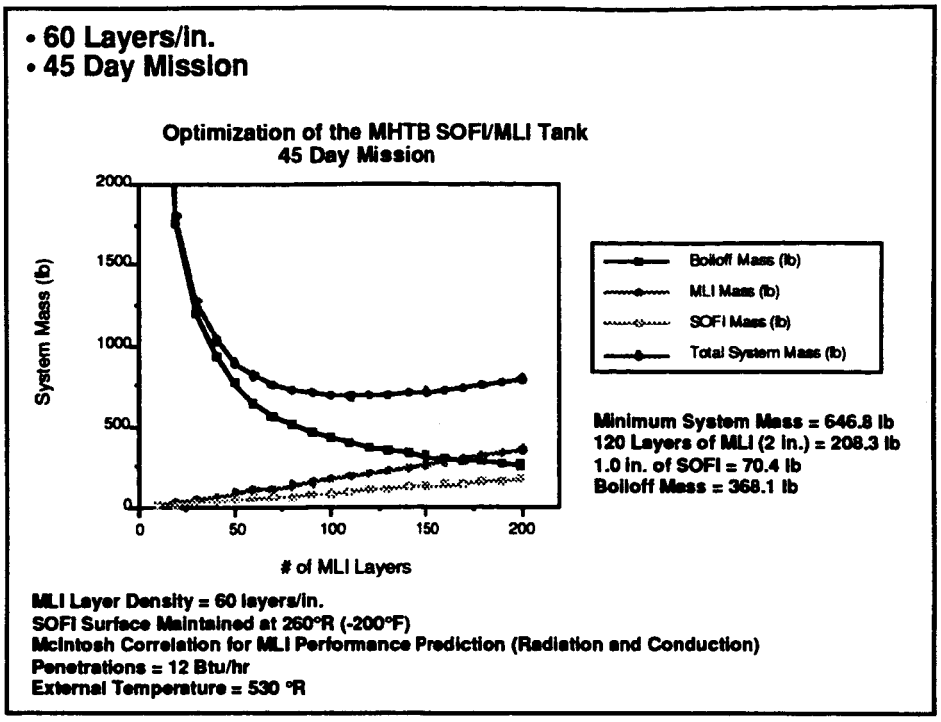

Figure 3.2.2-3 SOFI/MLI Optimization

In order to achieve a low density MLI layup, alternative fabrication techniques had to be considered. The conventional method of alternating layers of reflective material and spacer material produces a relatively high density blanket (45 to 90 layers/in.). Dr. McIntosh has developed a method of placing bumper strips between layers of DAM to create a low density MLI blanket. This process has been used on several commercial liquid helium dewars with much success. These bumper strips can be installed with variable thicknesses throughout the blanket to produce a variable density MLI blanket. The bumper strips act as standoffs between the layers and thereby greatly reduce the solid conduction. The bumper strips are two inch wide strips of spacer material which are applied at approximately two foot intervals around the tank. The bumper strips can be applied with multiple layers to provide a greater distance between reflective sheets. The greatest benefits from bumper strips is realized near the tank because solid conduction is the dominant term here. The number of bumper strips applied between the DAM layers can be reduced as the reflector layers move away from the tank surface because the temperature gradients are much smaller.

This concept leads to a variable density MLI layup was used for the MHTB tank. The variable density concept consists of a 45 layers MLI system with an overall effective layer density of approximately 25 layers/in. This initial variable density design consists of 10 layers of DAM

near the tank being separated by 5 bumper strips, the next 15 DAM layers being separated by 3 bumper strips, and the last 20 DAM layers being separated by 2 bumper strips.

In order to evaluate the effectiveness of this selected MLI layup, several sensitivities were completed, using the proposed thermal conductivity equation. The equation was used to predict the performance of a variable density MLI blanket and also assess the effect of interstitial pressure changes. Figures 3.2.2-4 through 3.2.2-7 show the optimization of a SOFI and variable density

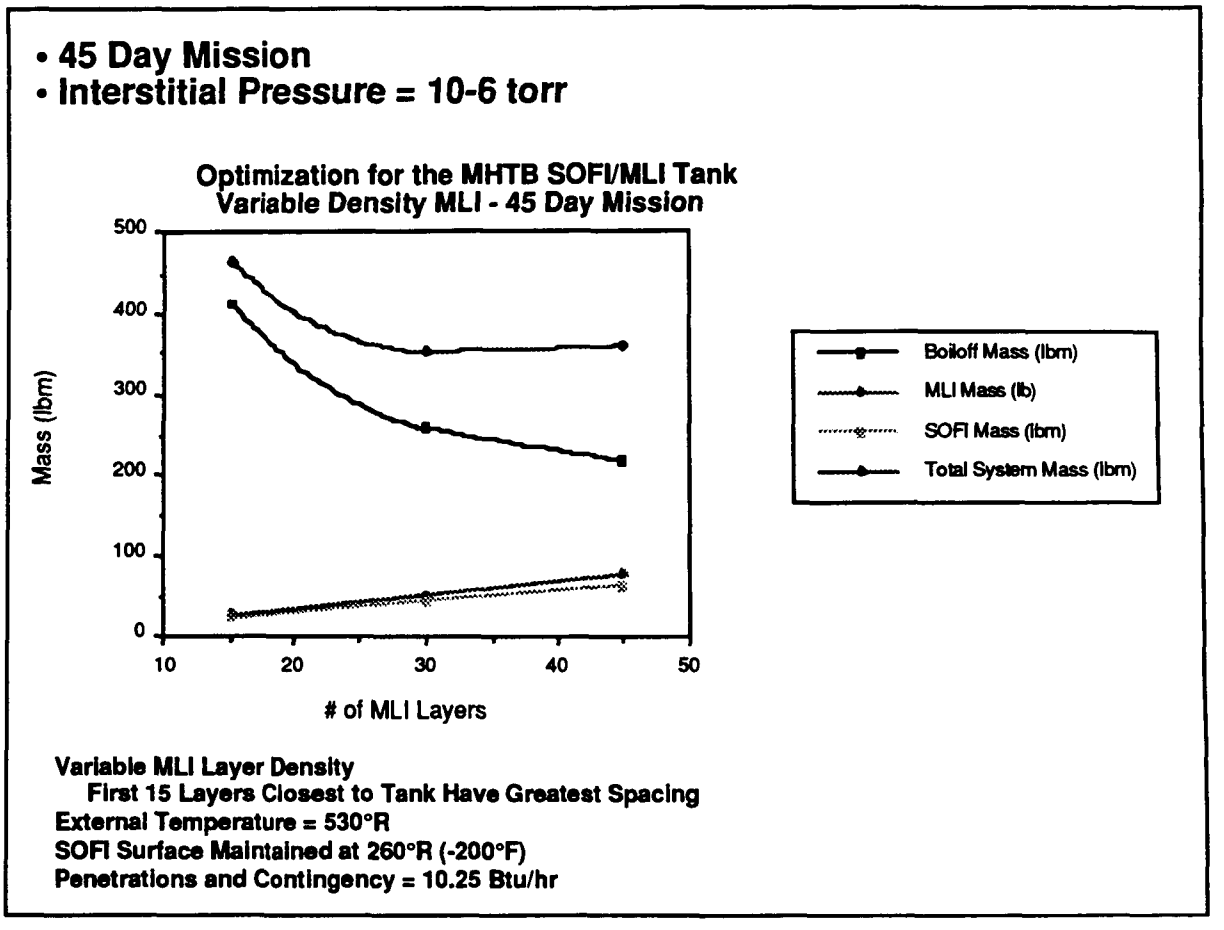

Figure 3.2.2-4 SOFI/MLI System Optimization - Variable MLI Density

MLI system for decreasing interstitial pressure. A 30 layer variable density system will provide the minimum system mass provided there is sufficiently low interstitial pressure (10^{-5} torr or less). Including 45 layers in the system does not tend to lower the system mass but simply trades the mass of the MLI for the boiloff mass. In the event the interstitial pressure is much higher (10^{-3} torr), the system is driven to more MLI layers because the mass of the additional layers is less than the mass of the boiloff.

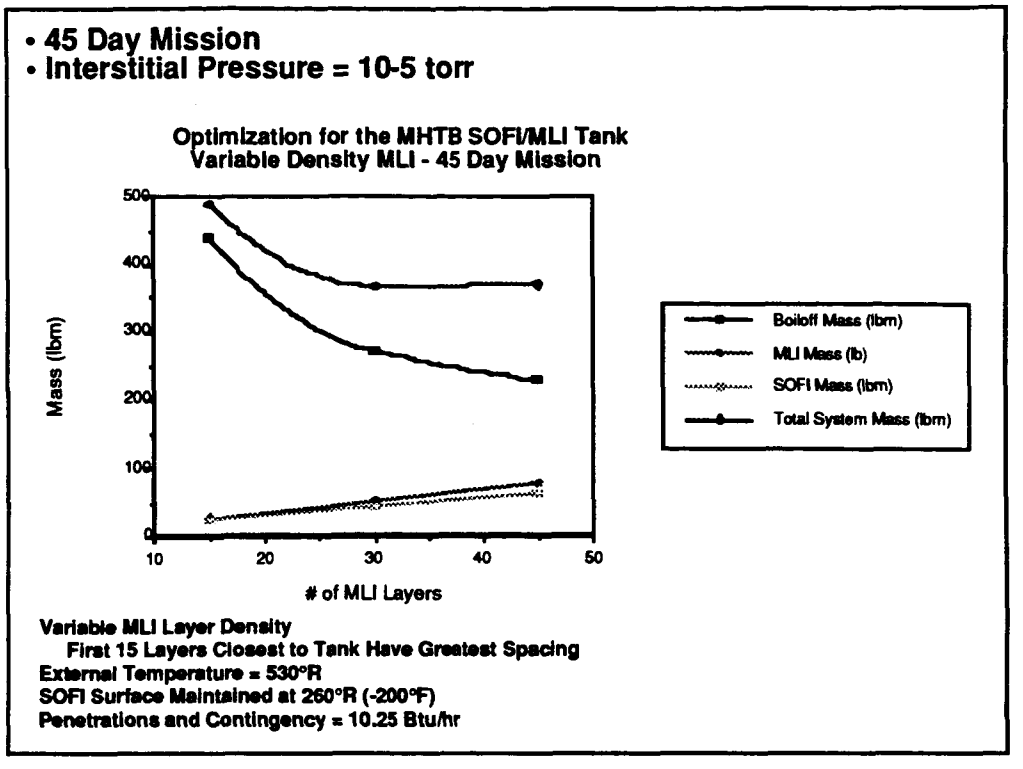

Figure 3.2.2-5 SOFI/MLI Optimization - Variable MLI Density

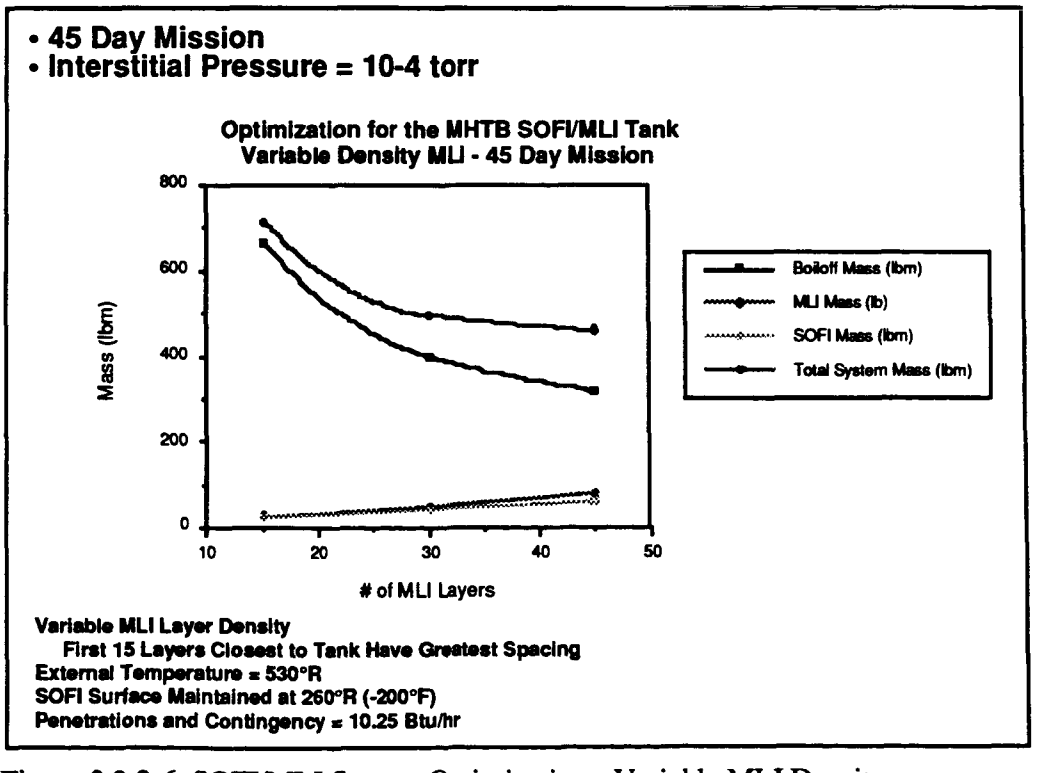

Figure 3.2.2-6 SOFI/MLI System Optimization - Variable MLI Density

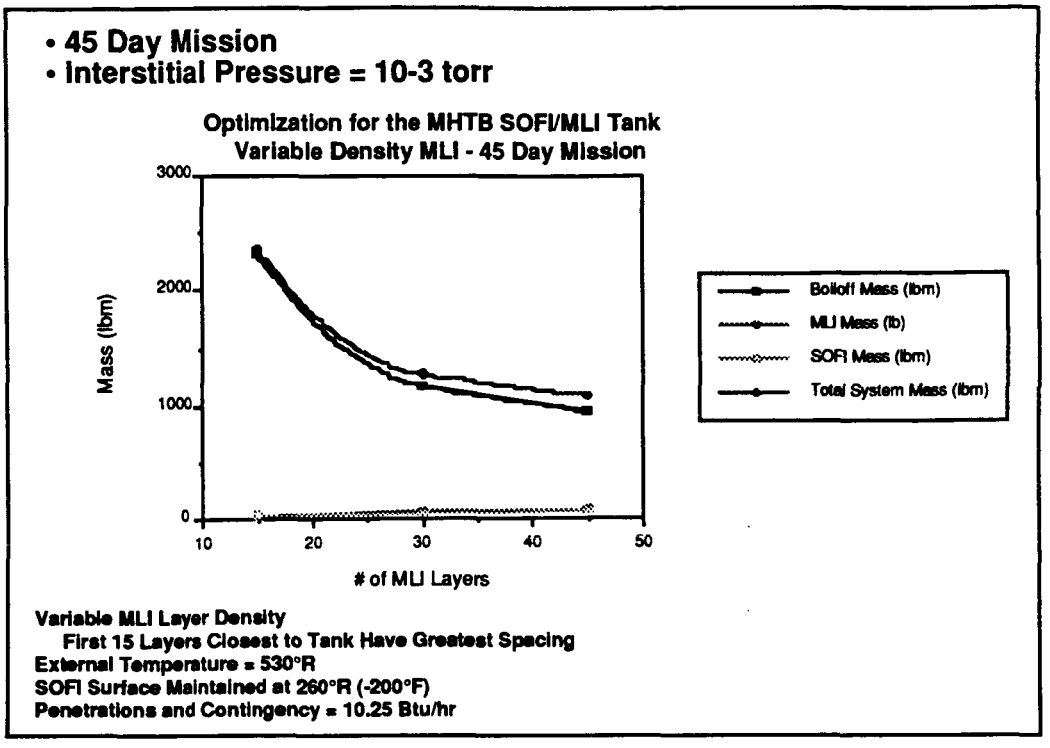

Figure 3.2.2-7 SOFI/MLI System Optimization - Variable MLI Density

3.2.3 MLI Sensitivity Analysis

The recommended variable density approach improves the overall system performance by reducing both the density and the thermal conductivity simultaneously. The density-thermal conductivity graph which was presented in Section 2.0 represents previously tested systems. Details regarding the variable density concept and sensitivity analyses are presented in this section. The average density for the variable density concept is lower than a constant density configuration because replacement of a complete layer of Dacron net with bumper strips reduces the surface area for that layer by 90%. This technique also reduces solid conduction, thereby reducing the thermal conductivity of the system while maintaining the overall robustness of the MLI layup. Table 3.2.3-1 provides the predicted values for the various MLI systems considered for the MHTB program. The predicted ρk values include the density of the DAM, Dacron net, bumper strips, and SOFI. The variable density MLI predicted values range from 2.5 to 2.9 x 10^{-5} Btu-lb/hr-ft^4-°R. These predicted values are at least two times better than for previously tested programs (with the exception of the MHTB constant density stacking).

Table 3.2.3-1 Density-Thermal Conductivity Values for SOFI/MLI Systems

MLI System	rho-k (x 10^5) (Btu-lb/hr-ft^4-R)
45 Layers	
Constant Density	9.72
Variable Density	2.94
3 Bumpers	3.64
6 Bumpers	3.04
10 Bumpers	2.81
30 Layers	
Variable Density	2.80
3 Bumpers	3.49
6 Bumpers	2.95
10 Bumpers	2.76
15 Layers	
Variable Density	2.56
3 Bumpers	3.36
6 Bumpers	3.32
10 Bumpers	3.60

The concept of variable density was introduced at the MHTB TCS Preliminary Design Review (PDR). Dr. McIntosh initially proposed a system which consists of a total of 45 layers of DAM separated by a layer of B4A Dacron net and various number of bumper strips layers. This concept applies 5 bumper strips between each DAM layer for the first ten layer closest to the tank, then 3 bumper strips between each DAM layer for the next 15 layers and finally 2 bumper strips between each DAM layer for the remaining 20 layers (see Figure 3.2.3-1). This concept basically breaks down the MLI blanket into three distinct sections. The section closest to the tank provides the greatest spacing between DAM layers since reduction of solid conduction is most important here. This section has 10 DAM layers, each one separated by 5-layer Dacron net bumper strips and one continuous Dacron net layer. The next section has 15 DAM layers, each one separated by 3-layer Dacron net bumper strips and one continuous Dacron net layer. This section provides greater radiation heat transfer protection while still maintaining a small solid conduction heat transfer path. The last section in the MLI blanket applies 20 DAM layers, each one separated by 2-layer Dacron net bumper strips and one continuous Dacron net layer. This section provides the greatest radiation heat transfer barrier and still keeps the solid conduction heat transfer component low. Further sensitivities have been completed to prove the validity of using this concept or selecting a preferred concept based upon the sensitivities.

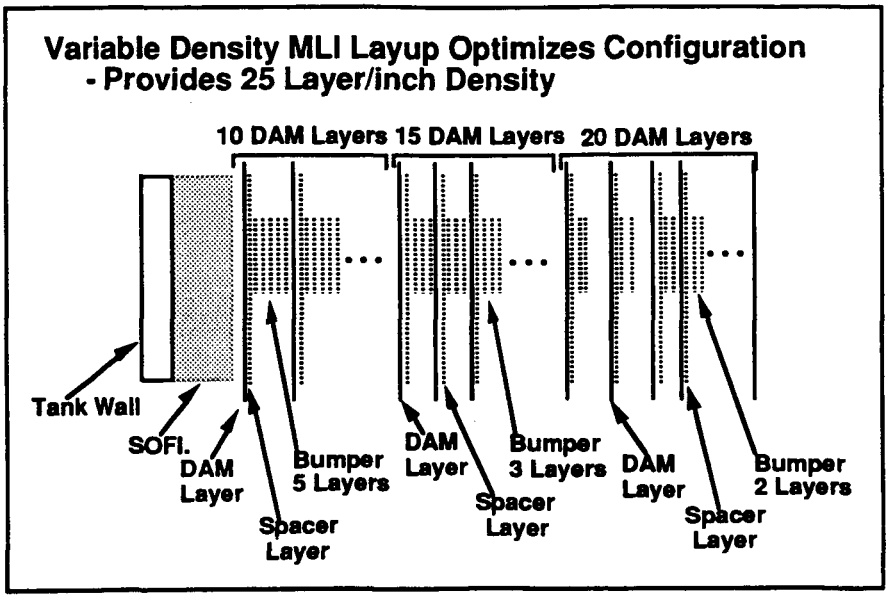

Figure 3.2.3-1 Recommended MLI Thickness and Layer Configuration

3.2.3.1 Sensitivity to the Number of Bumper Strips

The first sensitivity performed examined the number of bumper strips between the DAM layers. Every layer of DAM is separated by a complete sheet of B4A Dacron net and a given number of bumper strips. This sensitivity looked at putting the same number of bumper strips throughout the entire MLI blanket instead of the variable density layup to concentrate on the issue of number of bumper strips. The use of bumper strips in the MLI blanket can reduce the density for a 45 layer system from 75 layers/in. to nearly 20 layers/in. depending on the number of bumper strips installed. Figure 3.2.3-2 shows the sensitivity of the heat flux to the number of bumper strips placed throughout the entire MLI layup for a 45-layer system and a 30-layer system. The heat flux is reduced considerably by placing more bumper strips between the reflective material. The bumper strips essentially reduce the solid conduction through the MLI, so a relatively linear relationship is seen from 3 to 7 bumper strips. The addition of more bumper strips beyond approximately 7 layers has a decreased rate of return because the radiation component of the heat flux is now overwhelming the results. Therefore, placing approximately 6 or 7 bumper strips between the DAM is an effective usage of bumper strips.

To determine the appropriate number of bumper strips to apply between the various DAM layers, other limiting factors in the design like manufacturing constraints, mass and/or thickness must be evaluated. The manufacturing concern is maintaining the bumper strips height over the entire tank surface and not allowing the bumper strips to slide apart especially under launch g loads

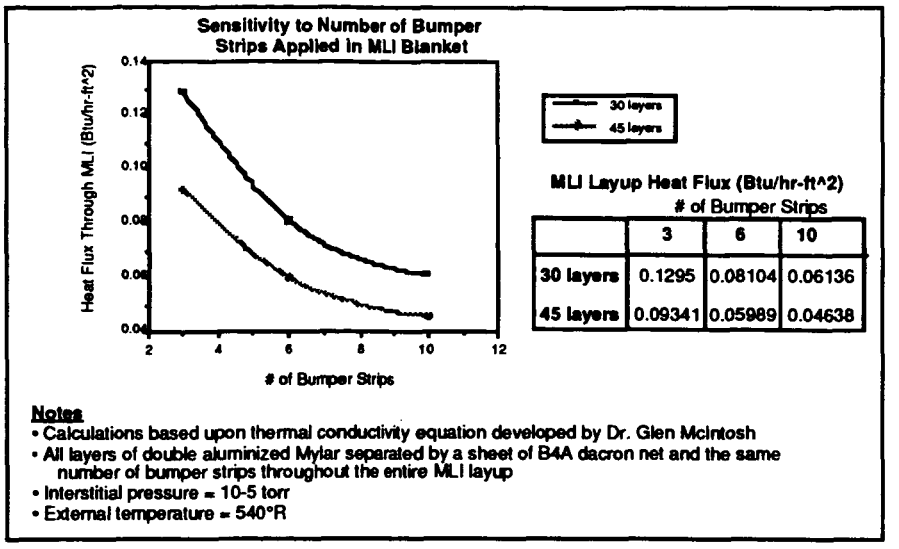

Figure 3.2.3-2 Sensitivity to Number of Bumper Strips

and vibration. Liquid helium dewars have been constructed which use 3 strips of thick glasspaper (8 mil) bumper strips between layers of 3 mil glasspaper and aluminum. This concept has proven successful for many over-the-road dewars which must operate reliably under rigorous g loads. The difference with the MHTB program is that Dacron net will be used in place of glasspaper. Dacron net has less contact friction than the glasspaper and may require some tacking to maintain the appropriate configuration. It is recommended that 5 to 6 bumper strips be used close to the tank wall and then reduce this number for the remaining layers of MLI to increase the robustness of the design.

3.2.3.2 Variable Density Sensitivity

The next sensitivity performed required varying the number of bumper strips throughout the MLI blanket system to produce the variable density layup as discussed in preceding paragraphs. Figure 3.2.3-3 shows the sensitivity to varying the number of bumper strips in different sections of the MLI blanket. The 30 layer system was evaluated because this was the recommended baseline from TCS Critical Design Review (CDR). The number of bumper strips in the first 10 cold layers was varied from 4 to 6 while the remaining blanket was held constant at 20 layers with 3 bumper strips and 5 layers with 2 bumper strips. The next graph to the right shows the number of bumper strips in the middle 20 layers being varied for 2 to 4 while the remaining blanket was held constant at 5 bumper strips in the 10 cold layers and 2 bumper strips in the last 5 warm layers. The last graph shows the sensitivity to varying the warm layer bumper strips from 1 to 3 while maintaining 5 bumper strips in the 10 cold layers and 3 bumper strips in the middle layers. This figure graphically illustrates how sensitive the cold layers are to changes in bumper

strip layers. Since the largest temperature gradient is observed in these layers, increasing the number of bumper strips in the cold layers dramatically improves the MLI performance. As the layers get warmer, applying more bumper strips has a less noticeable effect on the MLI

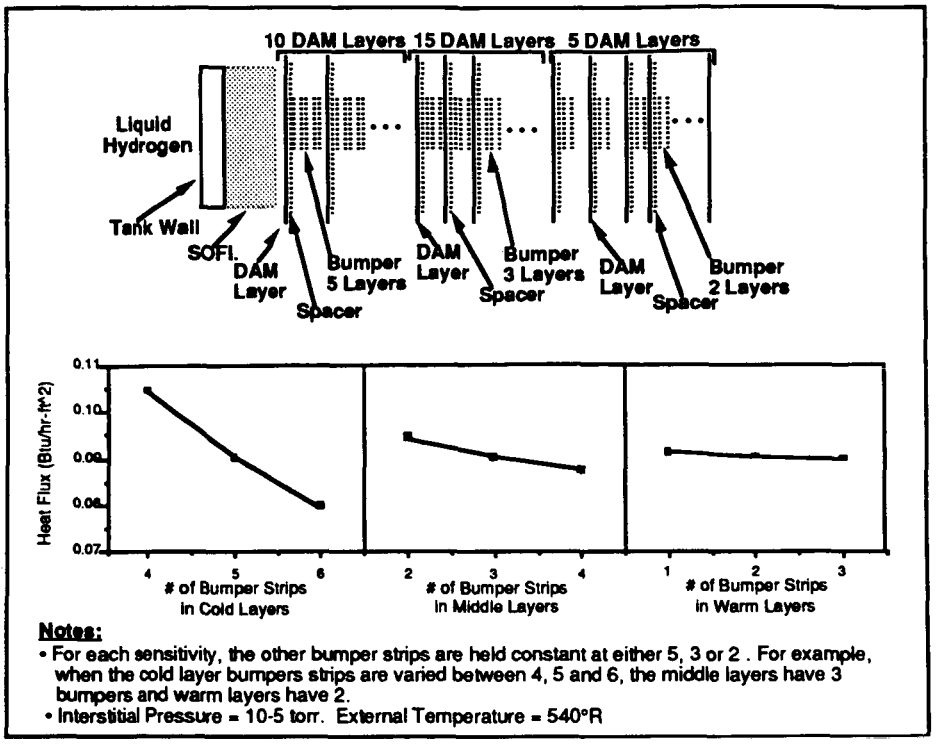

Figure 3.2.3-3 Sensitivity to Bumper Strips Placement in 30-Layer Variable Density

performance. Therefore, the variable density layup proposed at TCS CDR (5,3,2 bumper strips) provides good MLI performance and is a robust design for manufacturing.

3.2.3.3 Sensitivity to the Number of DAM Layers

Another sensitivity examined variable spacing limits within the DAM layers for a 30-layer variable density MLI blanket. The 30-layer variable density is the selected baseline and consists of three sections within the blanket. The cold section (next to the tank) is composed of 10 DAM layers with 5-layer bumper strips per each DAM layer, the middle section has 15 DAM layers with 3-layer bumper strips per DAM layer, and the warm section has 5 DAM layers with 2-layer bumper strips per DAM layer. This sensitivity evaluated the effect of moving two DAM layers into or out of each section to determine the impact to the overall MLI heat leak (see Figure 3.2.3-4). The number of DAM layers was held constant at thirty. Moving two layers into the cold section requires moving two layer from either the middle section or the warm section. Therefore, there are two lines on the graph - the solid line moves layers to a position near the cold section and the upper

dotted line moves the layers out to the warm section. The baseline MLI layup is also plotted for comparison.

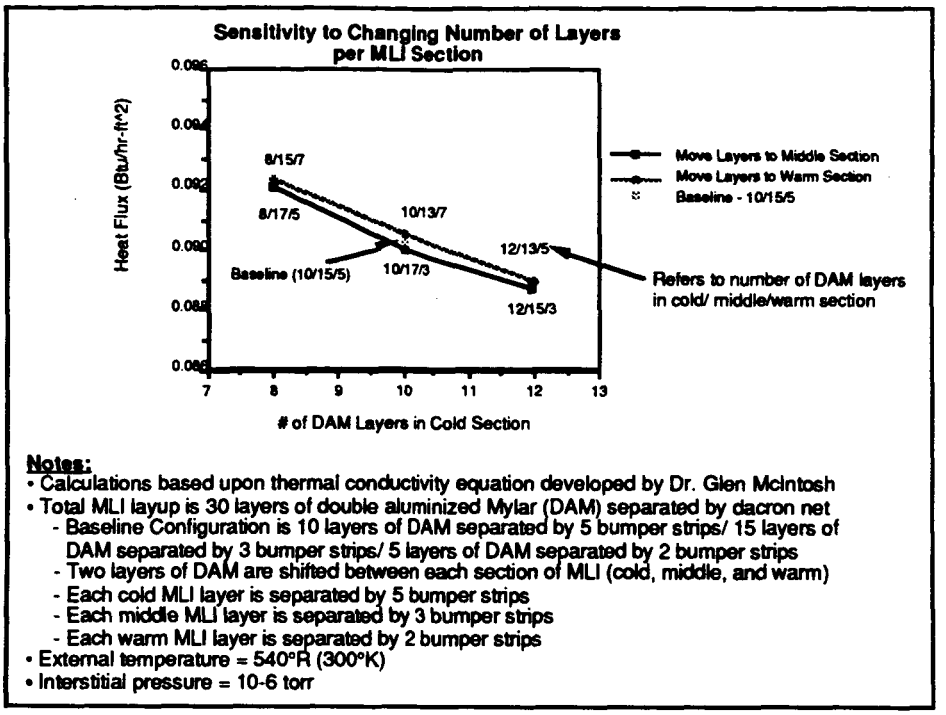

Notes:
- Calculations based upon thermal conductivity equation developed by Dr. Glen McIntosh
- Total MLI layup is 30 layers of double aluminized Mylar (DAM) separated by dacron net
  - Baseline Configuration is 10 layers of DAM separated by 5 bumper strips/ 15 layers of DAM separated by 3 bumper strips/ 5 layers of DAM separated by 2 bumper strips
  - Two layers of DAM are shifted between each section of MLI (cold, middle, and warm)
  - Each cold MLI layer is separated by 5 bumper strips
  - Each middle MLI layer is separated by 3 bumper strips
  - Each warm MLI layer is separated by 2 bumper strips
- External temperature = 540°R (300°K)
- Interstitial pressure = 10-6 torr

Figure 3.2.3-4 Sensitivity to DAM Layer Placement in 30-Layer Variable Density

The graph illustrates that the heat flux decreases with the addition of more DAM layers in the cold section. Adding two layers to the cold section decreases the heat flux by approximately 2%. Basically, this addition of DAM layers reduces the solid conduction between large temperature gradient layers. Conversely, moving the layers into the warm section reduces their effectiveness and also reduces the overall number of bumper strips used throughout the blanket. There are no dramatic differences in all these configurations illustrated on the graph (less than 2% between any two adjacent points). Thus, the results indicate the sensitivity to the number of bumper strips between layers is overshadowed by variation in the overall number of bumper strips.

The best performing MLI layup applies the most number of bumper strips throughout the entire layup. The reason for using the variable density layup is to improve the robustness (ease of manufacturing and handling) of the MLI. Basically, the bumper strips are not as effective as the DAM layers get warmer, therefore, the number of bumper strips can be reduced as DAM is applied to the tank. Using variable density MLI layup results in a heat flux of 0.090 Btu/hr-ft^2, while placing five bumper strips throughout the entire MLI layup results in a heat flux of 0.087 Btu/hr-ft^2 (at 10^{-6} torr interstitial pressure). This 3% difference in performance may be at the expense of the entire MLI layup since any damaged areas will produce heat leak that are magnitudes higher.

3.2.3.4 Mass and Thickness Sensitivity

The sensitivity to mass increases due to the addition of bumper strips is the next issue. The mass of the bumper strips is relatively small compared to the overall insulation mass. Table 3.2.3-2 illustrates the MLI mass sensitivity for different number of layers and bumper strips for the MHTB tank which has a surface area of 35 m^2 (374 ft^2). Masses shown are for the total MLI system, assuming the number of bumper strips shown is applied to all layers.

Table 3.2.3-2 Mass Sensitivity of MLI Systems (kg)

# of DAM Layers	# of Bumper Strips 3	6	10
15	10.62	11.49	12.65
30	21.25	22.98	25.30
45	31.87	34.47	37.95

The addition of a bumper strip layer increases the MLI mass on the MHTB tank by 3% which is not a significant driver for a few number of bumper strips. An additional factor which affects handling is the overall thickness of the MLI blanket using a different number of bumper strips. The thickness for various MLI configurations is shown in Table 3.2.3-3. The addition of bumper strips increases the MLI thickness, yet only the 10 layers system drives the thickness much beyond 2 inches. Therefore, the variations in mass and thickness due to bumper strips exhibit only a minor influence in the selection of the preferred MLI system. Again, the number of bumper strips shown is assumed to be applied to all layers of the MLI system.

Table 3.2.3-3 Thickness Sensitivity of MLI Systems (in.)

Configuration	# of Bumper Strips 3	6	10
15 layers	0.39	0.69	1.08
30 layers	0.79	1.37	2.15
45 layers	1.18	2.06	3.23

All the previous sensitivities have been based upon an interstitial pressure of 10^{-5} torr within the MLI blanket. This pressure level assumes good evacuation of the blanket to reduce the heat flux due to gas conduction. The gas conduction heat flux is dependent upon the interstitial pressure and will increase dramatically with an increase in interstitial pressure. Figure 3.2.3-5 illustrates the sensitivity to interstitial pressure. The graph shows the impact to the variable density system and the constant density system as the interstitial pressure is changed. The variable density

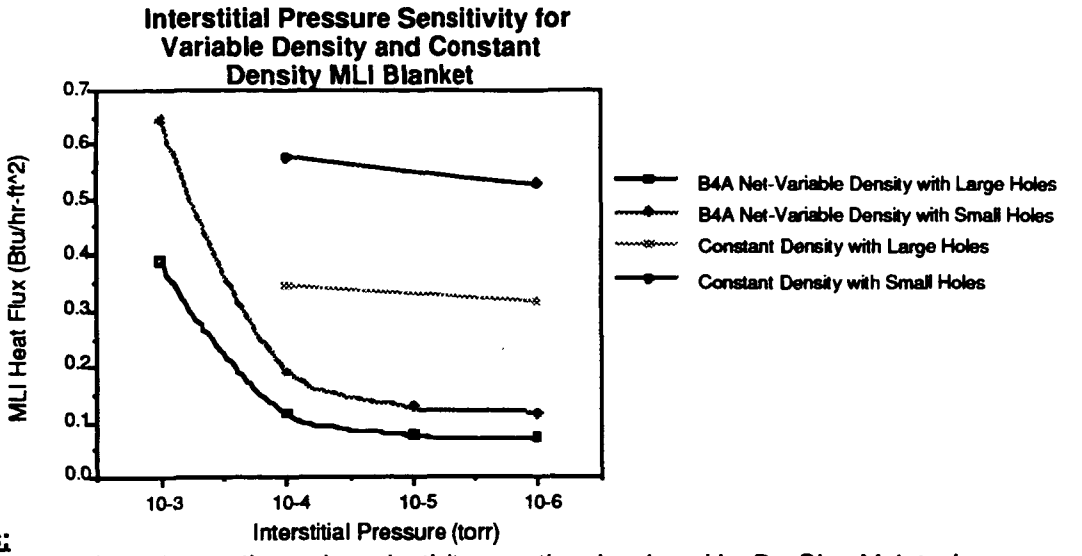

Notes:

- Calculations based upon thermal conductivity equation developed by Dr. Glen McIntosh
- 45 layers of double aluminized Mylar (DAM) separated by dacron net
- Variable density consists of 10 DAM layers separated by 5 bumper strips, next 15 DAM layers separated by 3 bumper strips and next 20 DAM layers separated by 2 bumper strips
- Constant density is all DAM layers separated by 2 layers of B4A dacron net
- Interstitial pressure refers to pressure within the MLI layers
- External temperature = 540°R (300°K)
- Small holes refers to standard perforation pattern developed by Sheldahl
  - 0.030 in. holes on 0.25 in. centers for 1.1% open area (67% increase in heat flux)
- Large holes are 0.50 in. holes for 1% open area

Figure 3.2.3-5 Sensitivity to Pressure Level

predicted performance for both small hole perforation pattern and large hole perforation pattern is also shown on the graph. Basically, the small hole perforation pattern will increase the heat flux by approximately 67% over a large hole perforation pattern. This same increase can be seen for the constant density small hole perforation pattern. The high interstitial pressure (10^{-3} torr) values were not calculated for the constant density case, but similar trends are expected. The performance of any system is not changed dramatically below 10^{-4} torr, but above this level the gas conduction plays a large role in the heat flux. Therefore, it is important to evacuate the blanket as rapidly as possible to achieve a 10^{-4} torr level, and the use of a large hole perforation pattern improves the performance of the MLI system at a given pressure. The remaining question is whether or not venting with large holes is comparable to that with small holes.

3.2.3.5 Dacron Net Sensitivity

A final sensitivity was performed to compare the use of B4A Dacron net to B2A Dacron net in the event that B4A net was not available. The B2A net has twice the mass of the B4A net due to

its tighter weave and its effect on the thermal performance is shown in Figure 3.2.3-6. The heat flux is increased by nearly 50% when using B2A net instead of the B4A net. This decrease in performance can be directly attributed to the increased solid conduction of the heavier net.

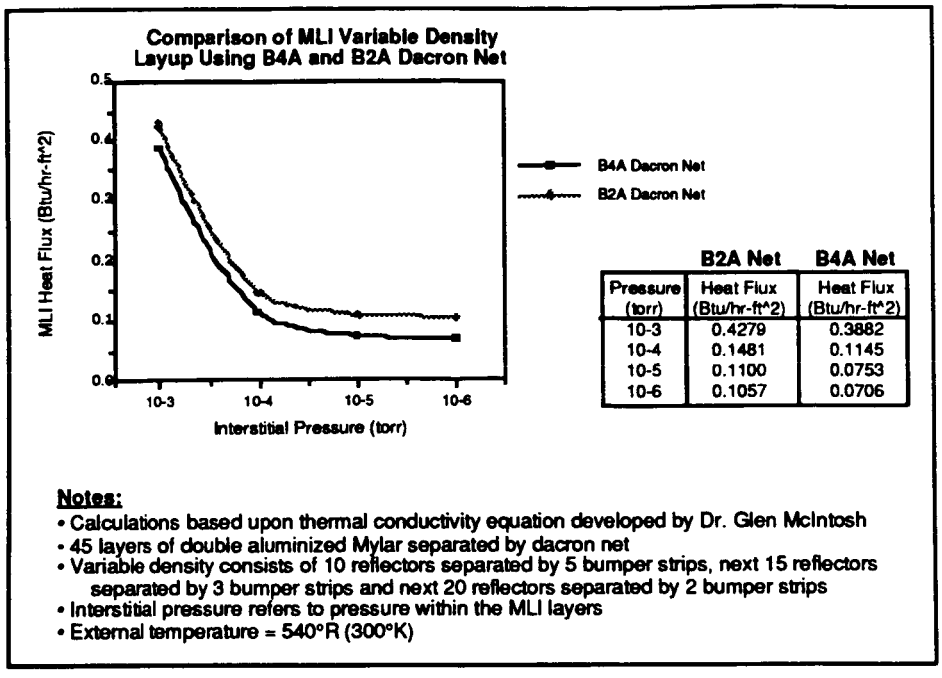

Pressure (torr)	B2A Net Heat Flux (Btu/hr-ft^2)	B4A Net Heat Flux (Btu/hr-ft^2)
10-3	0.4279	0.3882
10-4	0.1481	0.1145
10-5	0.1100	0.0753
10-6	0.1057	0.0706

Notes:
- Calculations based upon thermal conductivity equation developed by Dr. Glen McIntosh
- 45 layers of double aluminized Mylar separated by dacron net
- Variable density consists of 10 reflectors separated by 5 bumper strips, next 15 reflectors separated by 3 bumper strips and next 20 reflectors separated by 2 bumper strips
- Interstitial pressure refers to pressure within the MLI layers
- External temperature = 540°R (300°K)

Figure 3.2.3-6 Comparison of Dacron Net (B2A to B4A)

3.2.4 MLI Perforation and Percent Open Area

3.2.4.1 Rapid Ascent

Perforations in the DAM have historically been included in the design to enhance the outgassing of trapped gases. Perforating the DAM allows the trapped gases to escape through the MLI in a direction normal to the layers. In the event the DAM is not perforated, the trapped gases must migrate to the edges and seams to escape. For the MHTB application, the roll wrap process will produce a long tortuous path through which the molecules must escape . The side seams will also be overlapped which could inhibit the venting of any trapped gases. Therefore, the percent open area of the DAM can influence the venting rate. A calculation of the MLI delta pressure for 1% open area and a current Shuttle pressure profile was completed. The purpose of this calculation is to determine the impact of the pressure change on the MLI blanket and whether structural damage will occur. The pressure profile selected for analysis was the Shuttle cargo bay launch pressure history shown in Figure 3.2.4-1. This pressure profile is similar to the Titan pressure profile and has a more severe pressure change during the first 100 sec than the Saturn V vehicle. The delta pressure through the Mylar is plotted against the launch ascent time in Figure 3.2.4-2. The graph also shows the Shuttle pressure profile for comparison to the Mylar pressure

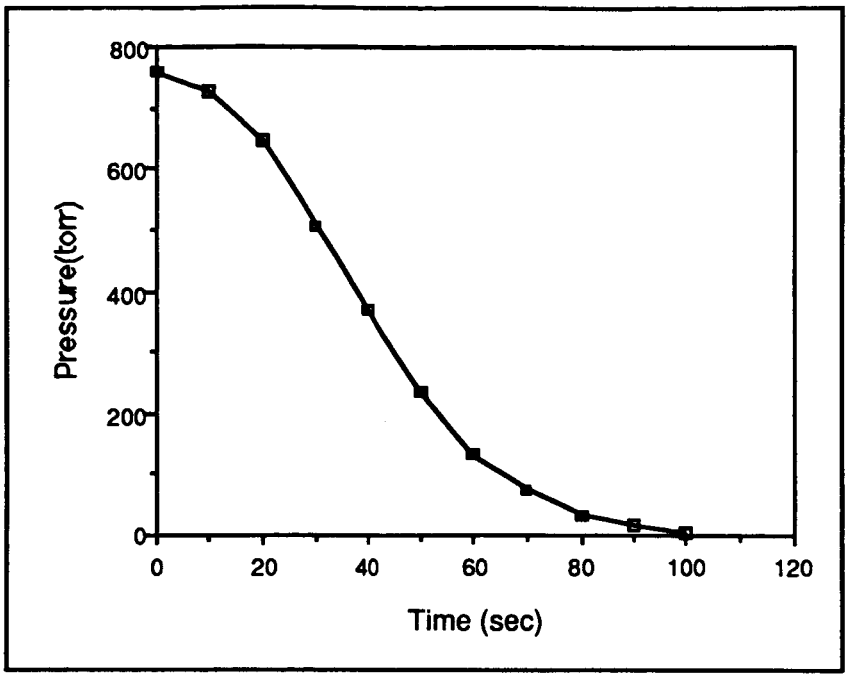

Figure 3.2.4-1 STS Cargo Bay Launch Pressure History

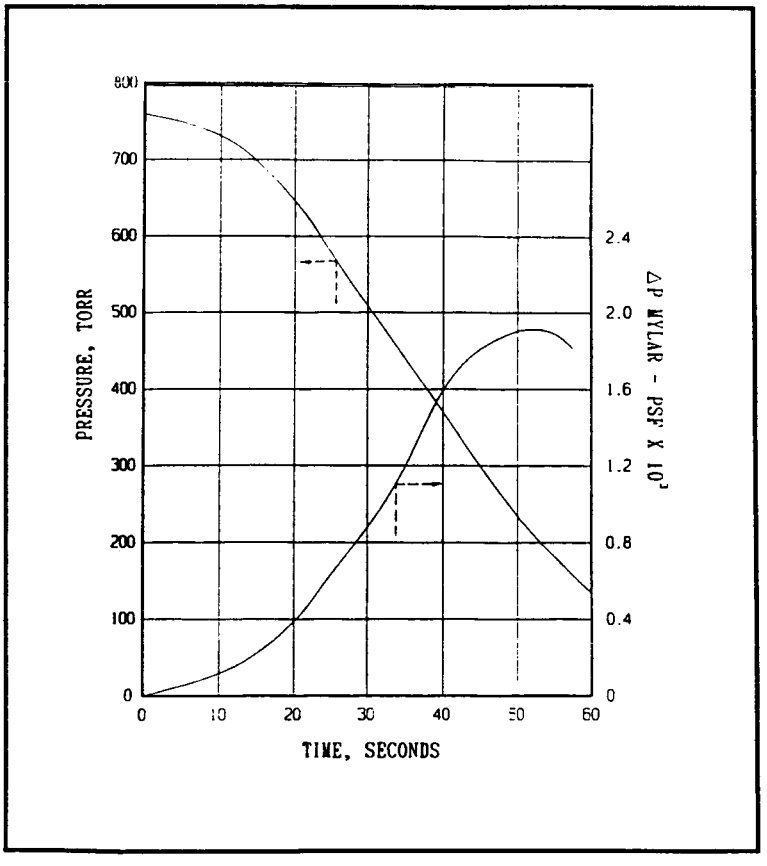

Figure 3.2.4-2 Calculated MLI Differential Pressure

differential. The maximum pressure differential is calculated to be less than 2.0 x 10^{-3} psf. However, sample MLI testing conducted at Lewis Research Center indicated orders of magnitude higher than predicted delta pressure with the large holes. The tests compared the MLI venting ability of a large hole 1 % open area MLI sample, a 2% open area large hole MLI sample, and a small hole 2% open area MLI sample.

Except for venting, the preferred configuration from a thermal consideration is no perforations at all. Yet, there is a physical requirement for venting during ascent and the first few hours on-orbit. Venting must be allowed during this period to prevent damage to the MLI system from differential pressure, and to achieve a good vacuum level within the MLI blanket to reduce the heat transfer. A typical large hole perforation pattern is shown in Figure 3.2.4-3 for 1% open area.

Preliminary results of the tests performed by LeRC on the MLI blanket indicate that the 1% large hole blanket did not vent as fast as predicted. The 2% large hole, however, vented adequately, and was selected as the baseline for the MHTB. The 2% hole pattern used for the LeRC test utilized the same holes shown above in Figure 3.2.4-3, with additional holes added as necessary to achieve 2%. The pattern used for the MHTB DAM is the same pattern as in Figure 3.2.4-3, with revised spacing to achieve 2%. This should provide marginally better venting performance, and more predictable radiation performance. Preliminary performance of the three blanket configurations is shown in Figure 3.2.4-4.

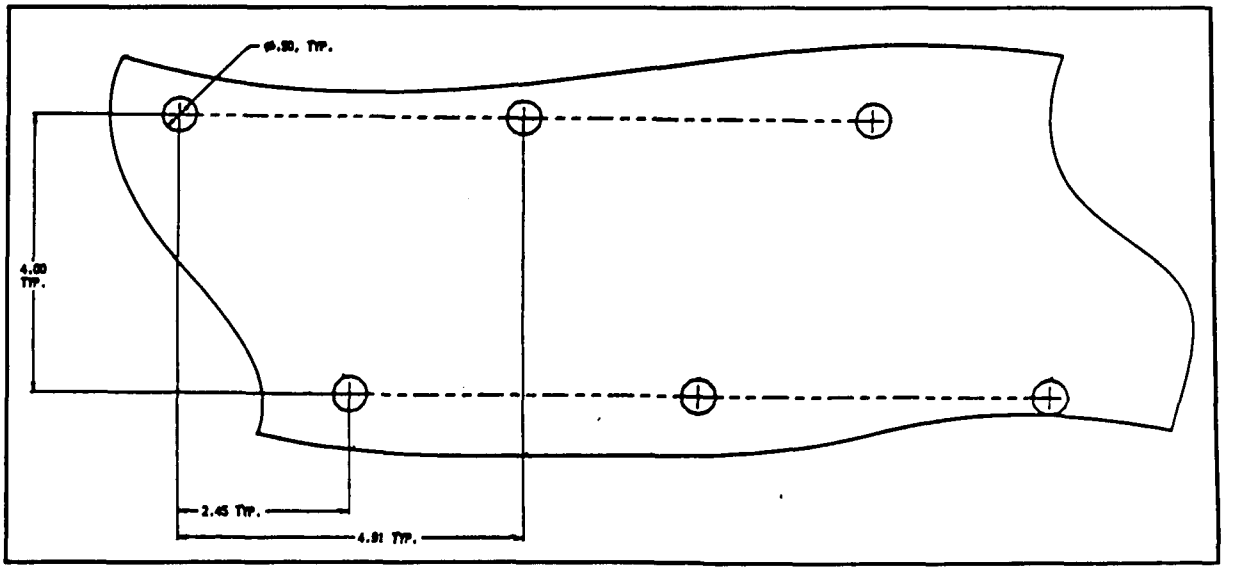

Figure 3.2.4-3 Typical DAM 1% Open Perforation Pattern

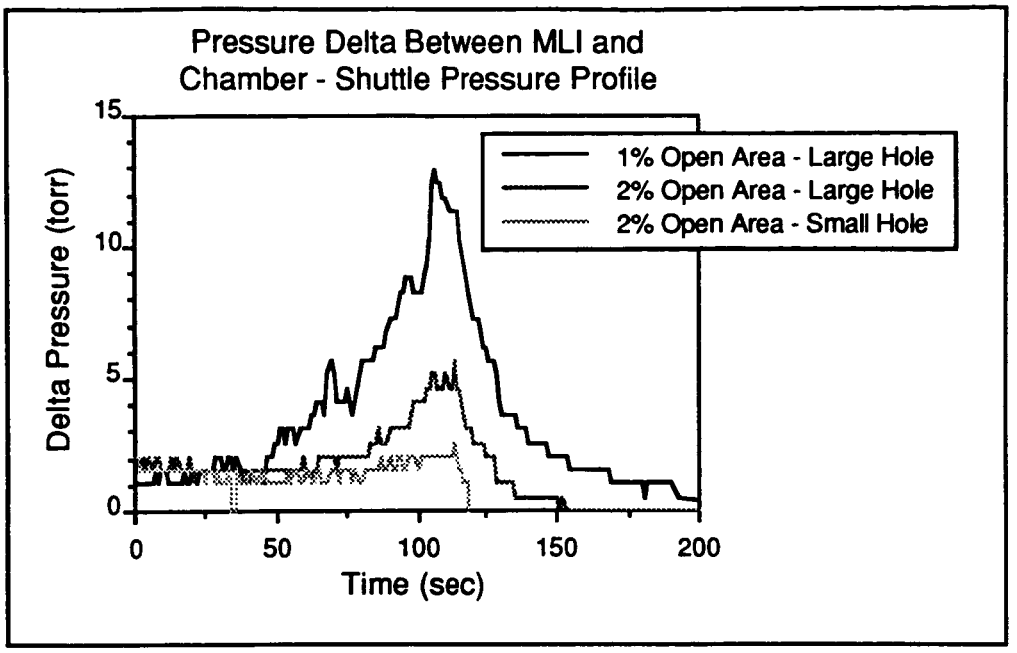

Figure 3.2.4-4 DAM Hole Size Performance - LeRC Test Data

3.2.4.2 Water Diffusion During Ground Hold (Small Hole Only)

A further concern is to assess the impact on the mean free path through the MLI for venting with many small holes in comparison to several large holes for 1% open area. The purpose of this calculation was to determine the purge time necessary to diffuse trapped water vapor from the MLI blanket during ground operations and the on-orbit diffusion of trapped gases/sublimating solids. An analysis has been completed to assess the ground hold outgassing capability of an MLI configuration using different purge gas temperatures (see Appendix B). This analysis was presented at the TCS PDR showing that the MLI will release trapped water vapor in a reasonable time period. This calculation was based on rate of diffusion and a mean free path length of 25 inches within the MLI layers. Figure 3.2.4-5 shows the water vapor concentration as a function of purge time. The vapor concentration will approach 10^{-6} lb/ft^3 after approximately 700 minutes (12 hours) of purging. Therefore, the MHTB tank should be purged for approximately 12 hours using a relatively warm (580°R) nitrogen purge to reduce the water concentration level in the blankets. The hole size was not a strong driver in this analysis since the mean free path is only slightly effected by hole size. The perforation pattern is a much bigger driver, but the worst case perforation pattern was assumed since a 25 inch mean free path was used for this analysis.

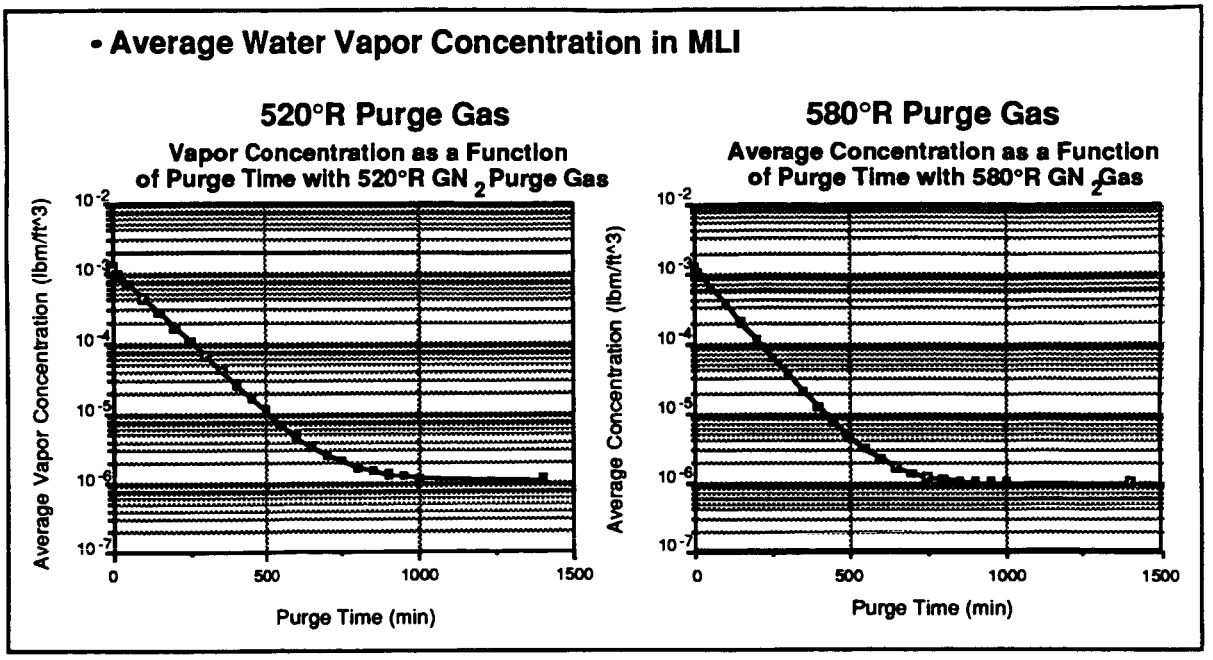

Figure 3.2.4-5 Water Vapor Removal from MLI

3.2.4.3 Perforation Effect on Heat Flux

Another concern is the effect of hole size and perforation pattern on venting of trapped gases on-orbit. When considering thermal effects on the MLI due to perforations, the Lockheed investigation shows that any perforations increase the heat leak through the MLI system due to radiation tunneling. Further evaluation showed that many small holes for perforation create a greater heat leak than a few large holes (see Reference 1, page 4-44). Figure 3.2.4-6 illustrates the impact to thermal performance due to changes in perforation hole size (Reference 2). The small holes increase the heat flux up to 38% for a 1% open area perforation pattern and can be explained by looking at the radiation phenomenon from small holes (Reference 3). The radiation heat transfer is negligible until the angle with the surface is at least 10°, even from very high emissivity surfaces. For a reflector spacing of about 1 mm (1/2 mm may be closer on the average), Figure 3.2.4-7 shows the physical characteristics of radiation heat transfer from a point source.

For a 1 mm gap, the effective radiation radius (R) is 5.67 mm. A 1 mm diameter black hole effectively radiates to an area of 120 mm^2 while a 1/2 inch hole radiates to an area of 454 mm^2 which is 3.8 times larger than the 1 mm diameter black hole. But the 1/2 inch hole area is 161 times larger than the 1 mm hole. For the same total orifice area, the small holes have a radiation area which is about 42.5 times larger. For 1/2 mm spacing between reflectors, the ratio of hole area to radiation area is 21.2. This is not the whole story because the separator material will block much of the low angle radiation, but it does illustrate that many small holes can have a larger radiation impact than a few greater diameter holes.

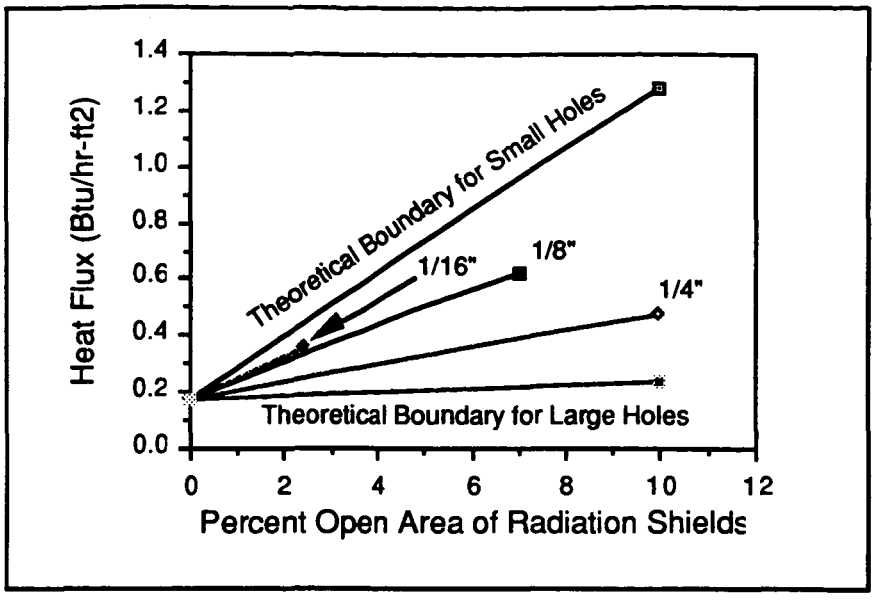

Figure 3.2.4-6 MLI Perforation Hole Size vs. Heat Flux

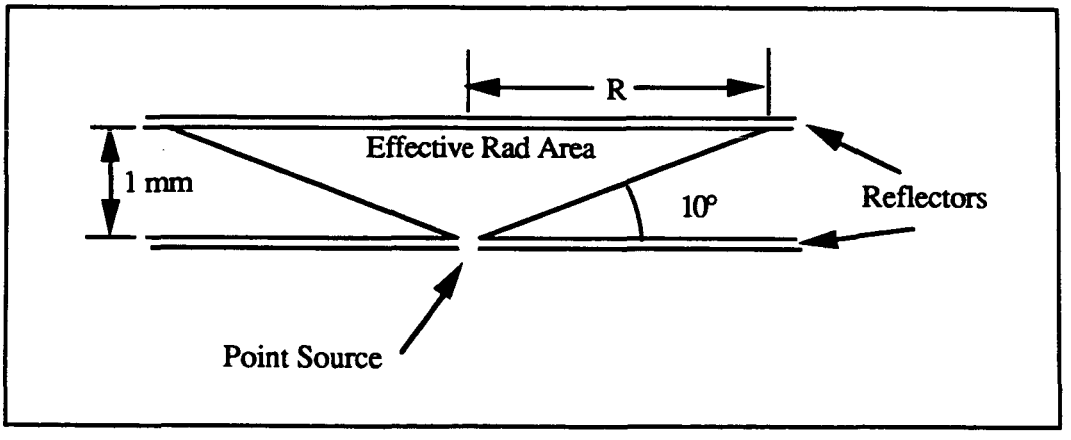

Figure 3.2.4-7 Radiation Point Source Heat Transfer

3.3 Instrumentation

The instrumentation described here was the baseline at CDR, and any updates or changes made during the actual installation at MSFC are not available to present in this report. Instrumentation consists primarily of temperature and liquid level sensing, which is used in conjunction with tank pressure to describe the state of the contents. Temperature sensors are placed on the tank wall, throughout the insulation, and on the tank penetrations. Silicon diodes are used on the tank and SOFI surface to increase the accuracy of those measurements. Thermocouples are used in the MLI to minimize disruption of the insulation and are used on the heater shroud for control sensors. A typical instrumentation profile through the MLI blanket is

shown in Figure 3.3-1. Silicon diodes are placed on the tank wall as indicated in Figure 3.3-2 to provide an understanding of thermal stratification on the tank wall as the liquid level drops. Silicon diodes are placed on the SOFI surface in the profiles indicated in Figures 3.3-2 and 3.3-3. The thermocouples in the MLI blanket are placed over the SOFI silicon diode to predict the temperature gradient through all the insulation. The MLI thermocouples are integrated into the insulation during the roll wrap process.

In addition to the silicon diodes placed on the tank wall, silicon diodes are placed on several penetrations to understand the temperature profile along the penetration. Two diodes are placed on the manhole cover to estimate the temperature of the top of the cover which could be several hundred degrees warmer than the tank exposed to liquid. The fill and vent lines also have silicon diodes placed on them to understand the temperature gradient along the lines. The instrumentation port has several diodes on the surface to understand the temperature gradients on this large thermal mass. Two of the four low heat leak tank supports have several small diodes near the tank wall to estimate the temperature gradient and predict the heat leak from these supports.

A capacitance probe is installed in the tank to measure liquid level during testing. Two internal temperature rakes are installed with the primary rake being accessed through the instrumentation port. The secondary rake is installed through the Rockwell top flange and has spacing of silicon diodes along its length that is offset relative to the primary rake. These instruments will measure any possible thermal stratification in the tank during the pressure control

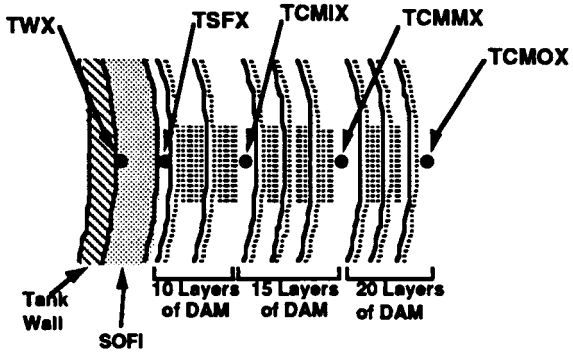

Instrumentation List

Location	Indicator	Type	Number
Tank Wall	TWX	Diode	6
SOFI	TSFX	Diode	6
MLI - Inner	TCMIX	*Thermocouple**	6
MLI - Middle	TCMMX	*Thermocouple**	6
MLI - Outer	TCMOX	Thermocouple	6

* Change From Original Instrumentation List
(Use 36 AWG Wire on Thermocouples)

Figure 3.3-1 TCS Instrumentation - Insulation Profiles

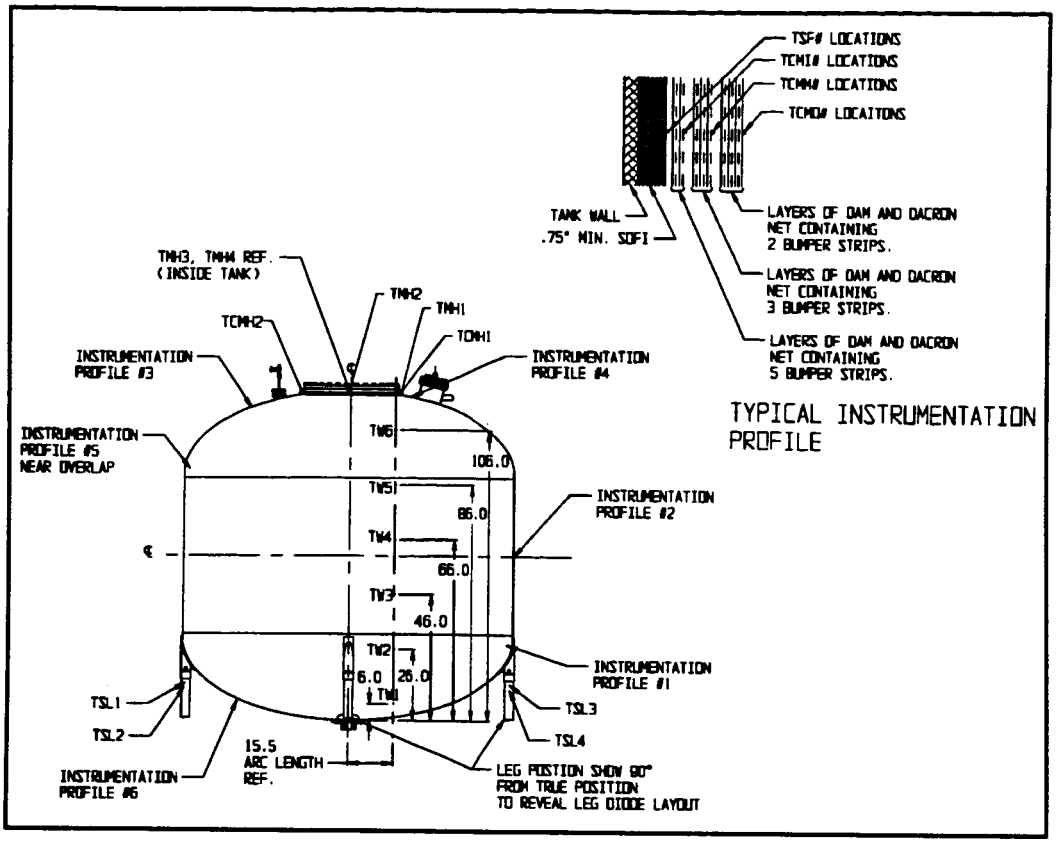

Figure 3.3-2 Instrumentation Planned at CDR

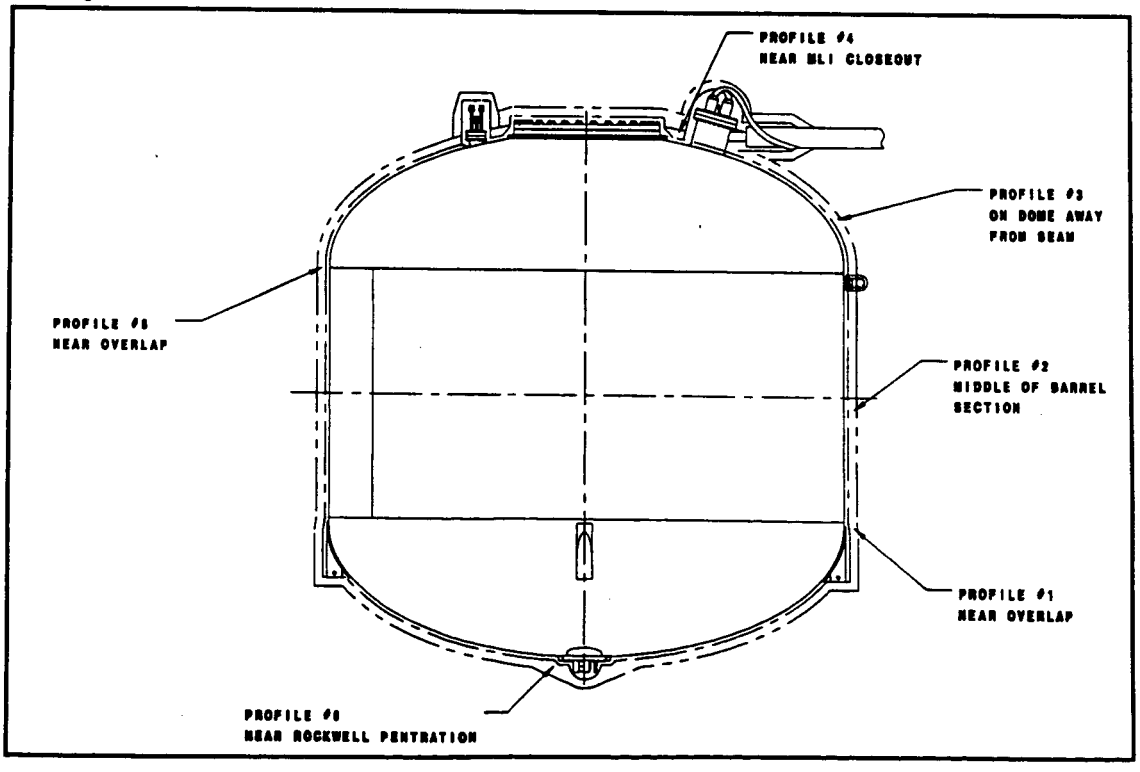

Figure 3.3-3 MLI Instrumentation Profile Locations Planned at CDR

testing. The external penetration instrumentation measures the temperature gradients to predict the heat leak through the penetrations.

4.0 MLI Application Plans at CDR

The application of the MLI insulation utilizes a commercial roll wrap technique to apply the layers of MLI as opposed to past techniques which involved manual fabrication of individual blankets. These individually constructed sections of the reflective and separator material were then installed on the tank by either sewing, tacking, grommeting or taping. These techniques ensure a well constructed blanket but require extensive hours for fabrication and installation. The other drawback of these techniques is the number of seams which allow radiation tunneling and conduction between adjacent layers of reflective material resulting in an increased heat flux into the tank. The alternative method which has been developed for this program uses a commercial roll wrap technique which has been used for Superconducting Super Collider liquid helium storage dewars. The reflective material and separator material are dispensed as continuous sheets onto the tank which eliminates the blanket seams and tunneling effects.

The MLI application tooling is a unique fixture to dispense DAM, Dacron net and bumper strips. Similar fixtures have been built and used for other commercial dewar insulation applications. The tooling plans described here are those planned prior to CDR, and were modified prior to and during implementation at MSFC. Figure 4-1 is an end view of the tank with application frames on each side for dispensing the DAM, Dacron net and bumper strips. The left side of the fixture holds the main Dacron net separator material dispenser which consists of two rolls of 54 inch wide material and a center roll of 18 inch wide Dacron net. Above these rolls are a series of dispensers for the bumper strips which are spaced every 24 inches along the tank. The bumper strips are applied between the layers of Dacron net sheet and DAM sheet which is dispensed from the other side. The DAM will be fed from a continuous 106 inch wide roll for the barrel section and a continuous 120 inch wide roll for the dome blankets. Figure 4-2 is the top view of the roll wrap tooling. It shows the main rolls for the Dacron net, the overlap roll of Dacron net and the bumper strips. The left side of the figure illustrates the process for the dome blankets. Five sets of bumper strips are applied on the dome blankets while only three sets are applied to the barrel section. The right side illustrates the view for the barrel section application process. To start the insulation process, the materials are rolled off the dispensing rolls and taped to the tank. When all layers have been secured and aligned, the tank is rotated at approximately one RPM at proper tension until the required number of layers have been applied. The fabrication of the dome blankets starts the roll wrap process. They must be rolled prior to rolling the barrel section because the dome blanket sections must be rolled on the head material winding fixture (see Figure 4-3) or rolled on the tank. The rolled dome blankets are cut from either the fixture or the

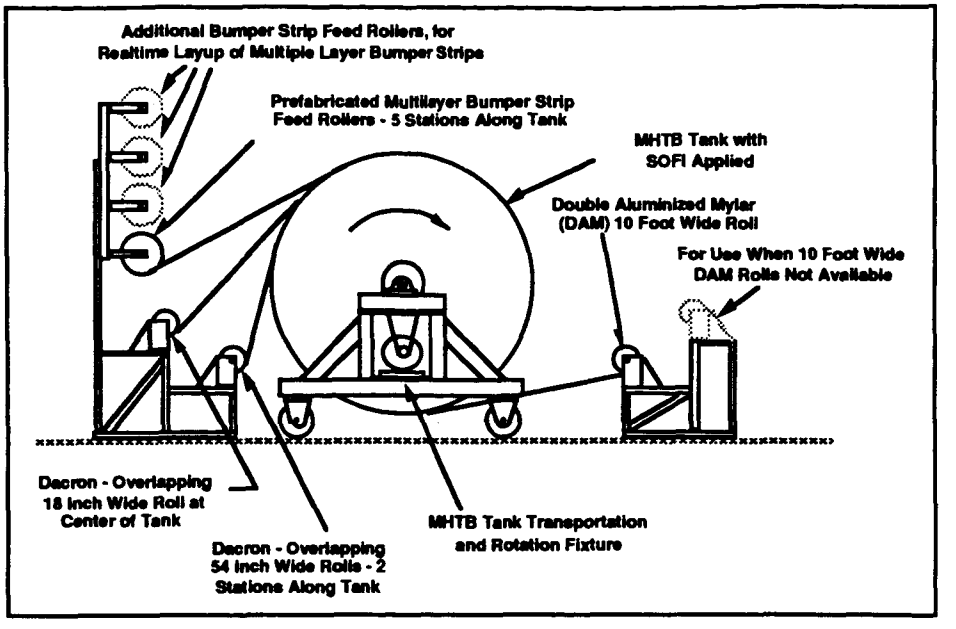

Figure 4-1 Roll Wrap Tooling, Front View - as Planned at CDR

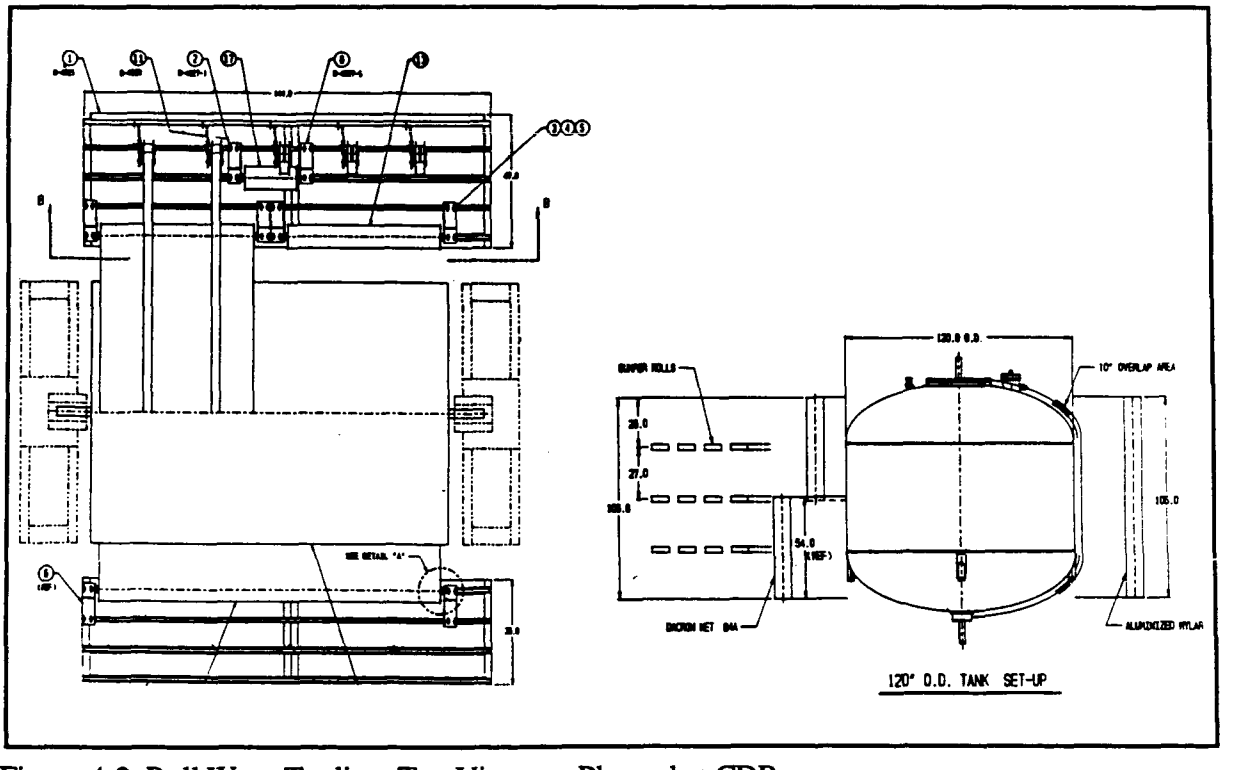

Figure 4-2 Roll Wrap Tooling, Top View - as Planned at CDR

tank and laid out on a working table. The dome blanket Mylar is a continuous 120 inch wide roll to make large enough circles to cover the domes. These circles are cut out from the blanket as well

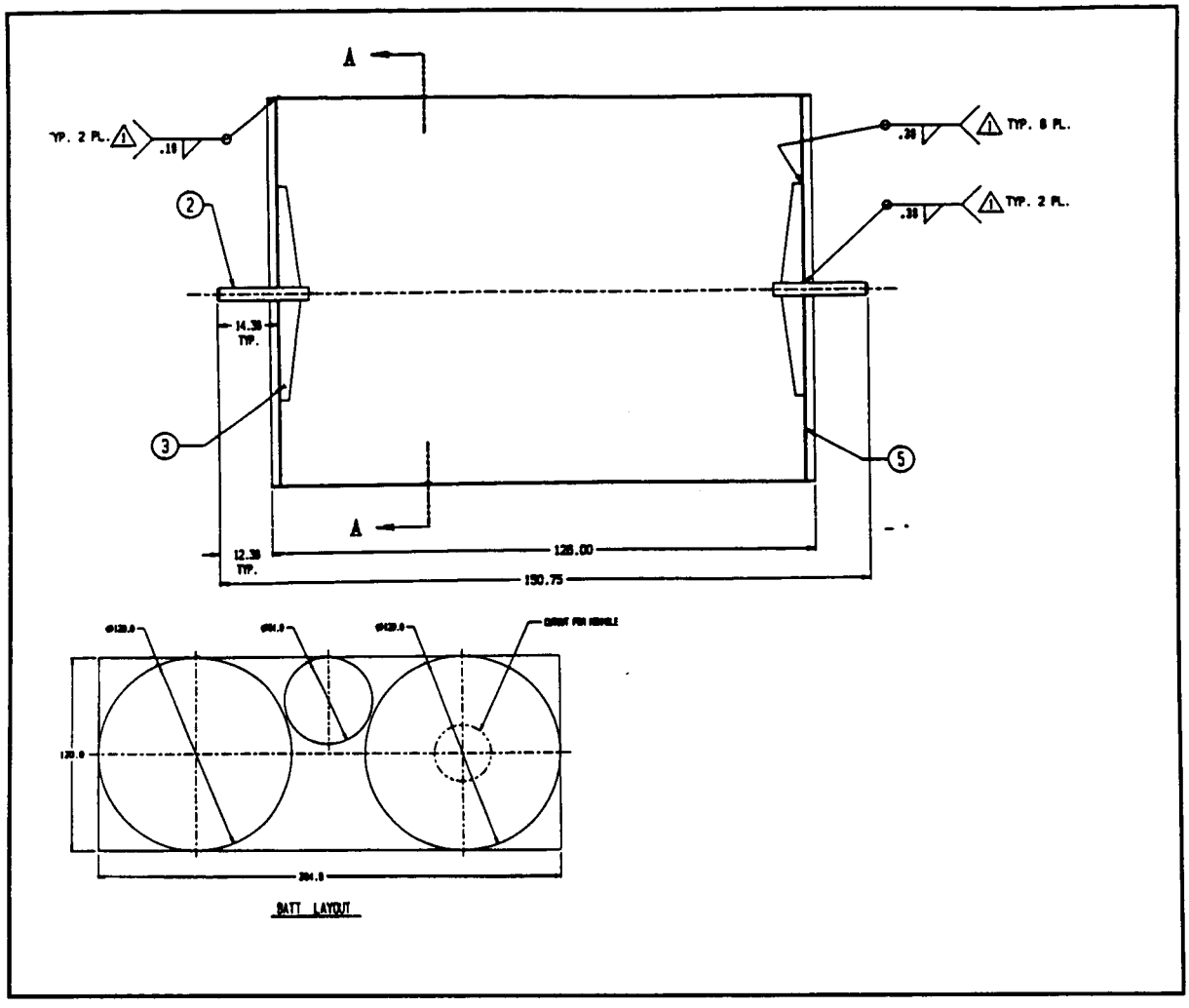

Figure 4-3 Head Material Winding Cylinder - as Planned at CDR

as the manhole cover blanket. The bumper strips within the dome blanket are rotated 90° every layer to create a lower density layup. Once the bumper strips have all been rotated, the penetration holes are cut out. Several penetration holes are required in the top dome blanket including the manhole, the instrumentation port, the fill line, the pressurization line, and the Rockwell hardware port. If a blind flange is used over the Rockwell hardware port, then a cutout is not be required for the initial insulation process. The penetration closeout procedures are discussed in Section 5.0. An alternative to use of either the head material winding fixture or the tank itself for creating the dome blankets is a manual layup accomplished on a horizontal table. This is somewhat more labor intensive, but eliminates the need to fabricate the head winding cylinder tool, and precludes potential damage to the SOFI or instrumentation, should the tank be used as a mandrel.

Once the penetration cutouts have been made, the blanket layers are ready to be applied to the tank either individually or as a complete layup using a dome head insulation fixture. This

fixture, as shown in Figure 4-4, basically allows all the dome blanket layers to be handled at one time during installation. The barrel section is now ready to be insulated. The MLI application fixture must be reconfigured to apply MLI to the barrel section. The insulation materials are rolled off the dispensing rolls and taped to the tank surface. Once the materials are aligned and secured, the motor driven application begins. The process is stopped periodically to apply instrumentation and changeout bumper strip rolls for the variable density layup. Once the barrel section is completed, the dome blankets are applied using the fixture. The individual layers are interleaved with the barrel section layers and taped in place. Aluminum tape is used to secure the layers at approximately one foot intervals around the circumference. The interleaving and taping continues until all the layers are secured. Instrumentation is applied intermittently within both the barrel section and dome blanket process.

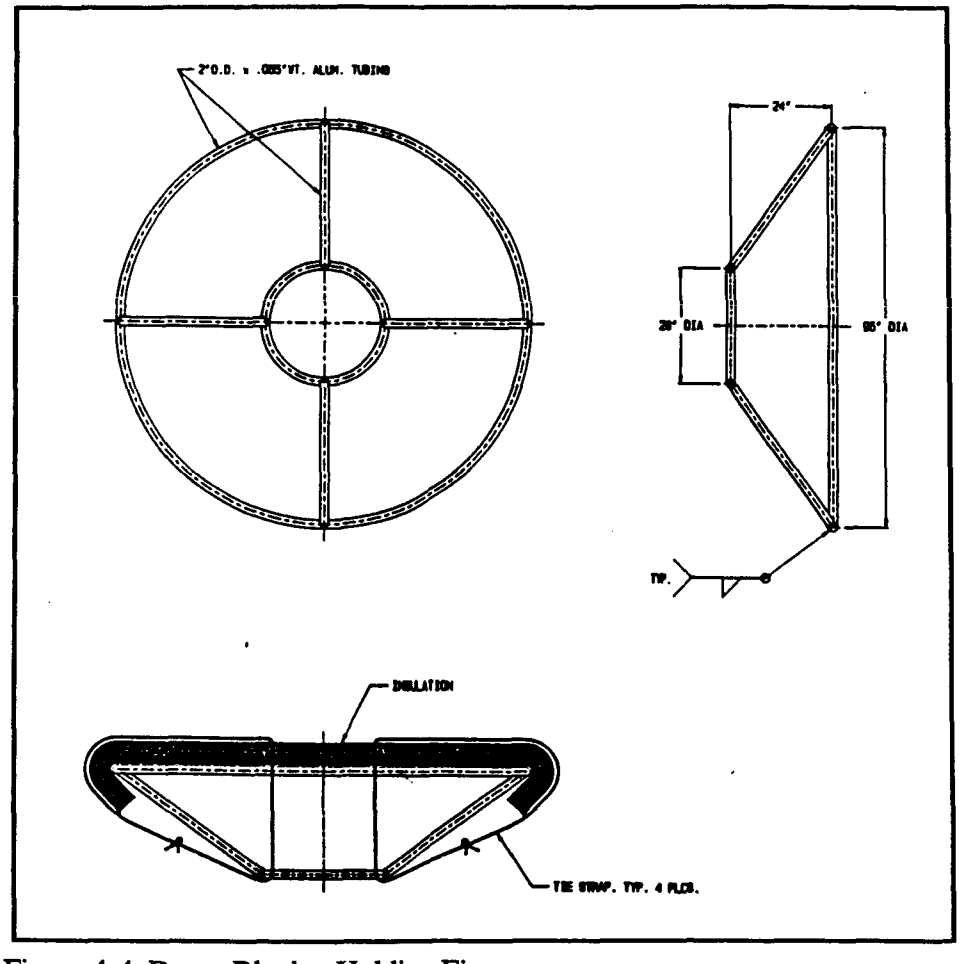

Figure 4-4 Dome Blanket Holding Fixture

4.1 Material Preparation

4.1.1 Bumper Strip Tacking

Prior to applying the bumper strips to the tank, they are tacked together to ensure the layers do not separate or slide apart. A process was developed to tack the bumper strips together which entails folding the Dacron net into the proper layers then tacking the strips together using a Swiftacher® (by Avery Dennison) tool which dispenses plastic tabs. This method produces a lower density bumper strip since the folds of the bumper strips help provide separation.

To make a bumper strip layup, a width of Dacron net is pulled through the net folder and then tacked before being spooled on the take-up roll. The net folder is a set of aluminum plates which guides the net into a folded configuration. This procedure can be used to produce bumper strip configurations from 2 to 6 layers.

The alternative to this method is to cut 2-inch wide strips and tack these strips together using the Swiftach® or fasten them together by heat sealing or sewing. This procedure is not as desirable because the bumper strips will not have the additional thickness spring on the sides.

4.1.2 Mylar Perforation

The Mylar was purchased on 120 inch wide rolls unperforated. The previous discussion on hole size and thermal degradation due to small holes led us to devise a plan to perforate the Mylar after receipt. The concern with perforating techniques was ensuring a clean cut on all the holes (otherwise the Mylar will tear) and the desire to maintain the same percent open area throughout the Mylar sheet. The suggested perforation technique was the use of a hollow tube drill which perforated the Mylar directly on the delivered cardboard cores from the manufacturer.

An additional concern with perforation after receipt is the change in percent open area (from inside to outside of roll) if the Mylar is too thick on the roll or the core diameter is too small. The Mylar can be purchased on either a 6 inch or 10 inch diameter core. An analysis was completed to determine the thickness of Mylar on a 6" and 10" core and the effect on percent open area. The concern is the change in the arc length for the material near the core. The insulation of the MHTB tank requires approximately 27,000 ft^2 for a 45 layer system (which becomes 33,000 ft^2 with margin). Applying 3350 feet of Mylar to a 6 inch core increases the roll diameter by 0.98 inches and increases the percent open area to 1.16% on the layers closest to the core. If the same order is split between two rolls, the percent open area changes to 1.09% on the inner layers. If the same amount of Mylar is applied to 10 inch cores, the percent open area increases to 1.03%. A total of 33,500 square feet of unperforated double aluminized Mylar was obtained on two separate 10 foot long rolls on a 10" core. This configuration provides an acceptable percent open area through the entire Mylar sheet when perforating.

4.1.3 MLI Acceleration Loads

The MLI must be attached well enough to the tank to withstand the loads encountered during launch. The roll wrap MLI is taped together at the seams with tape. The design acceleration load is 4.5 g's with a factor of safety of 2. The loads in the MLI must be transferred from the upper dome through the barrel section to the lower dome. The projected mass of a 45 layer system is 40 lb_m for the barrel section and 20 lb_m per dome blanket. The upper dome to barrel joint must then react (40+20) x (4.5 x 2) = 540 lb_f. The first question is the basic strength of the DAM. The tensile strength of a sheet of DAM is approximately 23,000 psi, which is 138 pounds per foot of length for a 0.5 mil film. Since the tank circumference times 45 layers of DAM is 1413 lineal feet of DAM, its total tensile capability is approximately 195,000 pounds, which is approximately 360 times higher than the requirement. Although the addition of vent holes will lower the capability somewhat, and little is known about precise Mylar strength at lower temperatures (although Mylar film is advertized to be pliable to -70 degrees C, which encompasses most of the MLI), the margin of strength appears to be very high.

The next question is the type and amount of tape required to transfer the loads from the dome blanket to the barrel section. The initial plan was to use Kapton tape, which was evaluated by Ball Aerospace (see Reference 4). It has a thickness of 0.0029 in, a tensile strength of 30 lb/in and a peel strength of 30 oz/in. Unfortunately, the Kapton tape has an emissivity on the order of 0.9, which could compromise the insulation characteristics of the MLI, and Kapton tape has a limited shelf life. The tape finally selected is aluminum backed polyester, which has a thickness of 0.0021 in, a tensile strength of 19.5 lb/in, and a peel strength of 40 oz/in. This tape has an emissivity of only 0.03, which is significantly better, and has a very long shelf life. Based on tape testing performed by Ball Aerospace on the Kapton tape, one piece of 1 inch wide tape is required every five feet around the tank circumference. The MHTB baseline is one piece every foot of circumference, so there is significant margin for either type of tape.

4.1.4 MLI Grounding planned at CDR

A requirement for the MLI blanket is that the MLI have a total resistance of less than 500 ohm. In order to achieve this resistance level, each layer of the MLI must be in electrical contact with surrounding layers. This concept defeats the thermal goals because each layer should be isolated from surrounding layers to achieve the best thermal insulation. Programs which have utilized individual MLI blankets have typically included grommets on a corner (penetrating all layers) to ground the blanket. These grommets were used to install a bonding jumper between each blanket and then each seam was covered with double aluminized Mylar tape. This recommendation was derived for an individual blanket assembly to assure no static charge buildup on an individual blanket and to prevent radiation tunneling.

The MHTB insulation concept differs from previous insulation designs in the fact that the barrel section Mylar is one continuous sheet. The Mylar has a resistance of 1 ohm per square. The barrel section Mylar is 8.83 feet wide and 1415 feet long for a 45-layer system. Therefore, the barrel section will have a resistance of 160 ohms. The dome blanket layers will be attached to the barrel section as illustrated in Figure 4.1.4-1.

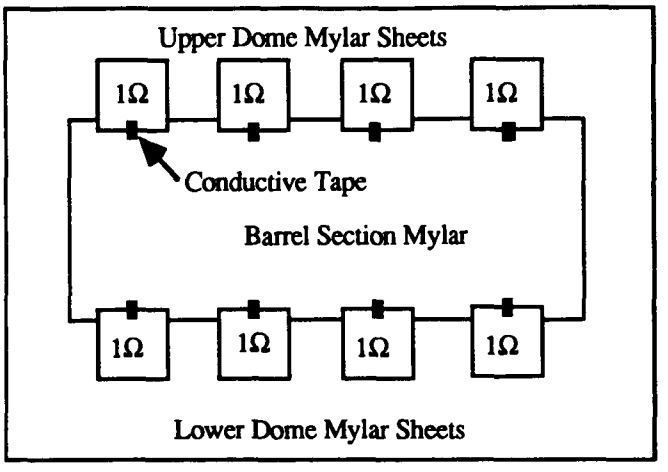

Figure 4.1.4-1 Mylar Resistance Diagram

The dome blankets will add surface area to the barrel section Mylar and add series resistance to the blanket. Each dome sheet is a 120" circle which will have a resistance of approximately 1 ohm. Therefore, all the dome sheets will add a total of 60 ohms to the barrel section resistance of 107 ohm for a total of 167 ohm resistance throughout the entire blanket. In-house testing was performed on the Mylar to verify the 1 ohm per square value. Several sheets of different sized Mylar were tested for resistance. A 4 x 5 ft sheet measured approximately 1.5 ohm. A 5 inch x 30 ft sheet measured 45 to 60 ohm resistance and a 5 inch x 60 ft sheet measured 100 to 120 ohm resistance. Therefore, the testing verifies the 1 ohm per square value.

The assembly of the MLI requires a least one strip of electrically conductive tape per sheet. The tape has a very low resistance (0.005 Ω) and provides contact between the dome sheet and the barrel section sheet. A continuous length of tape is not required over each seam since the seams are overlapping and contact will be made in every location that the Mylar is taped for structural attachment. Two pieces of 3M #1181 copper foil electrically conductive, pressure-sensitive adhesive tape are used to bond each dome DAM sheet to the barrel section DAM sheet. Bonding jumpers between sheets of Mylar were not included, because good contact will be established and the bonding jumpers could potentially damage the individual sheets of Mylar. The MLI is then grounded to the tank at a penetration(s), and to the vacuum chamber structure to complete the

ground. The attachment method and location(s) of these ground connections are left to the discretion of MSFC.

5.0 Penetrations

The test tank includes several penetrations which require foam and MLI closeouts to complete the insulation system. The penetrations included in the closeout considerations are the manhole cover, instrumentation port, vent line, fill line, lifting rings, pressurization line, the Rockwell hardware ports, trunnions, and tank legs. The foam closeouts are performed in the SOFI spray booth, the MLI application area and potentially in the test stand. All the MLI closeouts are performed in the MLI application area except the manhole cover brace point.

5.1 Foam Closeouts - CDR Plans

Foam closeouts are required over areas of the MHTB tank surface which are not adequately covered by the robotic spray application. This includes locations around penetrations, the dome ends, and the tooling attach point. These closeouts are performed using a pour-in-place foam material termed PDL-4034 which is the closeout material used on the ET program. This closeout foam is bonded to the adjoining SOFI material using a tie coat adhesive termed Conathane TU-400M. Thus, each of these closeouts will be characterized by a discernible "bondline" around the closeout perimeter. All closeouts which can be accomplished in the spray booth are completed before moving the tank to the MLI staging area. These spray booth closeouts include spraying the manhole cover with the exception of the bolt hole pattern and pressure check port, the 8-inch instrumentation feedthrough neck, the top Rockwell interface, and 4 inches from the weld line on the vent, fill, and pressurization lines. The bottom Rockwell interface and the tank leg receptacles are completely closed out in the spray booth. General closeout procedures for these areas are included in Appendix C. These procedures require updating during the actual closeout operations for documentation purposes. Photographs of the closeouts in various stages are also required.

After the tank is moved to the MLI application area, additional foam closeouts are required prior to the MLI application. The vent, pressurization, and fill lines are welded onto the tank line stubs, the tank legs are installed, then foam closeout operations are performed. Foam is applied the appropriate distance down the lines and legs to ensure no nitrogen condensation during testing. After the MLI application is completed, several foam closeouts are required. The lifting eyes on the side of the tank require a foam closeout and MLI closeout. The manhole cover bolts, pressure ports, instrumentation bolts, the bottom trunnion, and the top Rockwell interface require a foam closeout. The important factor during these foam closeouts is to ensure no foam is applied to the MLI, because the foam will degrade the MLI performance. Appropriate measures are taken during this final foam application to eliminate contamination of the MLI.

5.2 MLI Closeouts - CDR Plans

The MLI closeout procedures have been defined to create an understanding of the requirements to complete the insulation process. Preliminary closeout procedures are presented in Appendix C. These procedures are to be refined by MSFC to incorporate the thermal analysis for layer temperature matching. Substantial importance has been placed on MLI closeout operations to match MLI layer insulation temperature with penetration temperatures, so that conduction losses are minimized. The actual closeout procedure may differ from the procedures presented in Appendix C, so appropriate documentation shall be developed during the closeout to record final configurations. Step by step photographs shall be taken to document the closeout procedure.

5.3 Low Heat Leak Tank Supports

The tank is supported by four composite legs that are shown in Figure 5.3-1. This concept was selected because it is representative of the truss network which could be used on a flight vehicle to transfer the ascent acceleration forces into a liquid hydrogen tank. The legs consist of filament wound S-2 glass/epoxy tubes which are 3 1/16 inches in diameter and 1/16 inch wall thickness, bonded to a fittings which are attached to the tank. This filament wound glass/epoxy material has a uniaxial ultimate strength of 150,000 psi and a modulus of 8.0 to 8.5 x 10^6 at room temperature. Tie rods connecting the legs are included in the design to minimize deflection under conditions where side loads are applied.

6.0 Thermal Shroud

The heater shroud is installed between the cold wall of the chamber and the test tank to provide constant and variable boundaries for the TCS. The shroud is designed to maintain the outer MLI surface between 300° R and 550° R to simulate the temperature conditions in low earth orbit, during on-orbit transfer, and on the lunar surface. The shroud design, shown in Figure 6-1, is a stand alone fixture assembled around the test tank. The heater shroud is constructed of eight aluminum side panels which are bolted together, four top panels, and five bottom panels to provide complete thermal coverage of the TCS. All the panels have heater tape applied at approximately one foot interval to provide the necessary thermal environment. The panels are all 1100 series aluminum to enhance conduction within the panel and to minimize the thermal gradient between the electrical resistance heater strips. The heater tape spacing was determined by a thermal analysis to ensure minimal temperature gradients on the shroud. The input voltage to the heater strips is controlled by facility power controllers which utilize thermocouples on the shroud to sense the temperatures of heater shroud zones. There are eight zones on the side panels, four on top and five on the bottom.

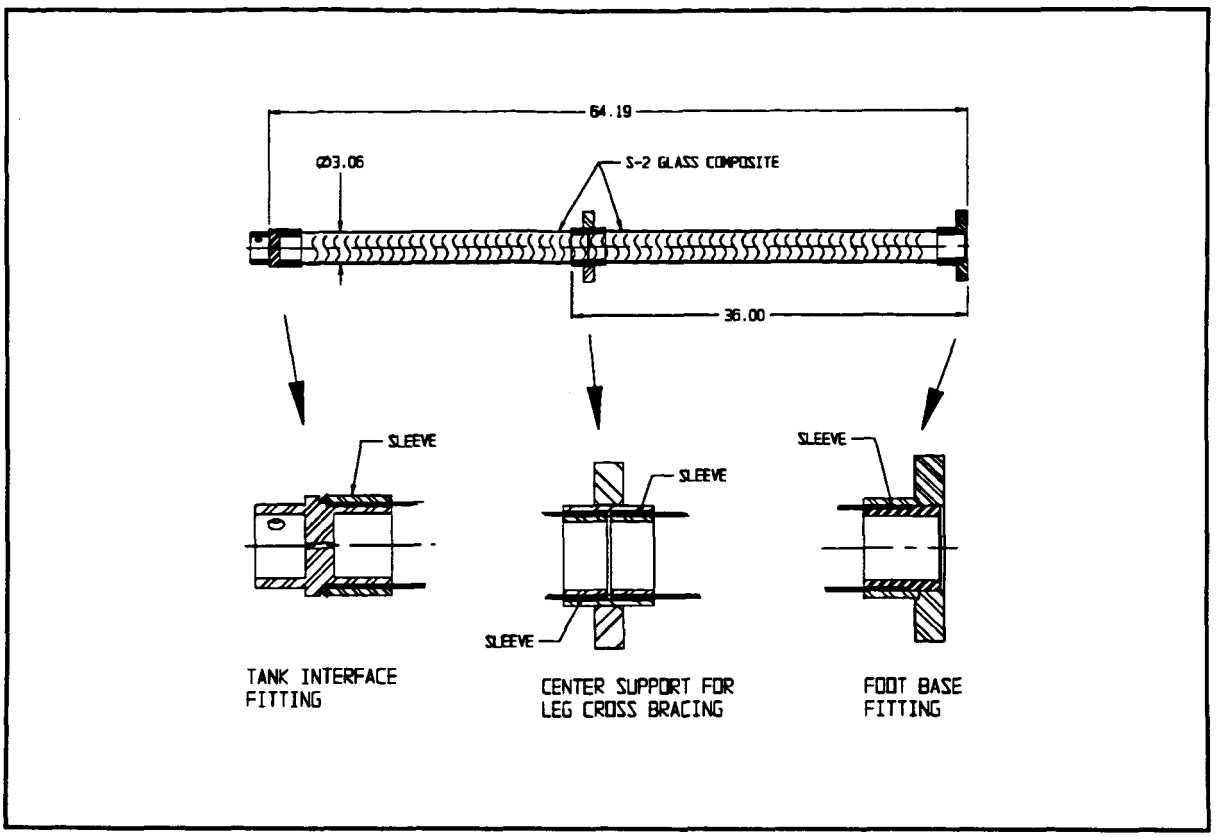

Figure 5.3-1 Composite Tank Leg Assembly

A thermal analysis was performed to size the electrical heaters for steady state and transient conditions. The thermal analysis investigated the sensitivity of the tank surface temperature to changes in heater tape spacing, the distance between the heater shroud and the tank, and the emissivity of all the surfaces (TCS surface, heater shroud inner and outer surface, and the cold wall surface). The analysis output predicted the required power density and the heater tape spacing to raise the temperature of the TCS surface from 300°R to 540°R in less than 2 hours and to maintain the temperature gradient on the TCS less than 5°R. For the analysis, the cold wall in the vacuum chamber was held at 150°R with an emissivity of 1.0 (black wall). The actual cold wall shows an emissivity of 0.9 and a steady state temperature of 190°R, resulting in a conservative analysis. The emissivity and the thermal conductivity of the shroud material are important considerations in the heater shroud design. A low emissivity surface on the shroud reduces the thermal gradients on the TCS surface and decouples the heater shroud from the cold wall. The largest heat loss under steady state conditions is to the cold wall which is at liquid nitrogen temperature. This loss can be minimized by applying a layer of low emissivity aluminized Mylar between the shroud and the cold wall. A high thermal conductivity material (pure aluminum) will

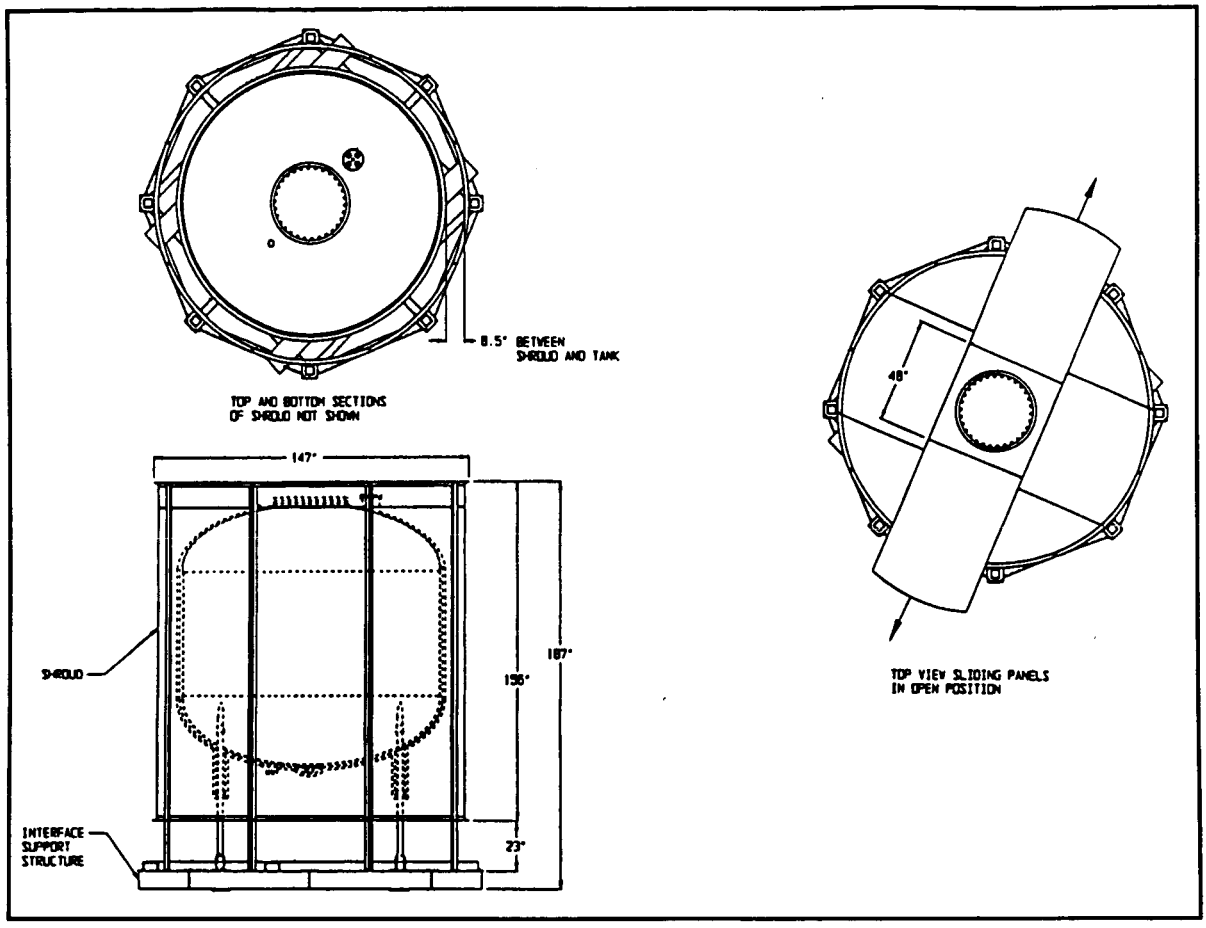

Figure 6-1 Heater Shroud Layout

reduce the temperature gradients on the shroud and consequently reduce the thermal gradient observed on the tank. Therefore, using the 1100 series aluminum provides this high thermal conductivity value while still maintaining structural capability.

A heater power density of 20 Watts/ft^2 provides enough heat to change the temperature from 300°R to 540°R in less than 2 hours. The analysis was based upon placing the shroud six inches from the TCS surface and using one foot spacing between the heater strips, which results in a steady state tank surface temperature gradient of approximately 1°R. The actual design of the shroud places the heater strips at 14 inch intervals and the heater shroud is approximately 8.5 inches from the tank surface. Under these conditions, the steady state temperature gradient on the tank surface is approximately 2°R and the temperature gradient on the shroud is approximately 18°R. This small gradient is within the requirements set for the heater shroud.

The shroud design includes several provisions for access to tank components and penetrations. The top of the heater shroud has two center panels which can be slid back, providing access to the manhole cover, instrumentation and fluid feedthroughs. The side panels can be

individually unbolted and removed. The bottom panels can also be removed, providing access to the location where the pressure control hardware will be installed for future tests.

7.0 SOFI/MLI Rotation Fixture

The SOFI/MLI rotation fixture is designed to rotate and handle the MHTB tank during SOFI application in the spray booth as shown in Figure 7-1. This fixture is also used to rotate the tank during the MLI application process. The fixture includes a removable assembly on the end for the MLI dome blanket operation. The tank is supported by the lifting rings during this operation. The fixture has overhead crane pickup points and castors for maneuverability and positioning. With the tank mounted in the fixture, the assembly has an overhead clearance of 10 foot 9 inches which is equivalent to the SOFI spray booth door height.

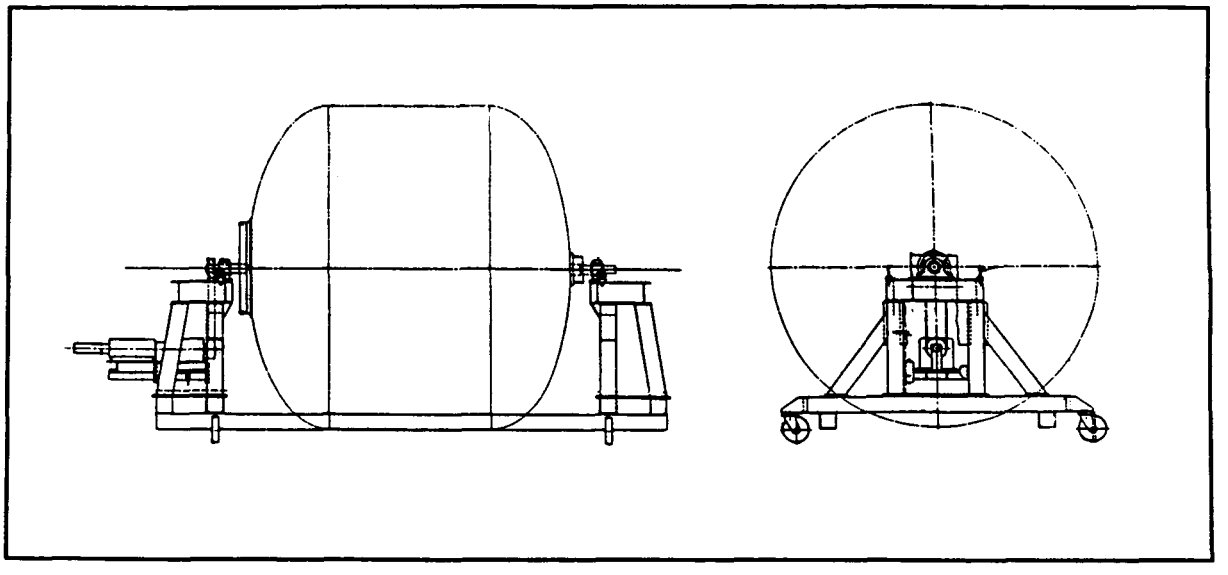

Figure 7-1 Rotation Fixture for SOFI/MLI Application

8.0 Tank Development

A significant portion of the contract activity was devoted to the design and fabrication of a large liquid hydrogen tank, its support structure, and interfaces with the MSFC thermal vacuum chamber located at Test Stand 300 in the East Test Area. The overall layout of the vacuum chamber, tank, support structure, the TCS hardware, and MSFC supplied scaffolding are presented in Figures 8-1 and 8-2. The Contract Statement of Work required that the tank be designed for long life cryogenic/vacuum life and include representative supports, fill and drain lines, instrumentation, and interfaces for the TCS and alternative CFM hardware supplied by other contractors. MSFC fills the role as system integrator in development of this testbed.

8.1 Tank Introduction and Development Objectives

There were several goals for the development of the MHTB test tank, which required a careful blending of flight-like characteristics and robustness. In order to have a safe, durable test

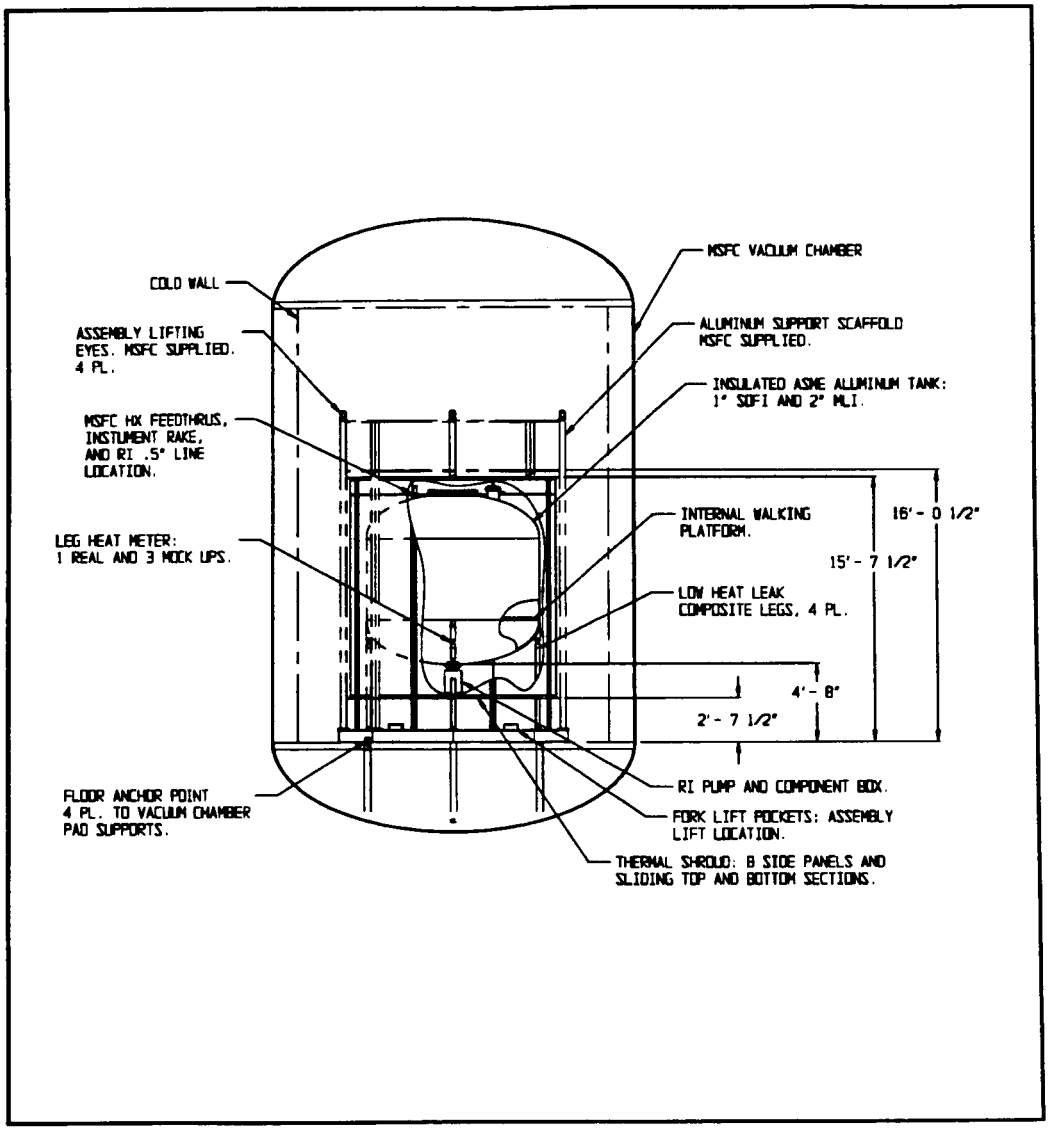

Figure 8-1 Test Bed General Arrangement in Test Cell 300 - Side View

bed that could be used for years of testing, we selected a fairly massive, aluminum, ASME coded tank, which sacrificed some of our ability to obtain precise transient thermal data, but provided a very robust testbed, as described below.

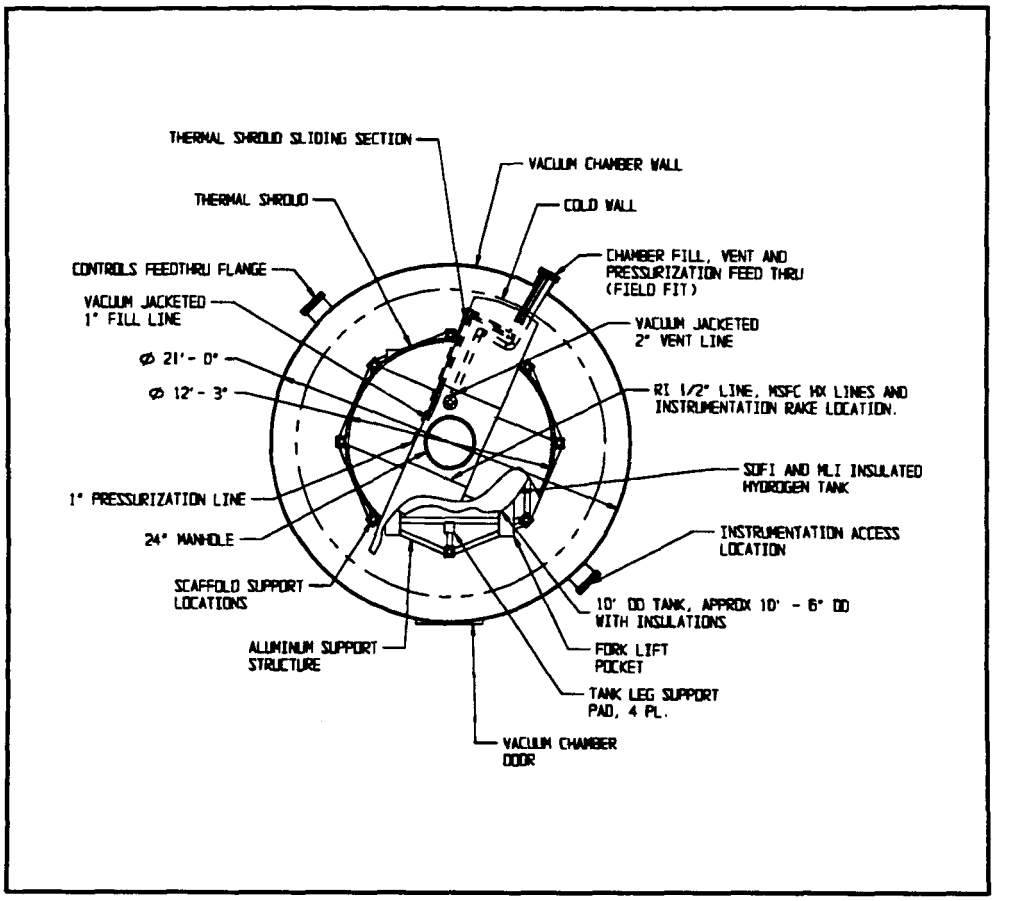

Figure 8-2 Test Bed General Arrangement in Test Cell 300 - Top View

The tank will be used to study thermal performance and pressure control over a wide variety of conditions. Pressure inside the tank can range from vacuum to 50 psid. External pressure will also vary from 760 torr to hard vacuum (10^{-7} torr) utilizing the rapid decompression of a simulated flight profile. It was this wide range of conditions and a concern for safety that led to the selection of an ASME-coded vessel. Coded vessels are not life limited by thermal/vacuum cycles and assure adequate safety margins for unexpected events. The ASME tank is one that must also meet rigid material quality requirements, be assembled by qualified fabricators, pass acceptance tests, and be verified by an independent nationally recognized inspector. The MHTB tank has met all the ASME requirements and is a coded vessel.

Another major driver in the design of the tank is its size, since it must contain adequate volume to be representative of a flight system. A typical flight hydrogen tank would be relatively large with a diameter of 8 to 25 feet and a length of 10 to 50 feet. As explained in the following paragraphs, a 10 foot diameter tank was chosen.

8.2 Tank Design and Dimension Selection

Keeping in mind objectives of low heat leak, a flight representative size of 10 foot diameter and 10 foot tall tank was chosen. The diameter was selected for a variety of reasons. It had to be large enough to represent a flight tank yet small enough to be installed in the thermal vacuum chamber at MSFC. The vacuum chamber has a usable 18 foot diameter (inside the cold wall) within which the tank and its associated hardware must be positioned. The 10 foot size was selected to allow adequate clearance for test personnel, the heater shroud, scaffolding, and facility service connections. A larger tank would compromise those clearances, therefore a 10 foot diameter was deemed a practical size.

Heat input is proportional to the tank surface area while fluid energy is proportional to tank volume. Therefore, tanks with low surface area to volume ratios are the best long term cryogenic storage vessels. "Square" tanks, that is a tank in which the height is approximately equal to its diameter, have low surface area to volume ratios and thus a height equal to the diameter was chosen. One other notable factor led to the selection of this tank size since this size is the next logical progression of earlier long term cold storage experiments. The earlier data can be used to compare scaling and thermal performance differences.

Once the overall dimensions were selected, other geometric concerns had to be resolved. First, the dome heads were chosen with a 2:1 geometry instead of the typical flight $\sqrt{2}$:1. The primary reason for this selection was manufacturability. A 2:1 head can be bump formed, a process where a flat plate is spun and repeatedly impacted with a computer controlled die head to achieve the proper geometry. A $\sqrt{2}$:1 head would required spin forming with intermittent annealing to relieve forming stresses, a very expensive and time consuming process. Since the selection of a 2:1 dome did not compromise the thermal system and the data could be mathematically correlated to other geometries, it was selected as a practical alternative dome head geometry.

Material selection for a flight tank would realistically be Weldalite or aluminum 2219, since these materials possess some of the highest strength to weight ratios. From a test environment stand point however, aluminum 5083 is a logical alternative for a variety of reasons. First, it is a proven cryogenic code material which has a proven history of safe operation in long life unlimited cycle vessels. Second, it has very high fatigue strength, is easy to weld (for future changes and modifications), has high corrosive resistance, and does not require solution heat treat after welding to obtain its optimum properties.

Once the material was selected, the ASME code clearly dictates the safe and acceptable thicknesses required for vacuum and pressure shells and domes. The shell thickness is driven by the wall stiffness requirement to resist vacuum collapse which lead to the next higher commercially available thickness of 0.5 inches. Further stiffening for vacuum collapse protection was added by welding two rolled angles under each of the dome head weld seams. These angles also provide

dimensional rigidity during manufacture, act as back up rings for welding, support internal scaffolding for test setups, and strengthen shipping and handling points. A summary of the tank design is shown in Table 8.2-1.

Table 8.2-1 Pressure Vessel Characteristics

Requirements	Design Features
Size	10 ft Diameter by 10 ft Long
Volume	639 cubic feet
Surface Area	374 square feet
Dome Geometry	2:1 Radius to Height Ratio
Material	5083 Aluminum
Design Temperature	Ambient to -435°F
Operating Pressure	50 psid Internal, 14.7 psid External
ASME Code	Section VIII, Division 1
Weight	2785 lb (Vessel without support structure)

8.3 Access and Penetrations

The penetrations, while each being unique have some common features (with the notable exception of the manhole which is discussed in section 8.3.7). First, penetrations were minimized to reduce the heat input. When possible, penetrations were combined with other functions or performed other functions within themselves to reduce the total number of penetrations. In order to minimize heat input, stainless steel plumbing is used since stainless steel has approximately 1/100th the conductivity of aluminum at LH_2 temperatures and can save a considerable amount of heat input. The tank is aluminum however, and to attach the plumbing, a 3003 aluminum to 304 stainless steel transition joint is used. (The tank material of 5083 aluminum will not bond to the stainless steel without the intermediate 3003 aluminum transition). The design of these joints were incorporated into the ASME reinforcement requirements by using the added cross sectional thickness of the transition as reinforcement. Combining functions helps to reduce bulk and thermal mass. Stainless steel plumbing is used throughout and allows the design to utilize proven cryogenic vacuum flanges. These flanges and their OFHC copper gaskets provide reliable helium leak tight seals at a reasonable cost. It should be noted that the copper in the gasket and the flange have very similar thermal expansion coefficients. Since there is very little relative movement

between the flange and gasket during chill down, the seals are freed from many of the problems which plague other cryogenic joints. These flanges have a proven track record in use on the Slush Hydrogen Test Facility (STF) and in the 24" manhole verification testing where they have remained leak tight even with direct LH_2 exposure.

8.3.1 Bottom 3" Spare penetration

The 3" spare penetration incorporates two functions: future test pressure plumbing and trunnion mounting. The trunnion transfers static and dynamic loads into the tank through this point (see Figure 8-3). This area required reinforcement to assure adequate strength. The reinforcement required for ASME provided a strong point which was combined with the trunnion design thus reducing the total amount of added material. This capped spare port can serve as plumbing access for future engine testing after the trunnion is removed.

8.3.2 PCS Bottom Penetration

The PCS bottom penetration provides many functions. First, it acts as a structural support for future pressure control hardware. The weight of the hardware and any associated dynamic loads are transferred through a 10" blind Conflat flange into the tank. Its second function is to provide internal support for a liquid hydrogen spray bar used for tank fluid mixing during the pressure control testing. This spray bar is also supported by brackets on the top of the tank which are aligned with the bottom spray bar mount. The penetration also functions as plumbing feedthroughs for the spray bar operation, and includes one 2" tube, one 1.5" tube and one 0.5" tube. A great deal of time, discussion, and effort went into the alignment of the inner support flanges and brackets, flange selection, and sizing of this penetration. A sectional view is shown in Figure 8-4.

8.3.3 PCS Top Penetration

The PCS top penetration consists of a flanged 3" tube. The flange supports a fiberglass instrumentation rake which can be removed without breaking the manhole seal. This rake supports 9 silicon diode temperature transducers. It is also the site of a 0.5" tube feedthrough used with the PCS. It is designed so that two other 0.5" ports can be added if future growth or testing requires such items. A sectional view of the penetration is shown in Figure 8-5.

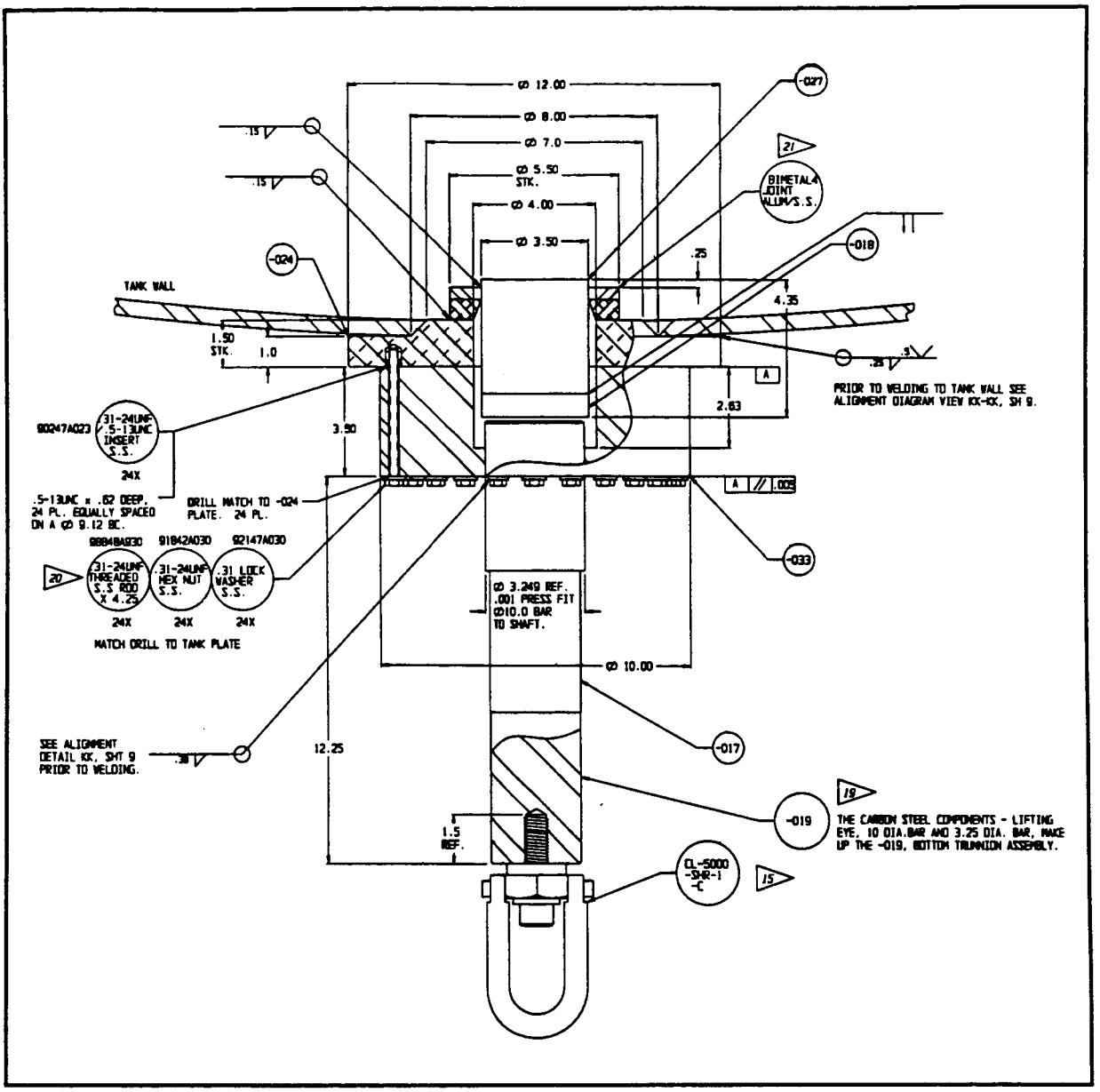

Figure 8-3 Trunnion Detail

8.3.4 Instrumentation Port and Vent Line

The development of the fluid lines was dependent on the development of the penetrations. The vent line, for example, incorporates not only the consideration for adequate venting, but capitalizes on the cooling energy of the vent gas. Internal instrumentation, the capacitance probe, diode wiring and pressure transducer ports are all located or routed to the vent penetration to take advantage of the escaping boiloff gas. The vent penetration/instrumentation port cross section is shown in Figure 8-6. The vent line exits the instrumentation port which includes a capacitance

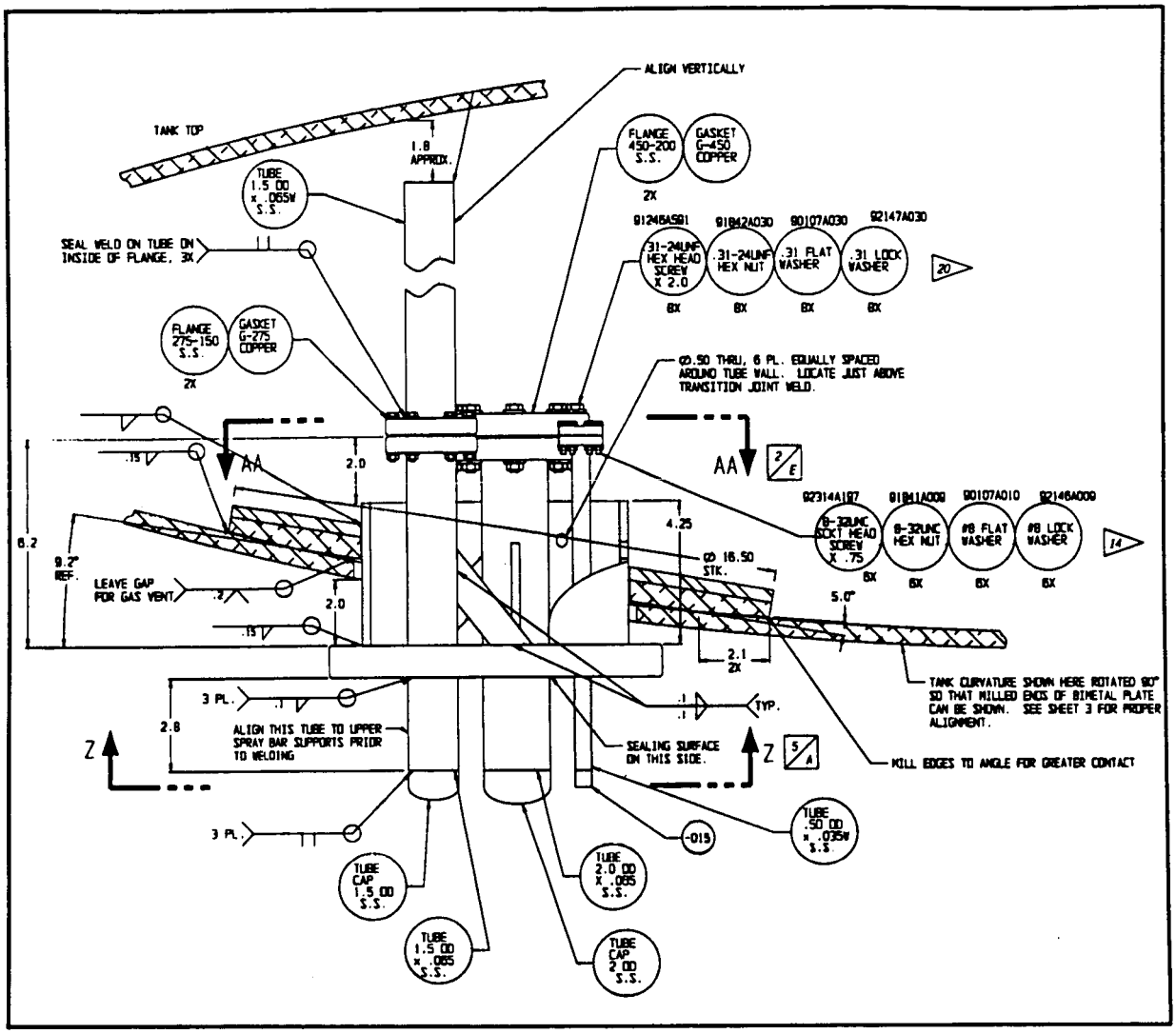

Figure 8-4 Bottom Penetration Detail

probe, instrumentation rake and electrical feedthroughs. As the cold gas is released to the vent line, it chills the instrumentation port as well as the wiring and plumbing which would tend to act as a heat source. The heat input of these items is considerably reduced while cold gas is flowing through the vent line. After leaving the tank penetration, the vent line transitions to a vacuum jacketed line to prevent cryopumping during ground hold or launch simulations. This line exits the vacuum chamber, and is routed through the measurement system for tank pressure control and gas flow.

The instrumentation port contains four 32-pin connectors and supports a fiberglass instrumentation rake. The rake and penetration are designed in a manner which allows for removal and service of the rake without the removal of the manhole. This allows for service of the

instrumentation rake assemblies without the major impact of removing the manhole insulation and gaskets. Each rake is equipped with 9 silicon diodes which allow temperature stratification measurement during the pressure control testing.

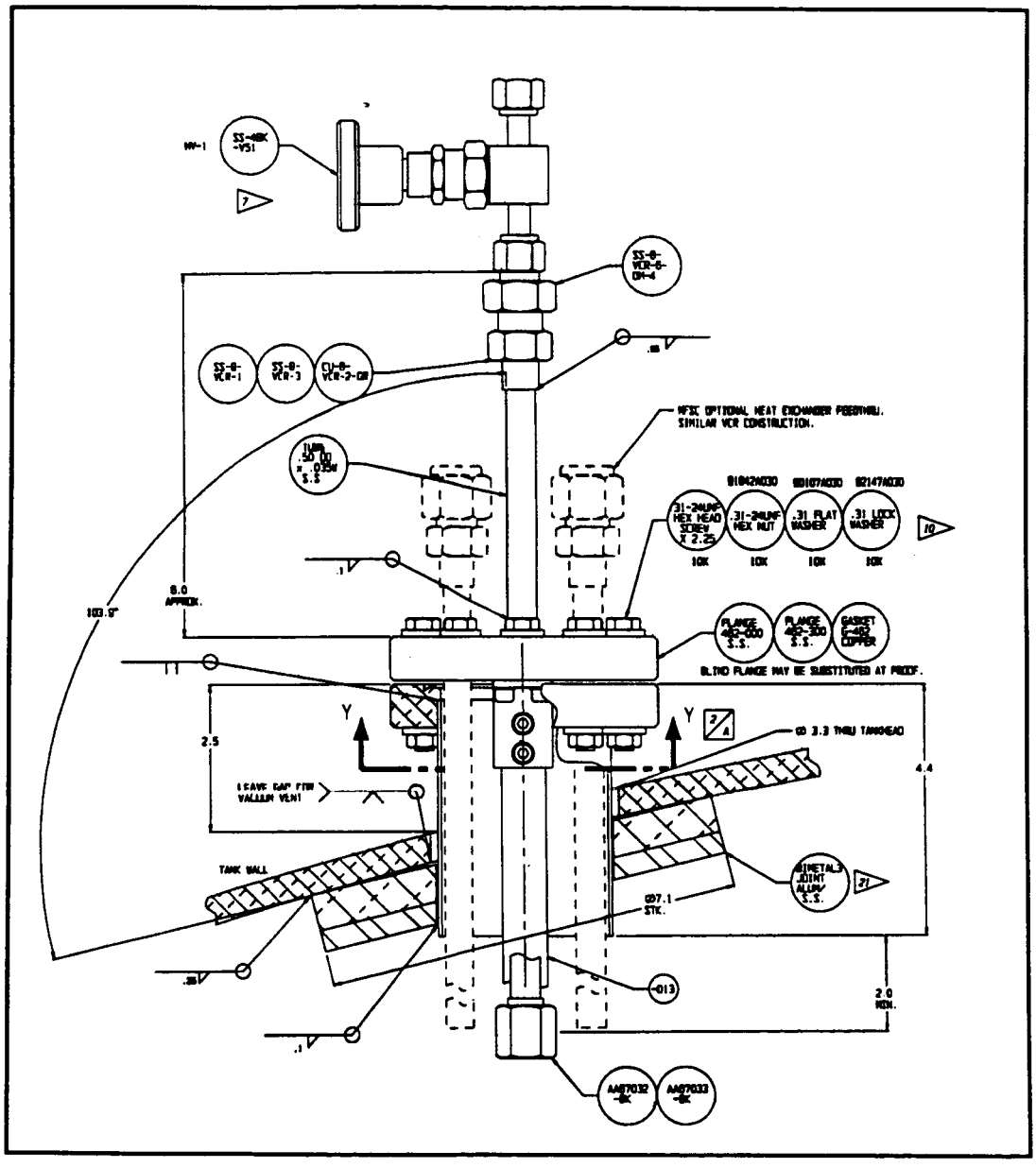

Figure 8-5 PCS Top Penetration Detail

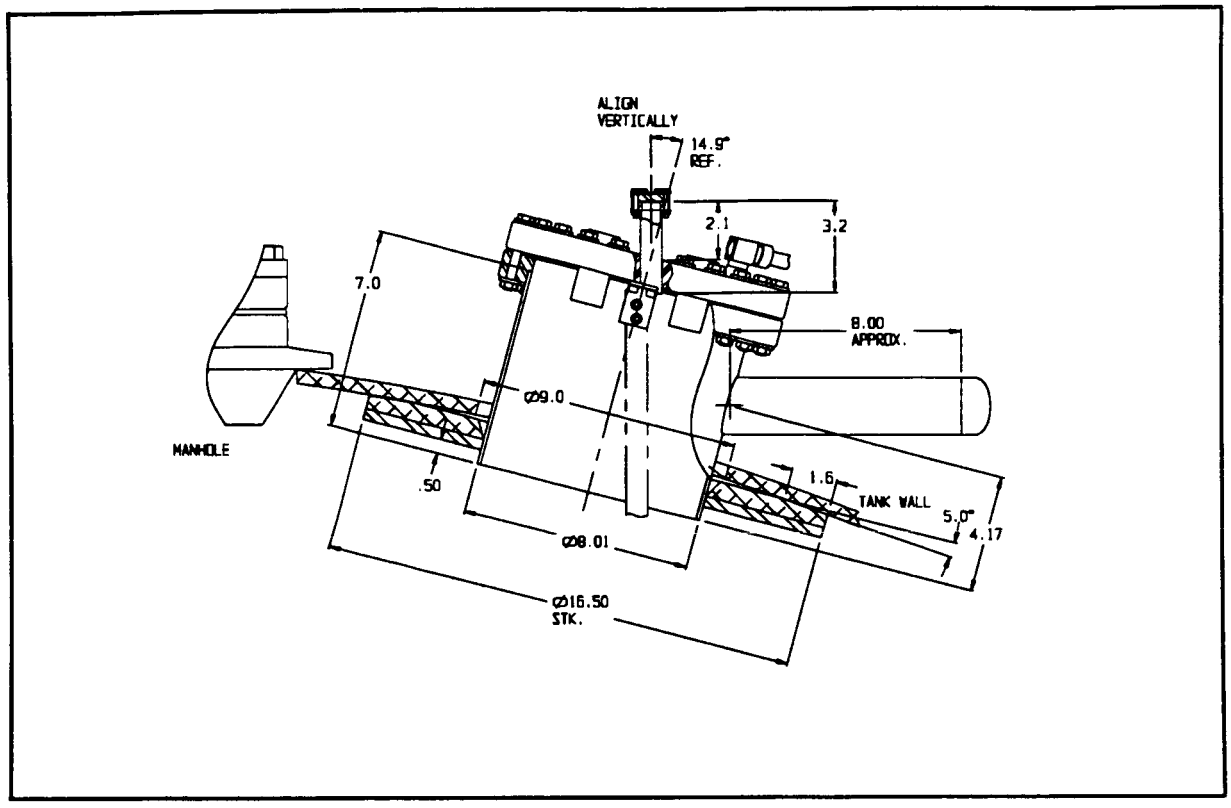

Figure 8-6 Vent Penetration/Instrumentation Port Detail

8.3.5 Fill Penetration and Line

The fill line, which is also used as a tank drain, is a 1" 300 series stainless steel line which acts as a dip tube drain inside the tank. It passes through an aluminum to stainless steel transition joint then transitions to a vacuum jacketed line after it leaves the tank. It follows a parallel path along the vent line and exits the vacuum chamber to the test cell's fill and drain system. The vacuum jacketed configuration was selected to prevent nitrogen condensation and cryopumping when the vacuum chamber is back filled to simulate ground operations.

8.3.6 Pressurization Penetration

The last plumbing line interface is the pressurization line. It is a 1" stainless steel line which connects to a MSFC-supplied diffuser on the inside of the tank. It then exits to the test cell's pressurization control system once it leaves the vacuum chamber.

8.3.7 Manhole

The 24" manhole was required for access during test set up, installation of internal working platforms, tank inspection, and maintenance or future modification. The development effort

dedicated to the manhole was extensive. This sealing system is used in a liquid hydrogen and hard vacuum environment, and requires a completely independent redundant sealing system so that testing may continue in the event of a failure. The flange of the secondary seal includes a port to detect the failure of the primary seal while keeping the leak contained. Both seals meet a stringent 10^{-9} scc/sec helium leak requirement, a leakage level which, to our knowledge, has never been demonstrated on a seal of this size. Development of this seal required liquid hydrogen testing combined with extensive helium leak detection to verify performance of each seal individually. A cross sectional view of the 24" manhole is shown in Figure 8-7.

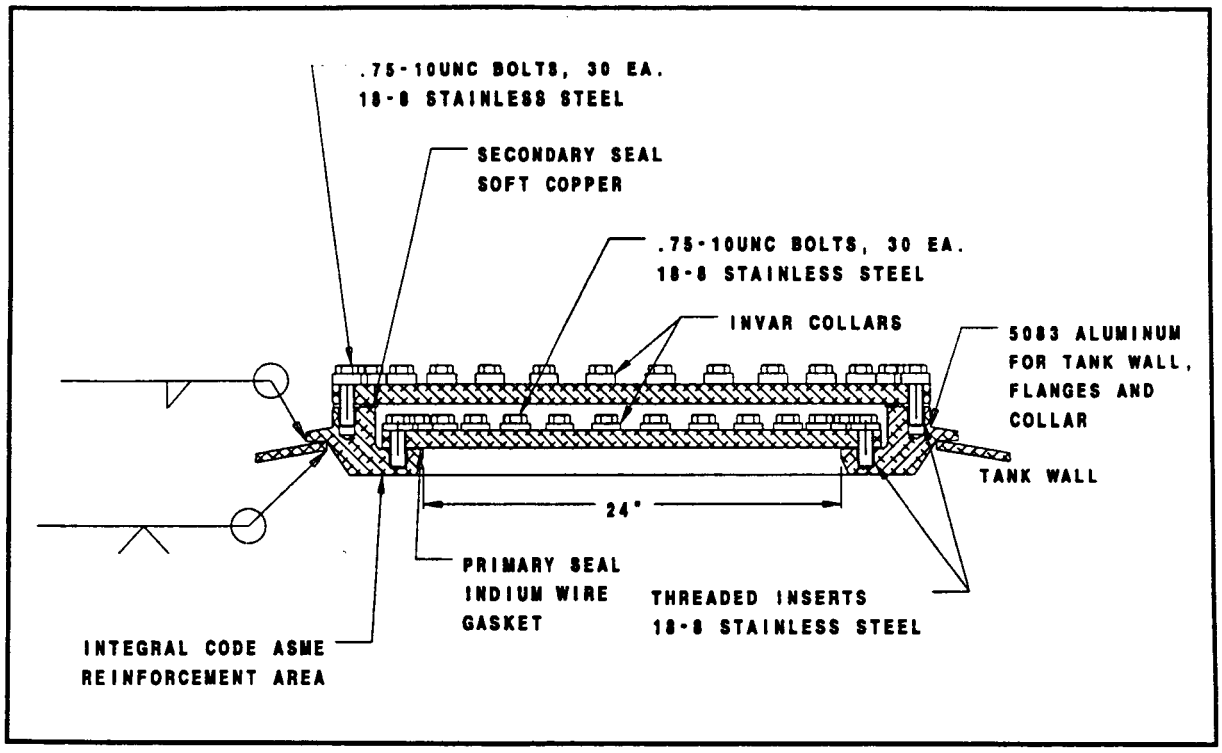

Figure 8-7 24 Inch Diameter Manhole Sectional View

The design of the primary seal incorporates an Indium crush wire (used much like an o-ring), tight tolerance machined sealing surfaces, Invar washers, 303 stainless steel self locking threaded inserts and 18-8 stainless steel cap screws. The combination of these items and their different thermal expansion coefficients act together to actually tighten the flanges as they chill down. The secondary seal uses a serrated tight tolerance surface and a 99.9% pure soft copper gasket and similar bolting to act as an independent system. Computer analysis also played a large part in the design of the seals. Computer area calculations were used to incorporate required ASME reinforced areas with sealing surfaces, thus strengthening a high stress area while minimizing tank weight.

The reinforced area was then capitalized on as a location for placement of a trunnion mount. The trunnions, which are required to spin the tank during the insulation processes, needed a high strength area for attachment to resist induced static and dynamic bending loads. The manhole reinforcement provided this location and allowed for the combination of code requirements with handling and sealing requirements for a more compact design. The manhole, as a trunnion mount, is shown in Figure 8-8.

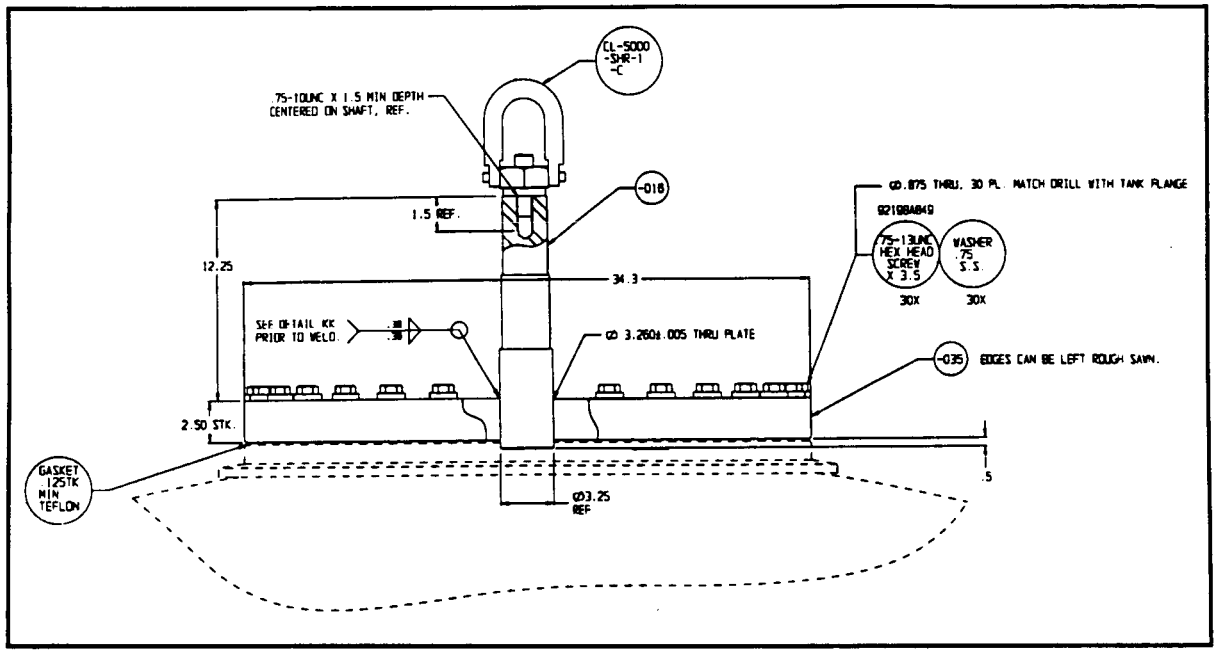

Figure 8-8 Manhole as a Trunnion Mount

8.3.8 Seal Verification Testing

A full seal development test was conducted early in the program for the primary seal material to verify it meets the leakage criteria of less than 1×10^{-8} scc/sec at liquid hydrogen temperatures. Since this concept had never been demonstrated on a 24" diameter manhole, a test fixture was built for the seal verification. The manhole seal was tested in a worst case configuration, that is, the sealing surface was always exposed to liquid hydrogen. In the MHTB final configuration, the manhole sealing surface is on the top of the tank, and is only intermittently exposed to liquid hydrogen.

8.3.9 Penetration Summary

Table 8-2 is included to summarize the list of all tank penetrations.

Table 8-2 Penetrations Summary

1) Manhole and Trunnion Mount - 24" Diameter
2) 1" Fill and Drain Line
3) 1" Pressurization Line
4) 8" Instrumentation Port (contains 2" Vent Line, Capacitance Probe, Electrical Feedthroughs and Instrumentation Rake)
5) Top 3" PCS (contains 0.5" Tube Feedthroughs and Second Instrumentation Rake)
6) Bottom 8" PCS (contains 0.5", 1.5", 2" Inner and Outer Tube Feedthroughs and 10" Blind Flange Support)
7) 3" Spare and Trunnion Mount

8.4 Shipping Configuration

Figure 8-9 shows the configuration for shipping the tank from Denver to Huntsville. Special tie downs and trunnion attachment lift points are incorporated in the shipping design. The shipping legs are a 5086 aluminum, all metal, shortened versions of the low heat legs which support the tank and anchor to the interface support structure for transportation. The tank is shipped on an air ride low boy trailer and is protected from weather by a sealed shipping container. Internal cleanliness is maintained by leaving a 5 psid GN_2 pad pressure on the tank. The internal tank temperature rakes are individually packed and shipped in separate containers. The silicon diodes and other instrumentation wiring are also shipped in a separate container so they can be more easily packaged and protected.

8.5 Internal Scaffolding at PDR

Figure 8-10 shows the removable scaffolding which can be used inside the tank for maintenance and other operations. It is designed to hold two people and is laid out to access all internal components. The open area allows the worker to access the flanges at the bottom of the tank, using the ladder shown in the manhole view. These flanges can not be reached from the platform.

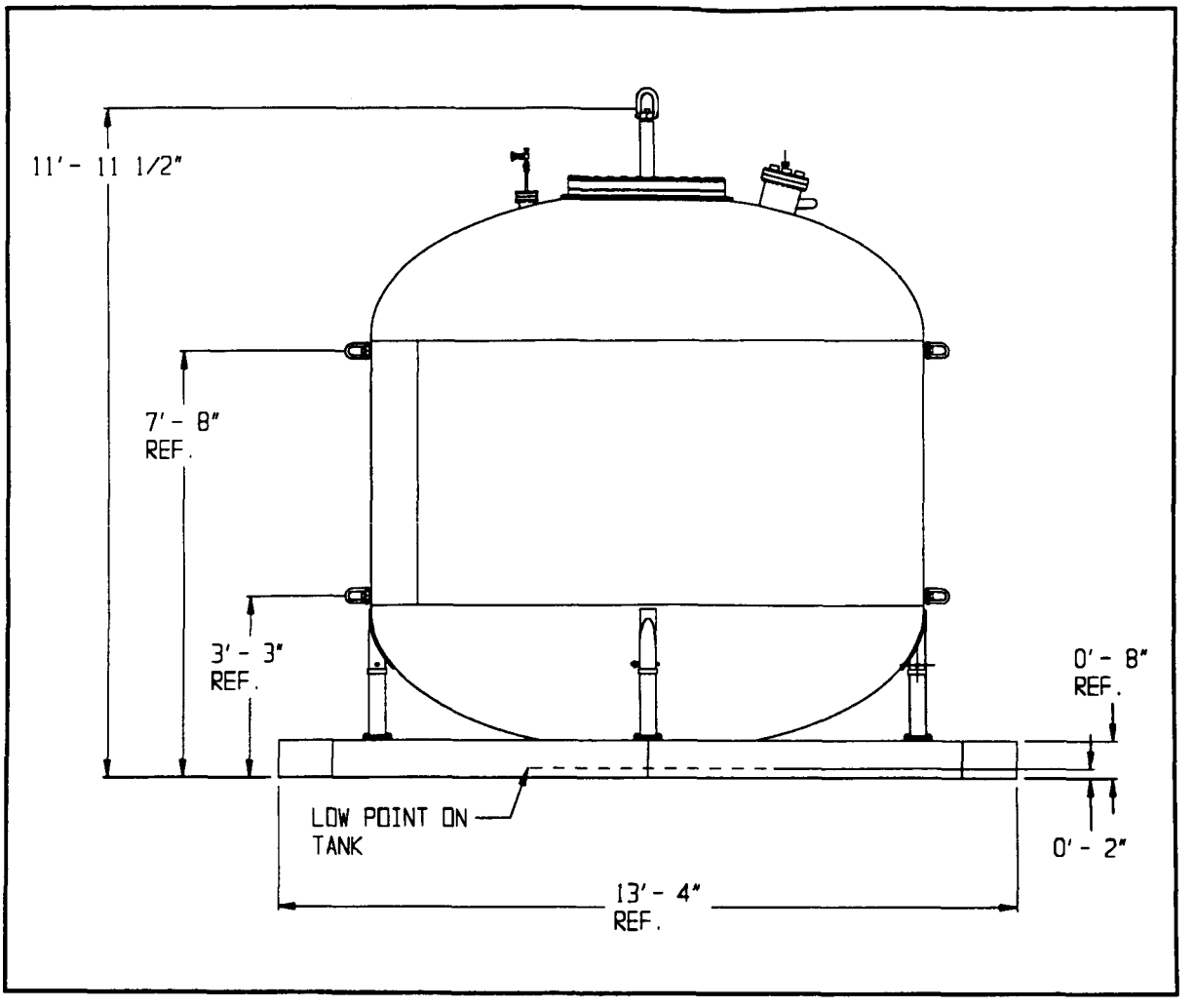

Figure 8-9 Tank Shipping Configuration

8.6 Interface Support Structure

The 6061 aluminum interface support structure is shown in Figure 8-11. It provides support for the tank during transportation, assembly and test. It interfaces with four hard points in the vacuum chamber floor, supports the thermal shroud and holds up the MSFC work platforms and scaffolding. The support structure is designed as a handling and transportation fixture and has the benefit of computer finite element modeling to ensure adequate safety margins under high shipping loads. This structure was also proof tested and dye penetrant inspected to verify its capabilities and fabrication.

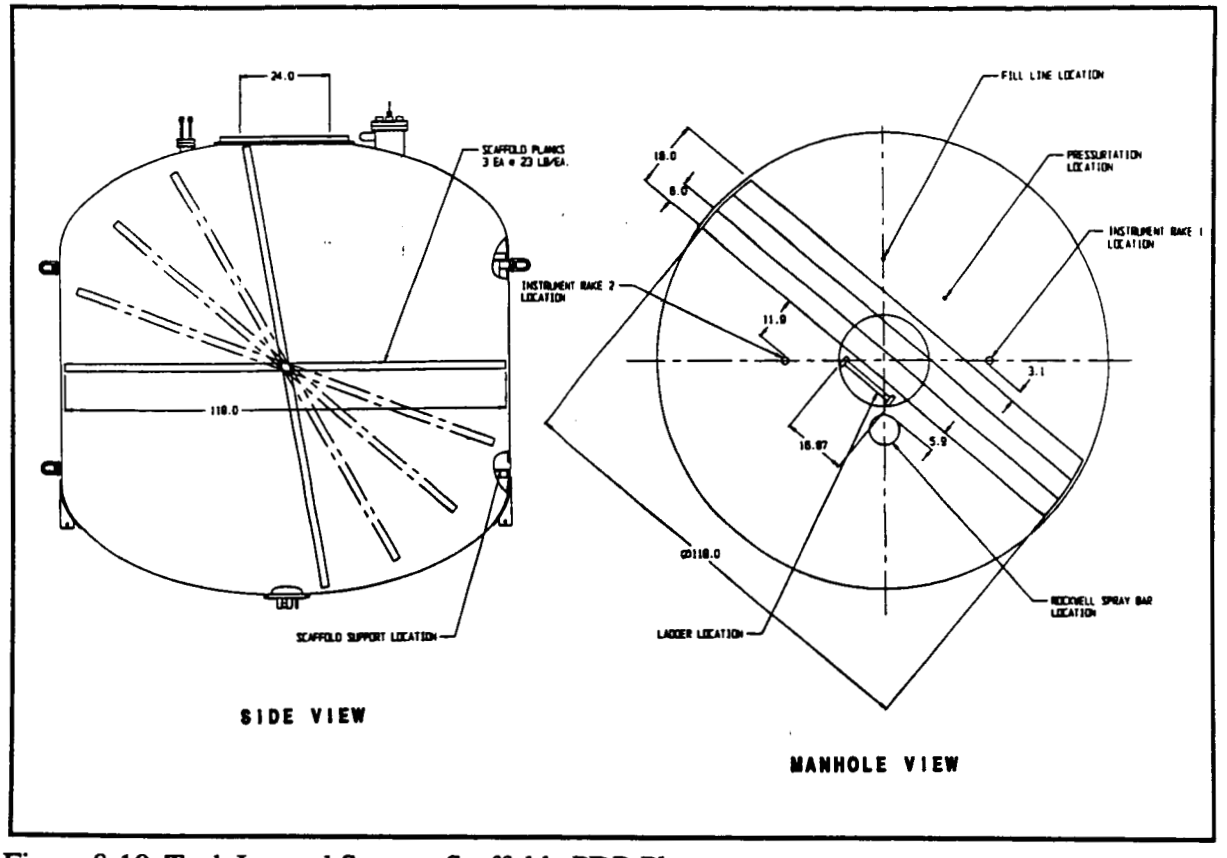

Figure 8-10 Tank Internal Support Scaffold - PDR Plans

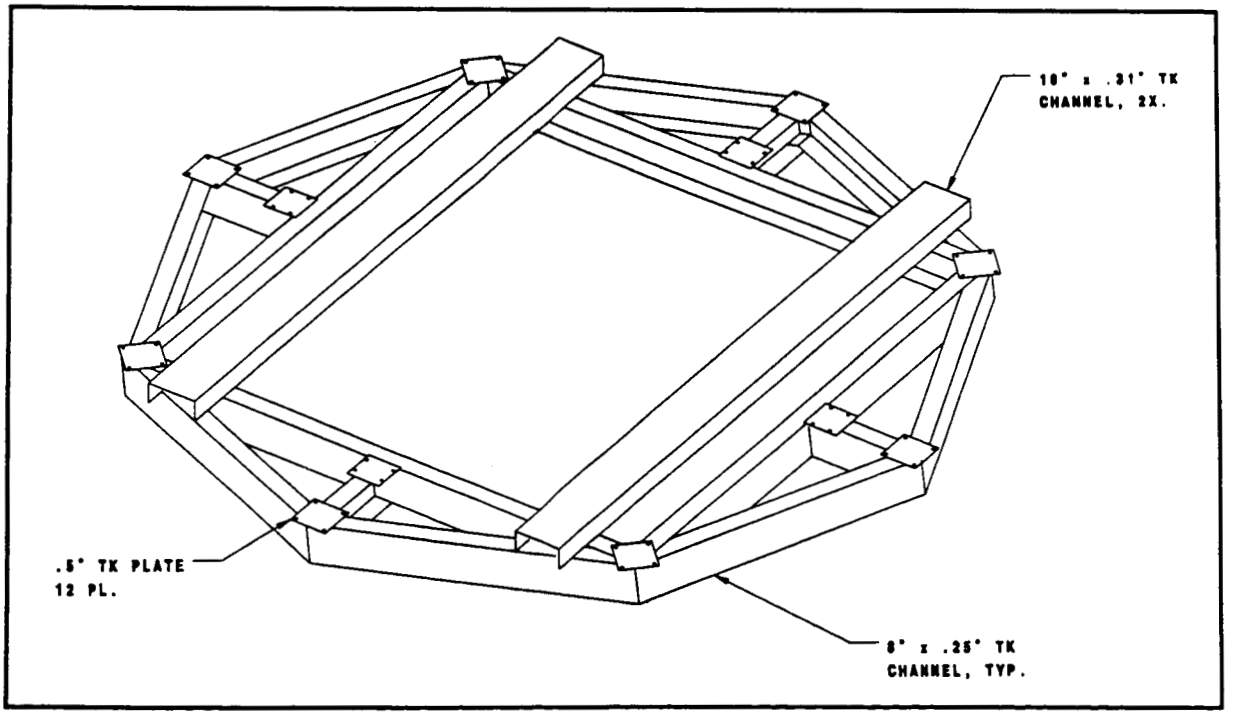

Figure 8-11 Support Structure

8.7 Tank Acceptance Testing

To ensure the safety and integrity of the fabrication of the pressure vessel and its associated hardware, a number of acceptance tests were performed. A summarized list of these tests are itemized below in Table 8-3. All of these items were satisfactorily completed and met all requirements. Results are made a part of the hardware data packages.

Table 8-3 Acceptance Test Requirements

Liquid Hydrogen Tank
Dye Penetrant Weld Inspection of Tank
1.25 Gas Stat. Proof Pressure Test
Vacuum Proof Test
Liquid Nitrogen Cold Shock and Leak Test of Indium Seal
Cleanliness Verification
Helium Leak Test
D-PRO Dimensional Inspection of Tank
ASME Inspection
Tank and Trunnion Weighing
Quality Verified Test Procedures
Quality Verified Fabrication Process Plan
Certified Materials
Interface Support Structure
Dye Penetrant Weld Inspection
Structural Proof Loading
D-PRO Dimensional Inspection

References

1. "Thermal Performance of Multilayer Insulations" Final Report; Keller, C.W., Cunnington, G.R., Glassford, A.P.; NASA CR-134477, Lockheed Missiles and Space Co., April 1974.

2. "Thermal Insulation Systems, A Survey" Glaser Peter, et al. NASA SP-5027, 1967.

3. Introduction to the Transfer of Heat and Mass, Eckert, E.R.G., McGraw-Hill, New York (1950), p. 203.

4. Multilayer Insulation Thick Blanket Performance Demonstration, Final Report, AL-TR-90-005, Ball Aerospace Systems Group, Mohling R.A., et al, April 1990, p.31.

APPENDIX A

10 Layer MLI Calculation

Design Parameters:

10 Reflectors with $\epsilon = 0.04$
11 separators for the temp. range from 300 to 270 K
3 continuous layers of B4A Dacron net per separator
Vacuum residual gas is nitrogen
Radiation absorptivity of separators is 0.95
Calculate Q/A for vacuum levels of 10^{-6} to 10^{-2} Torr

Detail Calculations:

B4A Dacron net:
Weight = 7.120 g/m^2 =0.0071202 kg/m^2
Solid Dacron density = 1,390 kg/m^3
Fiber diameter = 0.000777 m
Single layer thickness = 0.0001651 m
$\Delta X = 3 \cdot (0.0001651) = 0.0004953$ m
B4A wt. per DAM layer = $3 \cdot (0.0071202)$
$= 0.0213606$ kg/m^2
$\rho = 0.0213606/0.0004953$ m $= 43.12659$ kg/m^3
$f = 43.12659/1,390 =$ **0.03103**
$L_f = (\pi/4) \cdot (0.000777/0.03103) =$ **0.001967**

DAM and Composite:
Mylar thickness = 6.35E-6 m
Total layer spacing = 6.35E-6 + 0.0004953
L.S. = 0.0005017 m
N = 1/L.S. = 1/0.0005017 = 1993

Constants:
Let the first temperature be T1 and the second, colder, temperature be T2. Set up the thermal conductivity equation in the following form:

k1 = C1*(C3*(T1^2+T2^2)*(T1+T2)-C4*((T1+T2)/2)^3)

+ C5*P*(1-(.2)*(T1-78)/222)

+ C6(C7+C8*(800-T1)+C9*LN(T1))

C1 = 5.675E-8 W/m$^2 \cdot$K^4 (Stefan-Boltzmann const.)
C3 = 0.04/(2-0.04) = 0.020408
C4 = (4)*(0.001967)/(1993)*(0.95)^2 = 4.3743E-6
C5 = 1.1666 (Gas conduction factor for nitrogen)
C6 = (10E-2)*(0.03103)/0.0004953 = 0.626415
C2 = 1500 (Determined by iteration)
C7, C8, & C9 come directly from the MLI equation.

Calculation:

Now, turn to the TK Solver "Rule Sheet."
Write 10 equations for temperature as shown.
Write 11 equations for thermal conductivity, k1 through k11. (Note that the printout clips off some of the k_n terms. TK Solver accepts equations with up to 200 characters but will only print out 80.)
Write the equation for Q in terms of δT and k_n.
Shift up to the TK Solver "Variable Sheet."
Enter all of the constants in the imput column and solve. Note: For this example we let T0 = 300 in the k1 equation.

C2 must be iterated until the 10 shield temperatures are smoothly distributed over tne range from 300 down to 270 K. With C2 = 1500, read off the calculated value of Q = 0.5502 W/m^2.

20 Layer MLI Calculation

In this example, all of the data used above is retained but 10 more layers of DAM are added. This requires writing 10 more equations for temperature and k_n and calculating a new value for C2. The results of this exercise are shown on the last TK Solver "Variable Sheet." The 20-layer Q/A value is reduced to 0.2874 W/m^2.

RULE SHEET

Rule

```
T1 = SQRT(300^2-C2)
T2 = SQRT(T1^2-C2)
T3 = SQRT(T2^2-C2)
T4 = SQRT(T3^2-C2)
T5 = SQRT(T4^2-C2)
T6 = SQRT(T5^2-C2)
T7 = SQRT(T6^2-C2)
T8 = SQRT(T7^2-C2)
T9 = SQRT(T8^2-C2)
T10 = SQRT(T9^2-C2)
k1 = C1*(C3*(300^2+T1^2)*(300+T1)-C4*((300+T1)/2)^3)+C5*P*(1-(.2)*(300-78)/22
k2 = C1*(C3*(T1^2+T2^2)*(T1+T2)-C4*((T1+T2)/2)^3)+C5*P*(1-(.2)*(T1-78)/222)+C
k3 = C1*(C3*(T2^2+T3^2)*(T2+T3)-C4*((T2+T3)/2)^3)+C5*P*(1-(.2)*(T2-78)/222)+C
k4 = C1*(C3*(T3^2+T4^2)*(T3+T4)-C4*((T3+T4)/2)^3)+C5*P*(1-(.2)*(T3-78)/222)+C
k5 = C1*(C3*(T4^2+T5^2)*(T4+T5)-C4*((T4+T5)/2)^3)+C5*P*(1-(.2)*(T4-78)/222)+C
k6 = C1*(C3*(T5^2+T6^2)*(T5+T6)-C4*((T5+T6)/2)^3)+C5*P*(1-(.2)*(T5-78)/222)+C
k7 = C1*(C3*(T6^2+T7^2)*(T6+T7)-C4*((T6+T7)/2)^3)+C5*P*(1-(.2)*(T6-78)/222)+C
k8 = C1*(C3*(T7^2+T8^2)*(T7+T8)-C4*((T7+T8)/2)^3)+C5*P*(1-(.2)*(T7-78)/222)+C
k9 = C1*(C3*(T8^2+T9^2)*(T8+T9)-C4*((T8+T9)/2)^3)+C5*P*(1-(.2)*(T8-78)/222)+C
k10 = C1*(C3*(T9^2+T10^2)*(T9+T10)-C4*((T9+T10)/2)^3)+C5*P*(1-(.2)*(T9-78)/22
k11 = C1*(C3*(T10^2+T11^2)*(T10+T11)-C4*((T10+T11)/2)^3)+C5*P*(1-(.2)*(T10-78
Q = 6T/(1/k1+1/k2+1/k3+1/k4+1/k5+1/k6+1/k7+1/k8+1/k9+1/k10+1/k11)
```

(10 layer MLI)

VARIABLE SHEET

Input	Name	Output	Unit	Comment
	T1	297.4895	K	First reflector temperature
1500	C2			Difference of squares constant
	T2	294.95762		
	T3	292.40383		
	T4	289.82753		
	T5	287.22813		
	T6	284.60499		
	T7	281.95744		
	T8	279.2848		
	T9	276.58633		
	T10	273.86128		
	k1	.21794152		"k" between 300 K and first reflector
5.675E-8	C1			Stefan-Boltzmann const.
.020408	C3			Emissivity const. for e = 0.04
4.3743E-6	C4			Radiation absorption constant
1.1666	C5			Gas conduction coef. for nitrogen
.00013332	P		Pa	Vacuum level = 10E-6 Torr
.626415	C6			Solid conduction coefficient
.017	C7			Solid conduction term
.000007	C8			Solid conduction term
.0228	C9			Solid conduction Term
	k2	.21473218		"k" between first and second reflector
	k3	.21154727		
	k4	.20838696		
	k5	.2052514		
	k6	.20214076		
	k7	.19905521		
	k8	.19599491		
	k9	.19296004		
	k10	.18995077		
	k11	.18639868		
270	T11		K	Cold temperature
	Q	.550176	W/m^2	Heat leak per square metre.
30	δT		K	Total temperature difference

VARIABLE SHEET

Input	Name	Output	Unit	Comment
	T1	298.64695	K	First reflector temperature
810	C2			Difference of squares constant
	T2	297.28774		
	T3	295.92229		
	T4	294.55051		
	T5	293.1723		
	T6	291.78759		
	T7	290.39628		
	T8	288.99827		
	T9	287.59346		
	T10	286.18176		
	k1	.21865916		"k" between 300 K and first reflector
5.675E-8	C1			Stefan-Boltzmann const.
.020408	C3			Emissivity const. for e = 0.04
4.3743E-6	C4			Radiation absorption constant
1.1666	C5			Gas conduction coef. for nitrogen
.00013332	P		Pa	Vacuum level = 10E-6 Torr
.626415	C6			Solid conduction coefficient
.017	C7			Solid conduction term
.000007	C8			Solid conduction term
.0228	C9			Solid conduction Term
	k2	.21691984		"k" between first and second reflector
	k3	.21518761		
	k4	.21346249		
	k5	.21174451		
	k6	.21003369		
	k7	.20833007		
	k8	.20663365		
	k9	.20494448		
	k10	.20326257		
	k11	.20158795		
	T11	284.76306	K	
	Q	.2874425	W/m^2	Heat leak per square metre.
30	δT		K	Total temperature difference
	D1	52.398198		
	D2	51.970502		
	k12	.19992066		
	k13	.1982607		
	k14	.19660812		
	k15	.19496294		
	k16	.19332518		
	k17	.19169487		
	k18	.19007204		
	k19	.18845672		
	k20	.18684893		
	k21	.18516393		
	T12	283.33725		
	T13	281.90424		
	T14	280.4639		
	T15	279.01613		
	T16	277.5608		
	T17	276.09781		
	T18	274.62702		
	T19	273.14831		
	T20	271.66155		
270	T21		K	Cold temperature

Appendix B

Procedures for MLI and SOFI Closeouts

MHTB Tank

July, 1993

Table of Contents

Procedure for Top Dome Blanket Installation

1. Remove roll wrapped blanket from cylindrical fixture.

2. Layout blanket on working table and cut out circular pieces for domes and manhole cover.

3. For the top dome blanket, rotate each layer set (which consists of DAM, dacron net and bumper strips) 90° from the lower layer set.

4. Cut out penetration holes (manhole, fill/drain line, pressurization line, instrumentation port, RI hardware port) in top dome blanket.

5. Apply several layers of DAM, dacron net and bumper strips to the top dome SOFI surface using the dome heads handling fixture. Interleave the top dome DAM with the barrel section DAM. Tape the top dome DAM to the barrel section DAM using Kapton tape. Interleave the top dome dacron net to barrel section dacron net. Secure using Kapton tape.

6. Apply collars of DAM to appropriate penetrations. (Refer to individual penetration closeout procedure for details). Tape in position using Kapton tape.

7. Insulate each penetration with a layer of DAM and then a layer of spacer material. (Refer to individual penetration closeout procedure for details). Secure using Kapton tape.

8. Apply next layer(s) of top dome DAM, dacron net and bumper strips over previous layers. Interleave the top dome DAM with barrel section DAM. Secure using Kapton tape. Interleave top dome dacron net to barrel section dacron net. Secure using Kapton tape.

9. Repeat steps 6 through 8 until all top dome MLI blanket layers have been applied.

Procedure for Fill Line MLI Closeout

1. Trim back top dome MLI blanket from penetration, if necessary.

2. Apply collar of DAM over top dome blanket DAM.

3. Spiral wrap a layer of DAM, starting at the tank head and covering the DAM collar, along the fill line and over the vacuum jacket section to desirable location.

4. Secure DAM using Kapton tape.

5. Spiral wrap a layer of dacron net, starting at the tank head and covering the DAM, along the fill line and over the vacuum jacket section beyond the end of previous DAM layer.

6. Secure dacron net using Kapton tape.

7. Apply collar of DAM over top blanket DAM.

8. Starting at the end furthest away from the tank, spiral wrap a layer of DAM towards the tank, covering the previously wrapped dacron net.

9. Secure the DAM using Kapton tape.

10. Spiral wrap a layer of dacron net starting in the same location as the previous layer of DAM.

11. Secure dacron net using Kapton tape.

12. Repeat steps 2 through 11 until desirable layers of MLI are applied.

Note: Each layer of DAM should be wrapped the opposite direction of the surrounding layers of DAM.

FILL/DRAIN LINE
TYPICAL INSULATION

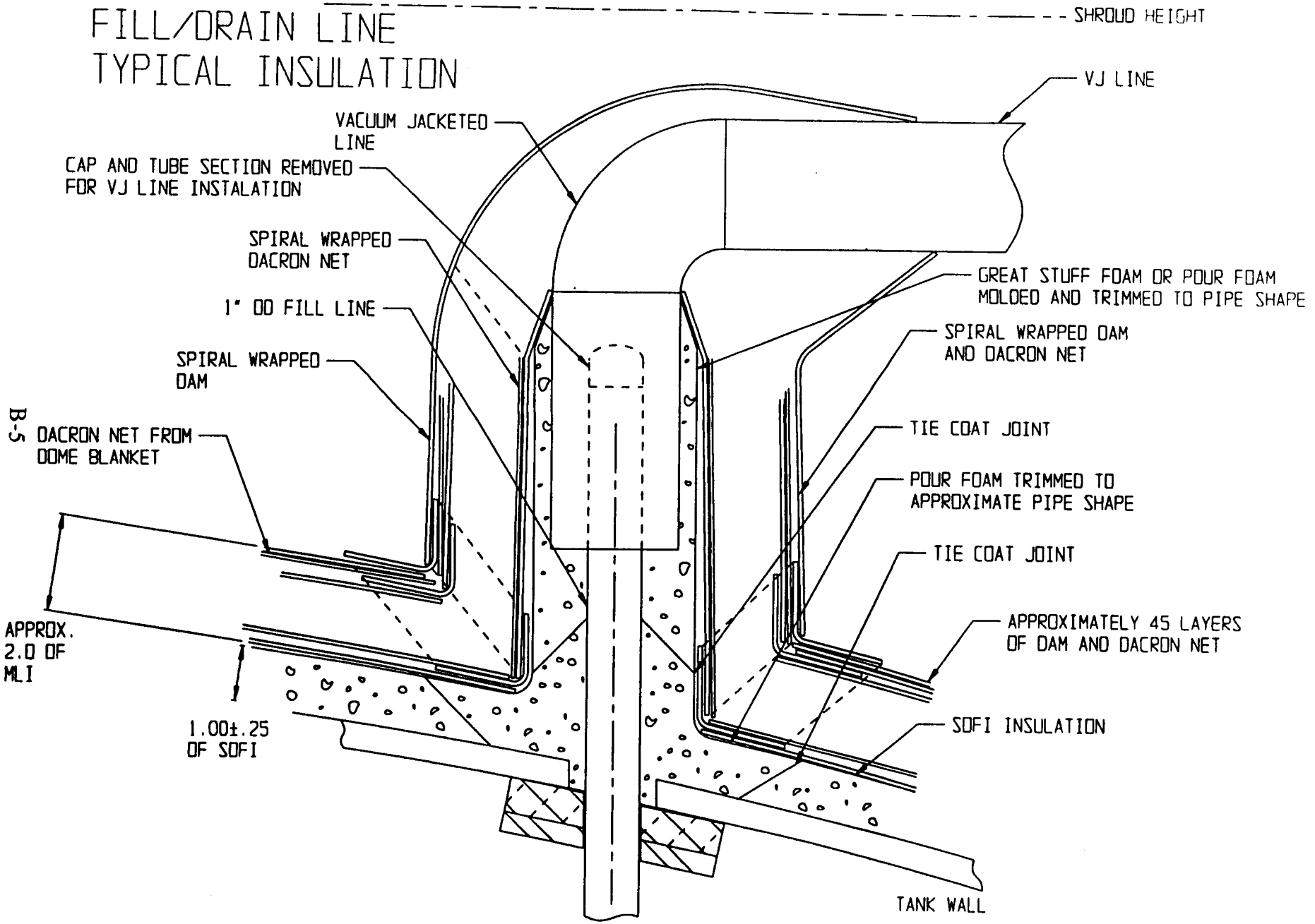

Procedure for Pressurization Line MLI Closeout

1. Trim back top dome MLI blanket from penetration, if necessary.

2. Apply collar of DAM over top dome blanket DAM.

3. Spiral wrap a layer of DAM, starting at the tank head and covering the DAM collar, along the pressurization line to end of SOFI application.

4. Secure DAM using Kapton tape.

5. Spiral wrap a layer of dacron net, starting at the tank head and covering the DAM, along the pressurization line and beyond the end of previous DAM layer.

6. Secure dacron net using Kapton tape.

7. Apply collar of DAM over top blanket DAM.

8. Starting at the end furthest away from the tank, spiral wrap a layer of DAM towards the tank, covering the previously wrapped dacron net.

9. Secure the DAM using Kapton tape.

10. Spiral wrap a layer of dacron net starting in the same location as the previous layer of DAM.

11. Secure dacron net using Kapton tape.

12. Repeat steps 2 through 11 until desirable layers of MLI are applied.

Note: Each layer of DAM should be wrapped the opposite direction of the surrounding layers of DAM.

PRESSURIZATION LINE TYPICAL INSULATION

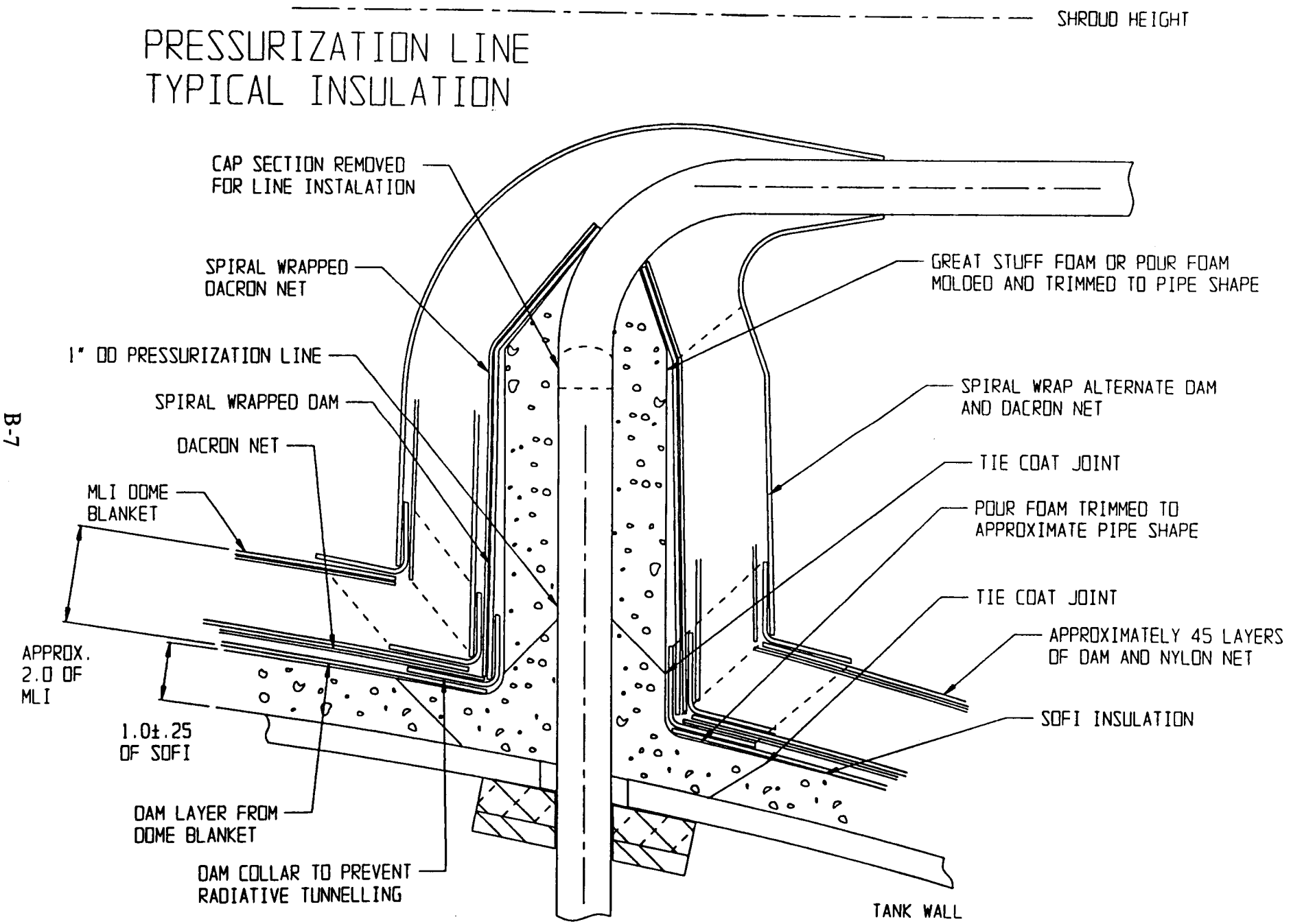

Procedure for Instrumentation Port MLI Closeout

1. Cut 3" radial slits in top dome blanket around instrumentation port and tape sections back from instrumentation port.

2. Apply one layer of slit cylinder DAM cutout around the instrumentation port.

3. Interleave lower portion of slit cylinder DAM with first layer of top dome DAM (nearest tank). Secure using Kapton tape.

4. Apply one layer of DAM disc over instrumentation port and interleave with slit cylinder DAM layer. Secure using Kapton tape.

5. Apply spiral wrap section of dacron net over DAM layer. Secure using Kapton tape.

6. Repeat steps 2 through 5 until desirable layers of MLI are applied.

Note: This procedure should be completed simultaneously with the vent line MLI closeout.

Procedure for Vent Line MLI Closeout

This procedure should be completed in conjunction with the instrumentation port MLI closeout.

1. Apply collar of DAM over vent line covering instrumentation port DAM.

2. Spiral wrap a layer of DAM, starting at the instrumentation port and covering the DAM collar, along the vent line and over the vacuum jacket section to desirable location.

3. Secure DAM using Kapton tape.

4. Spiral wrap a layer of dacron net, starting at the instrumentation port and covering the DAM, along the fill line and over the vacuum jacket section beyond the end of previous DAM layer.

5. Secure dacron net using Kapton tape.

6. Apply collar of DAM over instrumentation port DAM.

7. Starting at the end furthest away from the tank, spiral wrap a layer of DAM towards the tank, covering the previously wrapped dacron net.

8. Secure the DAM using Kapton tape.

9. Spiral wrap a layer of dacron net starting in the same location as the previous layer of DAM.

10. Secure dacron net using Kapton tape.

11. Repeat steps 2 through 10 until desirable layers of MLI are applied.

Note: Each layer of DAM should be wrapped the opposite direction of the surrounding layers of DAM.

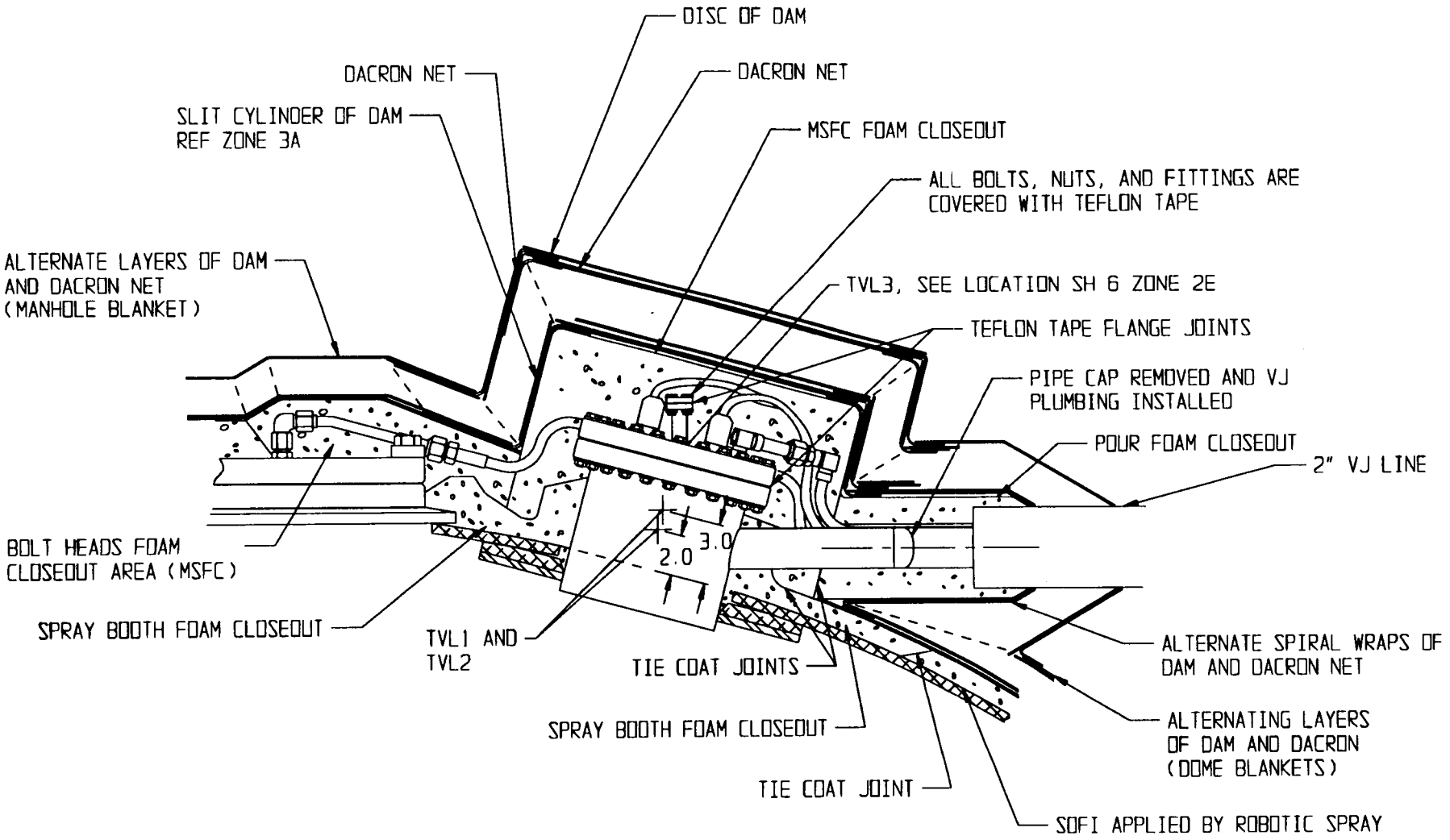

TYPICAL INSULATION OF TANK VENT PORT

Procedure for Rockwell Top Penetration MLI Closeout

1. Trim back top dome MLI blanket from penetration, if necessary.
2. Apply circular disc of DAM on top of blind flange.
3. Interleave lower portion of disc DAM into top dome blanket DAM.
4. Secure DAM using Kapton tape.
5. Apply circular disc of dacron net over DAM and interleave into top dome blanket dacron net.
6. Secure using Kapton tape.
7. Repeat steps 2 through 6 until desirable layers of MLI are applied.

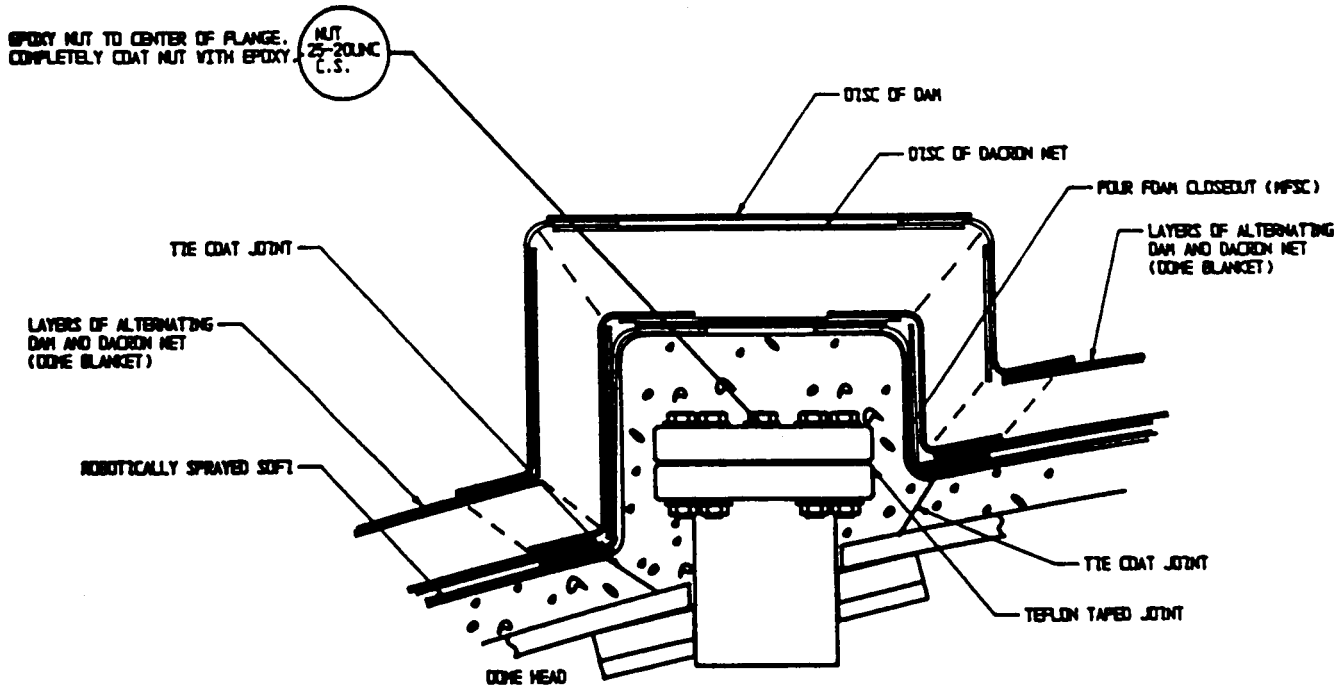

TYPICAL VCS FEEDTHRU INSULATION

Procedure for Manhole Cover MLI Closeout

1. Cut 6" radial slits in top dome blanket around manhole cover and tape sections back from manhole cover.

2. Apply complete manhole cover MLI blanket to manhole SOFI surface using handling fixture, if necessary.

3. Lay the first manhole cover layer of DAM (closest to the tank) in place over the SOFI.

4. Apply the first top dome slitted DAM layer (closest to tank) over the manhole cover DAM layer.

5. Secure the DAM using Kapton tape.

6. Lay the first layer of manhole cover dacron net (closest to the tank) over the previous layer of DAM.

7. Apply the first layer of top dome dacron net (closest to the tank) over the manhole cover dacron net.

8. Secure the dacron net using Kapton tape.

9. Repeat steps 3 through 8 until all layers have been interwoven.

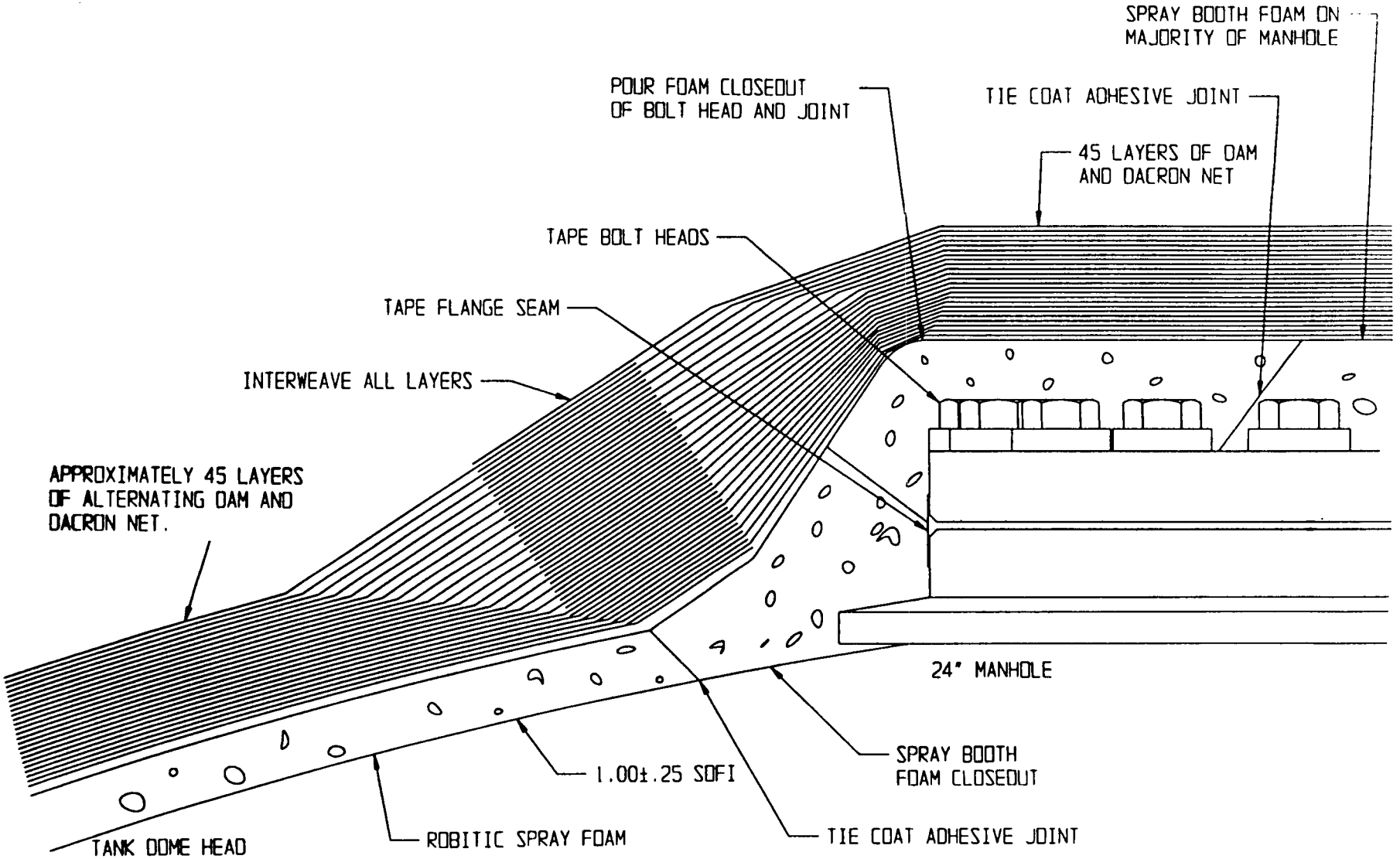

TYPICAL MANHOLE INSULATION

Procedure for Bottom Dome Blanket Installation

1. Remove roll wrapped blanket from cylindrical fixture.

2. Layout blanket on working table and cut out circular pieces for domes and manhole cover.

3. For the bottom dome blanket, rotate each layer set (which consists of DAM, dacron net and bumper strips) 90° from the lower layer set.

4. Cut slits in bottom dome blanket for tank legs.

5. Apply all layers of DAM, dacron net and bumper strips to the bottom dome SOFI surface using the dome heads handling fixture. Interleave the first layer of DAM (closest to SOFI surface) with the first layer of barrel section DAM. Tape the bottom dome DAM to the barrel section DAM using Kapton tape. Interleave the bottom dome dacron net to barrel section dacron net. Secure using Kapton tape.

6. Repeat step 5 until all bottom dome MLI blanket layers have been applied.

Procedure for Tank Legs MLI Closeout

1. Trim back bottom dome MLI blanket from penetration, if necessary.

2. Spiral wrap a layer of DAM, starting at the tank head along the tank leg to desirable location down the tank leg composite section.

3. Secure DAM using Kapton tape.

4. Spiral wrap a layer of dacron net, starting at the tank head, along the tank leg beyond the end of previous DAM layer.

5. Secure dacron net using Kapton tape.

6. Starting at the end furthest away from the tank, spiral wrap a layer of DAM towards the tank, covering the previously wrapped dacron net.

7. Secure the DAM using Kapton tape.

8. Spiral wrap a layer of dacron net starting in the same location as the previous layer of DAM.

9. Secure dacron net using Kapton tape.

10. Repeat steps 2 through 9 until desirable layers of MLI are applied.

Note: Each layer of DAM should be wrapped the opposite direction of the surrounding layers of DAM.

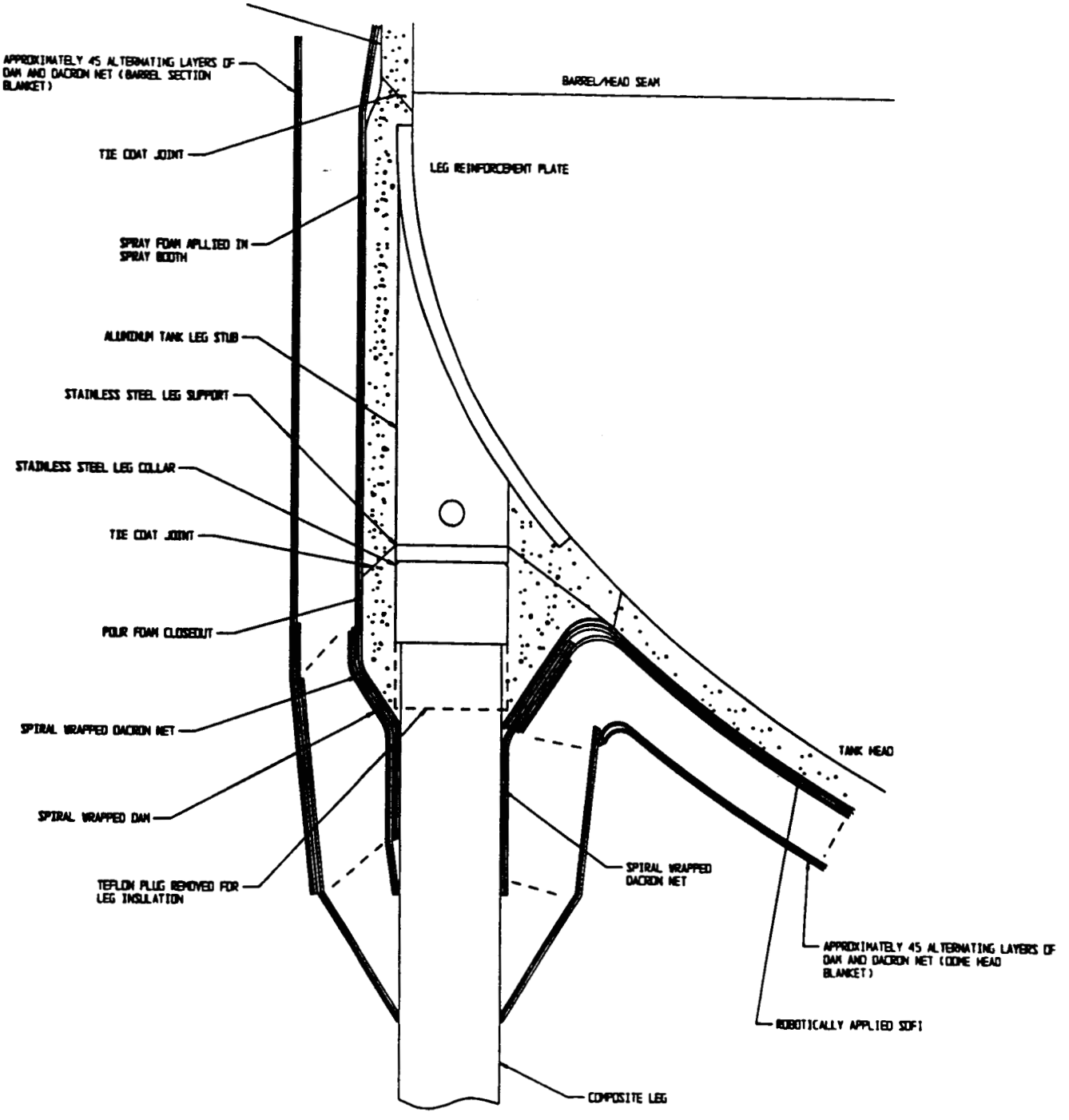

TYPICAL LEG INSULATION

Procedure for Rockwell Bottom Hardware MLI Closeout

(Utilize the closeout procedure developed for the instrumentation port as a guideline for this closeout)

1. Remove MLI and SOFI covering the Rockwell attachment.

2. Install Rockwell hardware on bottom dome.

3. Cut 3" radial slits in bottom dome blanket around Rockwell hardware and tape sections back from Rockwell hardware.

4. Apply one layer of slit cylinder DAM cutout around the Rockwell hardware.

5. Interleave lower portion of slit cylinder DAM with first layer of bottom dome DAM (nearest tank). Secure using Kapton tape.

6. Apply one layer of DAM disc over Rockwell hardware and interleave with slit cylinder DAM layer. Secure using Kapton tape.

7. Apply spiral wrap section of dacron net over DAM layer. Secure using Kapton tape.

8. Repeat steps 4 through 7 until desirable layers of MLI are applied.

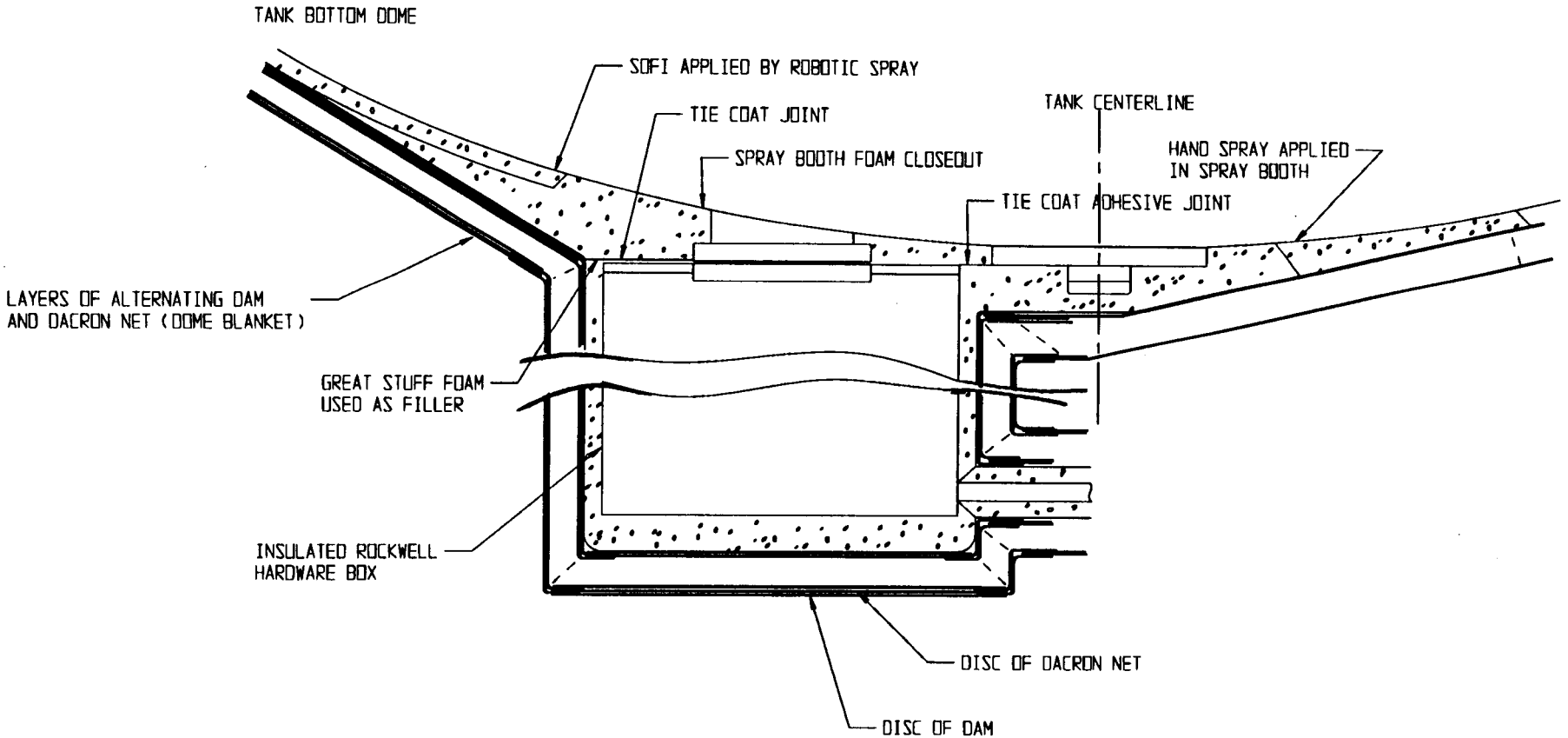

TYPICAL RI BOX INSULATION

Procedure for Fill Line SOFI Closeout

1. Trim back sprayed on foam until knitline thickness and total foam thickness requirements are satisfied.

2. Trim foam to scarf joint configuration.

3. Reactivate primer surface, if required.

4. Vacuum foam chips/dust from area.

5. Apply tie coat adhesive and allow to cure.

6. Prepare baggie for closeout Step 1.

7. Prepare foam materials, mix, and dispense into bagged area.

8. Allow foam to cure.

9. Remove bagging material.

10. Trim foam.

11. Remove foam scraps, vacuum remaining residue.

12. Repeat steps 5 through 12 for closeout Step 2 using either pour foam or Great Stuff as required.

FILL/DRAIN LINE
TYPICAL INSULATION

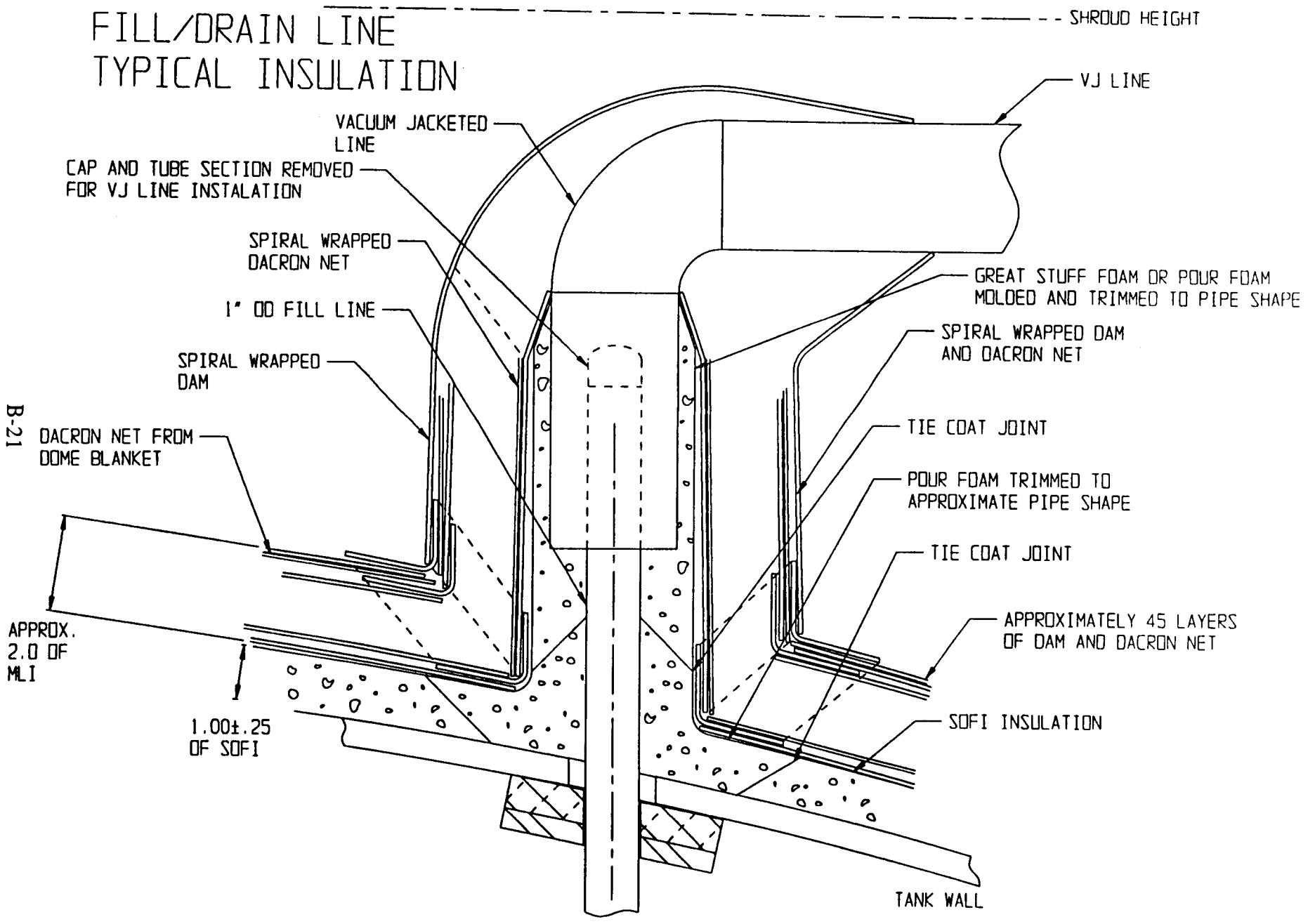

Procedure for Instrumentation Port SOFI Closeout

1. Trim back sprayed on foam until knitline thickness and total foam thickness requirements are satisfied.

2. Trim foam to scarf joint configuration.

3. Reactivate primer surface, if required.

4. Vacuum foam chips/dust from area.

5. Apply tie coat adhesive and allow to cure.

6. Prepare cardboard tube for closeout Step 1.

7. Prepare foam materials, mix, and dispense into cardboard tube area.

8. Allow foam to cure.

9. Remove cardboard tube.

10. Trim foam.

11. Remove foam scraps, vacuum remaining residue.

12. Repeat steps 5 through 12 for closeout Step 2 using either pour foam or Great Stuff as required.

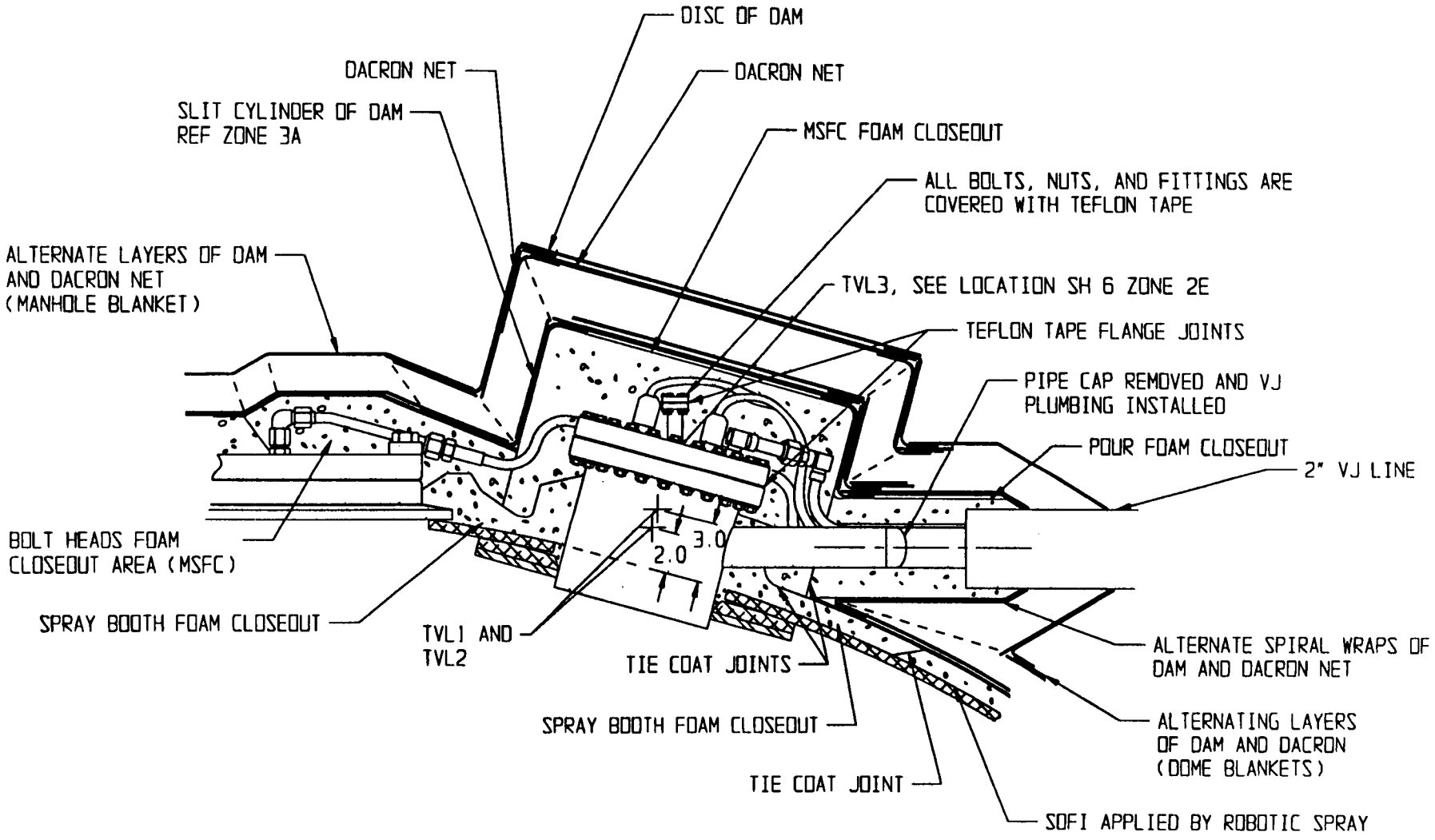

TYPICAL INSULATION OF TANK VENT PORT

NASA
National Aeronautics and Space Administration

Report Documentation Page

1. Report No.	2. Government Accession No.	3. Recipients Catalog No.
NASA CR-TBD		

4. Title and Subtitle
CFM Technologies for Space Transportation:
Multipurpose Hydrogen Test Bed System
Definition and Tank Procurement

5. Report Date
July, 1993

6. Performing Organization Code

7. Author(s)
E. C. Fox, J. B. Sharpe
E. R. Kiefel, D. R. Sheahan
G.L. McIntosh, M. E. Wakefield

8. Performing Organization Report No.
None

10. Work Unit No.
203604

9. Performing Organization Name and Address
Martin Marietta Astronautics
Flight Systems
Denver, CO 80201

11. Contract or Grant No.
NAS8-39201

13. Type of Report and Period Covered
Contractor Final Report

12. Sponsoring Agency Name and Address
NASA George C. Marshall Space Flight Center
Huntsville, AL 35812

14. Sponsoring Agency Code

15. Supplementary Notes
Project Manager: Mark Fisher and Leon Hastings, Space Propulsion Branch,
Propulsion Systems Division, Propulsion Laboratory
George C. Marshall Space Flight Center

16. Abstract

Abstract: This report covers the development of a test bed tank and system for evaluating cryogenic fluid management technologies in a simulated upper stage liquid hydrogen tank. The tank is 10 ft long and is 10 ft in diameter, and is an ASME certified tank constructed of 5083 aluminum. The tank is insulated with a combination of sprayed on foam insulation, covered by 45 layers of double aluminized mylar separated by dacron net. The mylar is applied by a continuous wrap system adapted from commercial applications, and incorporates variable spacing between the mylar to provide more space between those layers having a high delta temperature, which minimizes heat leak. It also incorporates a unique venting system which uses fewer large holes in the mylar rather than the multitude of small holes used conventionally. This significantly reduces radiation heat transfer. The test bed consists of an existing vacuum chamber at MSFC, the test bed tank and its thermal control system, and a thermal shroud (which may be heated) surrounding the tank. Provisions are made in the tank and chamber for inclusion of a variety of cryogenic fluid management experiments.

17. Key Words (Suggested by Author(s))	18. Distribution Statement
Cryogenic, Cryogenic Fluid Management, CFM, Upper Stage, liquid hydrogen, LH2, test bed, storage, thermal control, propellant management, insulation, multilayer insulation, MLI, SOFI	Unlimited

19. Security Classif. (of this report)	20. Security Classif. (of this page)	21. No. of pages	22. Price
Unclassified	Unclassified	93	

NASA FORM 1626 OCT 86